University of Stavanger

Faculty of Science and Technology

MASTER'S THESIS

Study program/ Specialization: Petroleum Engineering/Drilling Technology	Spring semester, 2012 Open / Restricted access
Writer: Eirik Hansen	…… (Writer's signature)
Faculty supervisor: Gerhard Nygaard	
Title of thesis: Automatic Evaluation of Drilling Fluid Properties	
Credits (ECTS): 30	
Key words: Drilling fluid technology Instrumented Standpipe Drilling automation Flow loop	Pages: 92 + enclosure: 15 Stavanger, 12/06/2012

Frontpage for master thesis
Faculty of Science and Technology
Decision made by the Dean October 30th 2009

ABSTRACT

This thesis is structured in two main parts. First part covers the fundamental role of drilling fluid in the drilling process. It provides a description of the mud circulating system for conventional drilling operations, outlines the basic composition of drilling fluids, and describes the main functions and properties of drilling fluids. Furthermore it describes the current testing procedures and equipment and illustrates how testing is used in the evaluation of drilling fluid properties.

The thesis also covers the fundamentals of drilling fluid hydrodynamics, including drilling fluid rheology and the three most commonly used rheological models for characterizing drilling fluid flow in conjunction with frictional pressure loss calculations. Some of the weaknesses and limitations of the current testing regime will also be discussed.

The second part will present a description of a new concept “Instrumented Standpipe” enabling automated measurements of important drilling fluid parameters during drilling operations. The Instrumented Standpipe concept is based on continuous pressure monitoring of the flow path between the mud pump and the swivel. These pressure measurements can provide valuable real time information about the fluid density, frictional parameters and rheological parameters. The major part of this chapter is related to the practical installation and implementation of a small scale Instrumented Standpipe set up on an existing flow loop, and validation of its performance through experimental testing.

ACKNOWLEDGEMENTS

The master thesis is the final work in the Petroleum Technology master program at the University of Stavanger. This thesis was conducted during the spring of 2012, and is a part of a larger collaboration between IRIS, Statoil, NTNU and UiS regarding intelligent drilling.

My previous work experience with conventional testing of drilling fluid properties, from working two years at the Halliburton's Drilling Fluid Laboratory, and my genuine interest of new and innovative technologies made the choice of this particular thesis obvious.

Working with this thesis has been very interesting, challenging and overall a great learning experience. I have utilized a lot of the knowledge acquired throughout my five years of studies, but also been challenged in areas where I had little preexisting knowledge especially related to the practical instrumentation and implementation of measuring instruments on an existing flow loop.

Even though the thesis to a great extent consisted of independent work there are many persons I would like to thank for helpful advices and guidance in moments of need. A special thank to *Gerhard Nygaard* who provided me with this interesting and challenging task. I would also like to thank *Sivert B. Drangeid* and *Hermonja A. Rabenjafimanantsoa* at the *Institute of Petroleum Technology, UiS*, and *Magnus T. Torsvik*, *Aibel*, for constructive discussions and practical support. I also want to express my gratitude to *Erling Grindhaug* for proofreading of this thesis.

Lastly I would like to thank my friends and family for all their support throughout my five years of studies.

CONTENT

ABSTRACT ..... **II**

ACKNOWLEDGEMENTS ..... **III**

LIST OF FIGURES: ..... **VII**

LIST OF TABLES: ..... **X**

1 INTRODUCTION: **1**

1.1 Objective and Scope of Work 2

2 FUNDAMENTALS OF DRILLING FLUID TECHNOLOGY **3**

2.1 Composition of Drilling Fluids 4
2.2 The Drilling Fluid Circulating System 5
2.3 Functions of Drilling Fluids 8

2.3.1 Control formation pressure 9
2.3.2 Remove cuttings from wellbore 13
2.3.3 Seal permeable formations – fluid loss control 14
2.3.4 Keep cuttings and weight material suspended during circulation interruptions 14
2.3.5 Release sand and cuttings at surface 15
2.3.6 Cool, clean and lubricate the bit and the drill string 15
2.3.7 Maintain wellbore stability in uncased sections 15

2.4 Properties of Drilling Fluids 16

2.4.1 Fluid Density – mud weight 17
2.4.2 Fluid Rheology 20

2.5 Rheological Models 24

2.5.1 The Bingham Plastic Model 24
2.5.2 The Power Law Model 26
2.5.3 Herschel-Bulkley model 27

2.6 Conventional testing of drilling fluid 29

2.6.1 Determination of drilling fluid density (mud weight) 30
2.6.2 Determination of viscosity and gel strength 32

2.7 Frictional Pressure Loss Calculations 37

3 AUTOMATIC EVALUATION OF DRILLING FLUID PROPERTIES 45

3.1 Instrumented Standpipe concept 45
3.2 Flow loop description 48
3.3 Implementation of differential pressure transmitters on flow loop 51

3.3.1 Matlab scaling factor 53
3.3.2 Verification of scaling factor 54

3.4 Pre-testing of small scale Instrumented Standpipe set up on flow loop 57

3.4.1 Pump characteristics 57
3.4.2 Inconsistent measurements for DP transmitters 57

3.5 Results of small scale testing with Instrumented Standpipe set up on flow loop 63

3.5.1 Formulas used in the Matlab plots 64
3.5.2 Measurements at 20% of maximum pump rate 65
3.5.3 Measurements at 25% of maximum pump rate 66
3.5.4 Measurements at 30% of maximum pump rate 67
3.5.5 Measurements at 35% of maximum pump rate 68
3.5.6 Measurements at 40% of maximum pump rate 69
3.5.7 Measurements at 45% of maximum pump rate 70
3.5.8 Measured pressure losses compared to theoretical at different flow rates 71
3.5.9 Fluid density estimation for different pump pressures 73
3.5.10 Measured friction factor vs. theoretical friction factor at different flow rates 74

CONCLUSION & LESSONS LEARNED 75

FURTHER WORK 76

ABBREVIATIONS 77

NOMENCLATURE 78

BIBLIOGRAPHY 80

APPENDICES **83**

A – Operating procedures 83

A.1 API Recommended practice for determination of mud density using the Pressurized Mud Balance [3] 83
A.2 API Recommended procedure for determination of viscosity using the Marsh Funnel (scanned from [3]) 84
A.3 API Recommended procedure for determination of viscosity and/or gel strength using a direct-indication viscometer (scanned from [3]) 85
A.4 Procedure for startup and shutdown of flow loop [26] 87

B - Technical documentation related to the installation DP transmitters on the flow loop 88

B.1 Table of analog input ports on control card (PCI 6221) 88
B.2 Circuit diagram for Differential Pressure transmitters 90
B.3 Terminal blocks (rekkeklemmer) in the control cabinet 91

C – Matlab script for measured data and plots 93
D – Error analysis 95
E – Excel calculations 96

E.1 Comparison of rheological models 96
E.2 Statistical analysis of measured data quality 97

LIST OF FIGURES:

Figure 2.1 – The drilling fluid circulation system [2]. 5

Figure 2.2 – The pore pressure gradient and fracture pressure gradient strongly influence the mud weight and casing program for the entire well. 12

Figure 2.3 - Mud processing circle [9]. 16

Figure 2.4 – A comparison of the effect of temperature and pressure on ESD a typical WBM and OBM [18]. 18

Figure 2.5 - Velocity profile for laminar flow of a Newtonian fluid in a round pipe, where the longer arrows indicate higher velocity..... . 21

Figure 2.6 - Velocity profile for turbulent flow. 21

Figure 2.7 - Schematic diagram of laminar and turbulent flow regime [1]. 22

Figure 2.8 - Rheogram for a Newtonian fluid. 23

Figure 2.9 - Rheogram for a typical Bingham plastic fluid. 24

Figure 2.10 - Effective viscosity [μ_e] for a Bingham plastic fluid. The effective viscosity will decrease when shear rate increased. 25

Figure 2.11 - Graphical comparison of measured rheological values compared to expected values for the Bingham, Power Law model and The Herschel-Bulkley model [Table presented in appendix E.1]. 28

Figure 2.12 – Halliburton's pressurized mud balance. 31

Figure 2.13 - Fann VG 35 Viscometer "Standard of the Industry". 33

Figure 2.14 - Schematic drawing of the basic components in a concentric cylinder viscometer [19].. 34

Figure 2.15 - Example of circulation pressures, for a typical well without any surface back pressure and uniform mud density throughout the well. [2]. 38

Figure 2.16 - Chart for obtaining Critical Reynolds number for Bingham plastic fluids [20]..... 44

Figure 2.17 - Chart for obtaining friction factors for Power Law fluids [20] 45

Figure 3.1 - Schematic of the Instrumented Standpipe setup. PT_1, PT_2, PT_3 and PT_4 are the pressure transmitters along the flow path [25]. 46

Figure 3.2 – Picture of the flow loop 49

Figure 3.3 - Process flow diagram (PFD) for the flow loop..... 50

Figure 3.4 - Picture of DP transmitters and their placement on the flow loop..... 51

Figure 3.5 - Levels included in the link between the DP transmitters and the PC input card..... 52

Figure 3.6 – Graphical presentation of scaling factor argument..... 53

Figure 3.7 - Differential pressures at 30% of maximum pump rate measured during working hours. 58

Figure 3.8 - Differential pressures at 30% of maximum pump rate measured after working hours.... 58

Figure 3.9 - Differential pressures at 40% of maximum pump rate measured during working hours. 59

Figure 3.10 - Differential pressures at 40% of maximum pump rate measured after working hours.. 59

Figure 3.11 - Comparison of Matlab data obtained during and after normal working hours. 60

Figure 3.12 - Box plot comparison of data quality for DP display readings obtained after work hours and during work hours, at 30% of maximum pump rate. 61

Figure 3.13 - Box plot comparison of data quality for DP display readings obtained after work hours and during work hours, at 40% of maximum pump rate. 62

Figure 3.14 - Measurements at 20% of maximum pump rate 65

Figure 3.15 - Measurements at 25% of maximum pump rate 66

Figure 3.16 - Measurements at 30% of maximum pump rate 67

Figure 3.17 - Measurements at 35% of maximum pump rate 68

Figure 3.18 -Measurements at 40% of maximum pump rate 69

Figure 3.19 - Measurements at 45% of maximum pump rate 70

Figure 3.20 - Measured pressure losses compared with the theoretical pressure loss for different flow rates..... 71

Figure 3.21 - Pressure difference between: DPver and DPhor, DPver and $(dP/dL)_{teo}$, and DPhor and $(dP/dL)_{teo}$..... 71

Figure 3.22 - Graphical presentation of estimated fluid densities at corresponding pump pressures 73

Figure 3.23 - Graphical comparison of the measured friction factor coefficient and theoretical friction factor coefficient at different flow rates. 74

LIST OF TABLES:

Table 2.1 - NORSOKs well barrier acceptance criteria fluid column [10]. 9

Table 2.2 - Nomenclature and practical input units for equations presented in Table 2.3 and Table 2.4 42

Table 2.3 - Equations for determining frictional pressure loss for non-Newtonian fluids [20] 43

Table 2.4 - cont. Equations for determining frictional pressure loss for non-Newtonian fluids [20] ... 44

Table 3.1 - Relationship between voltage signal and mBar obtained with the Rosemount HART 375 Field Communicator. 53

Table 3.2 - Correlation between display reading and Matlab data logger for DP 1 @ 30% of maximum pump rate. 55

Table 3.3 - Correlation between display reading and Matlab data logger for DP 1 @ 40% of maximum pump rate. 55

Table 3.4 - Correlation between display reading and Matlab data logger for DP 2 @ 30% of maximum pump rate. 55

Table 3.5 - Correlation between display reading and Matlab data logger for DP 2 @ 40% of maximum pump rate. 55

Table 3.6 - Flow loop hard data and fluid properties used in all subsequent calculations. 63

1 INTRODUCTION:

In today's modern oil and gas industry, where most of the easiest petroleum prospects are nearing depletion, the industry is forced towards increasingly more challenging and marginal prospects. New technology and innovation is a must to overcome these challenges and enable the future exploitation of these underground resources in a safe and sustainable manner.

The current method of evaluating drilling fluid properties is primarily based on manually performed tests, this applies to both onshore drilling fluid laboratories and at the actual drill site. Many of these standard tests are virtually unchanged since they originated in the middle of the last century [1, 2]. Although these tests still proves to be sufficient for their purpose, it is safe to say that they have not kept up with the development in the rest of the upstream industry when it comes to automation, digitalization and optimization. There is hardly any doubt that many of these standard tests could be automated, and the potential benefits of such automatization could be great.

Currently the routine standard tests, defined by the API standard [3], are typically performed two times per each 12 hour shift during drilling operations. Whereas the drilling fluid density is manually measured every fifteenth minute. This means that critical down hole decisions may be based on data that potentially could be several hours old and may not truly reflect the actual condition of the drilling fluid [4].

Automation of the routine tests opens the possibility more frequent measurements and real time collection and utilization of data. Random errors in measurements caused by human inaccuracy can practically be eliminated, thus provide more precise and consistent data. Another important aspect of automated testing is the reduction of direct contact between the drilling fluid and personnel, which means less exposure of potentially hazardous fluids. Ultimately automation can reduce the overall drilling risk and cost through real time hydraulic optimization, reduced rig site staffing, and better control of the bottom hole pressure.

In recent years two of the major providers of drilling fluids services namely Halliburton and M-I SWACO have developed and tested various ways of automated testing and real time monitoring of drilling fluid properties. Halliburton recently introduced their *Real Time Density and Viscosity (RTDV) Measurement unit*. That is described as a fully automated unit that measures the density and six speed rheology of drilling fluids per API standards. The system is installed near the mud tanks and measurements are performed at an average frequency of 1 test per 20 minutes [4]. While M-I

SWACO just as recently introduced a collection of discrete sensor packages for automatic monitoring of drilling fluid parameters including; density, temperature, electrical stability, water content in oil based fluids, elemental analysis, solids content, particle-size distribution, and multi-temperature rheological properties [5].

1.1 Objective and Scope of Work

In this thesis the potential of a new concept, Instrumented Standpipe for automated measurements of important drilling fluid parameters during drilling operations is discussed. The Instrumented Standpipe concept is based on continuous pressure monitoring of the flow path between the mud pump and the swivel. These pressure measurements can provide valuable real time information about the fluid density, frictional parameters and rheological parameters.

The main objectives of this study include:

1) Provide an overview of the various functions of the drilling fluid and their primary properties.
2) Give an introduction to the current testing equipment and procedures, especially related to evaluation of density and rheological properties of the drilling fluid.
3) Implementation of the Instrumented Standpipe concept to an existing flow loop and validation of its performance through experimental testing.

2 FUNDAMENTALS OF DRILLING FLUID TECHNOLOGY

The objective of this chapter is to provide a basic understanding of the role of drilling fluids in the modern petroleum drilling industry. It will in short and simple terms explain the essential equipment and procedures for fluid handling and testing, and their purpose and properties. The composition of the drilling fluids will be addressed in a very general terms.

The use of drilling fluids goes far beyond the petroleum industry. Already during the Chou dynasty (1122 – 250 B.C) it likely that water was used in the aid of removing cuttings and softening the rock when drilling brine wells [*1*]. Up to the early 1900s removal of drilled cuttings was the sole concern of the simple water based drilling fluids that mostly got their viscosity from natural clays in the cuttings. During the 1920s, dense material was added to the drilling fluid in order to control the formation pressure. In the 1930s; several more additives came into use, issues concerning fluid loss and filter cake build up was recognized and a few simple tests was developed. Some of these tests are very similar to the once used this day! There were now three different drilling fluid properties that were recognized and systematically controlled; sufficient density to control formation pressure, sufficient viscosity to transport cuttings out of the well, and fluid loss control. This marks the birth of the modern drilling fluid industry [*1, 2*].

Even though drilling fluid technology new has become severely more advanced, are these three parameters, along with separation of drilled solids from the mud, still considered the most important parameters [*2*].

The drilling fluid in the borehole serves as the first line of defense against well control problems. Close monitoring of the properties of the drilling fluid can provide early warning signs of impending well control problems, and are thereby a key factor for safe operations.

2.1 Composition of Drilling Fluids

Drilling fluid, often referred to as drilling mud, is a generic term used for different types of fluids used in conjunction with petroleum drilling and production of oil and gas. Drilling fluid technology constitute a vital part of the entire drilling process, from drilling to the completed well. Drilling mud is basically a heterogeneous mixture of various chemical additives in a base fluid. The most important consideration when formulating a drilling fluid, regardless of mud type, is to ensure that it can endure the stresses they meet down hole [6]. The composition also determines the performance aspect of the drilling fluid.

Every well is unique. So the drilling fluid program must be thoroughly planned and customized in order to suit the subsurface conditions for each well. Thus a considerable amount of drilling fluid formulations have been developed over the years and their composition has become very complex as more and more demands must be met. However, can drilling fluids be classified in three general groups according to their principal constituent [*1*]:

- **Water-based muds (WBM)** have water as the continuous phase. The water may contain several dissolvable substances (e.g. salts, surfactants, polymers) and various insolvable components (barite, clay and cuttings) in suspension.
- **Oil-based muds (OBM)** have oil as the continuous phase. Normally a mineral oil, diesel oil or a low-toxicity mineral oil is preferred. Because some water always will be present, the OBM must contain water-emulsifying agents to keep water suspended as small droplets in the base oil. It also contains various viscosifiers and suspending agents as well as weighting material (barite). Oil-based muds provide an unequaled performance with respect to penetration rate, wellbore stability, lubricity and thermal stability. They are however more expensive than WBMs and subjected to stricter regulations regarding their use, discharge and recycling.
- **Gaseous/foam based** Air or other gases is used to produce a foam like mud, in which gas bubbles are surrounded by a film of water containing a foam stabilizing substances (polymers or bentonite).

The first two (OBM and WBM) are by far the most commonly used.

2.2 The Drilling Fluid Circulating System

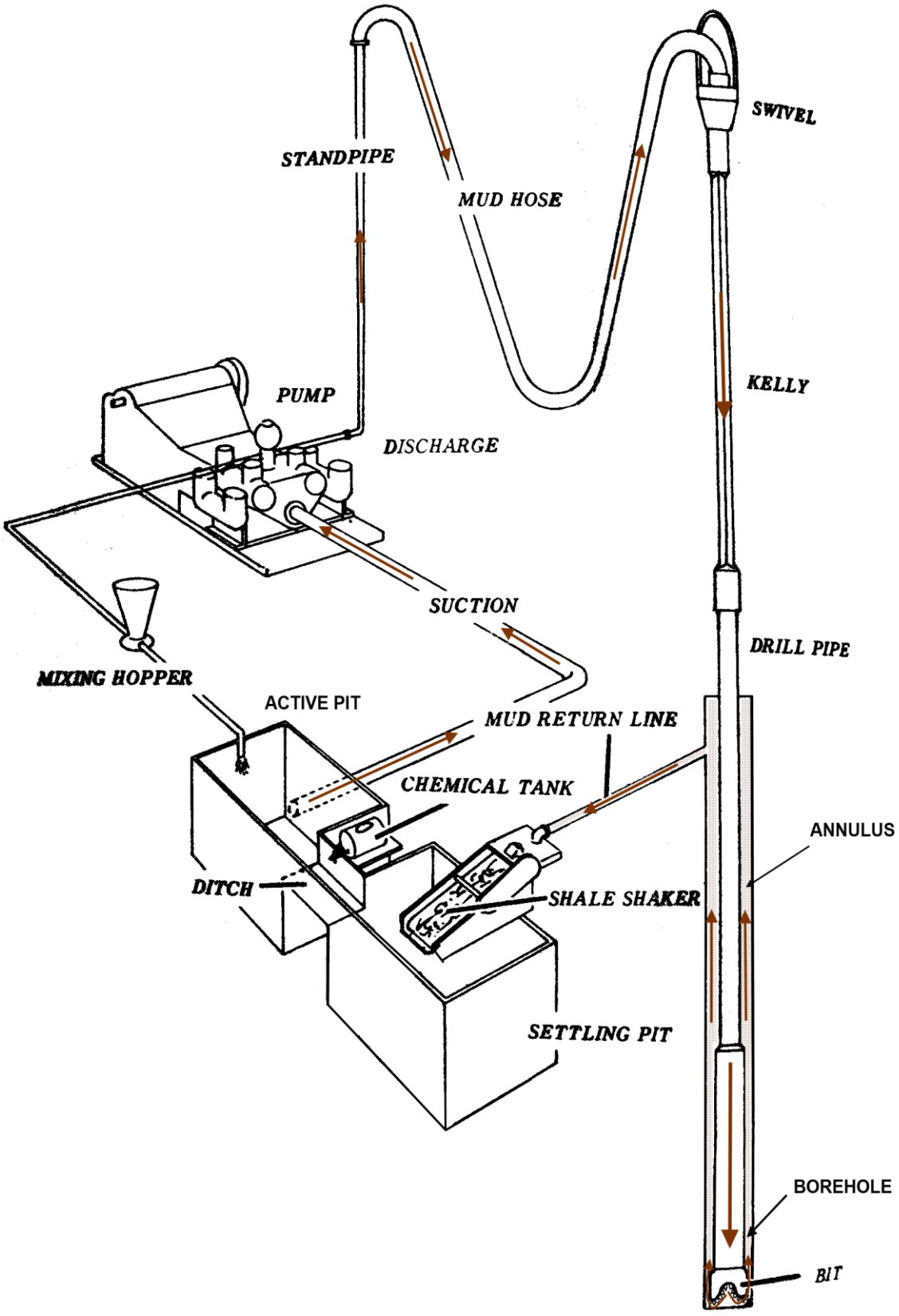

Figure 2.1 – The drilling fluid circulation system [2].

The heart of the drilling fluid circulation system is the big mud pumps that provide a pressure that drives the drilling fluid down the drill sting and back up the annulus. There are normally two or more of these powerful pumps, each capable of providing a pressure of several hundred bars and volume rate of thousands of liters per minute [1, 2, 7].

Figure 2.1 displays a schematic of a typical mud circulating system. Drilling fluid is pumped from the active mud pit up through the standpipe and the mud hose then continue through the top drive mechanism and down the drill pipe and BHA to the drill bit. In the drill bit the mud is forced through narrow nozzles resulting in a high velocity jet (70 – 150 m/s) acting on the bottom hole, thereby assisting the removal of material excavated by the bit. The nozzles cause a significant pressure loss, more than half of the pressure provided by the surface mud pumps is lost after the mud passes the nozzles [2, 7]. The remaining pressure forces the drilling fluid, now loaded with cuttings, up the annulus between the drill string and the borehole wall. The volumetric flow rate is more or less constant in and out of the well, but the annular diameter (flow area) will vary throughout the borehole and thereby affect the flow velocity in the annulus. The drilling fluids ability to transport cuttings out of the borehole depends partly on the flow velocity and the viscosity and density of the drilling fluid. This will be more thoroughly discussed later on, but in short, the flow velocity in all parts of the annulus must be greater than the settling velocity of particles/cuttings in the mud in order to bring them to the surface [2].

During drilling, there is a continuous supply of formation matter to the drill fluid. When the drilling fluid returns to the surface it could be contaminated with:

- Inert formation material (Gravel, sand, silt, feldspar)
- Reactive formation material (clays, limestone, colloidal solids)
- Formation fluids (water with different salts, oil)
- Gas from the formation (CO_2, H_2S, hydrocarbon gases)
- Unset cement from previous sections

These will mix and interact with the initially formulated drilling fluids and could cause adverse changes in its density, rheology, filter cake and other drilling fluid properties. Practically this could mean a lower rate of penetration (ROP), reduced hole stability, consume more chemicals, increased bit wear, higher torque and drag and increased risk of stuck pipe (differential sticking) [6, 8].

Drilling fluids are expensive and constitute a considerable share of the total drilling cost, so in order to keep the cost to a minimum, one wants to reuse as much of the drilling fluids as possible. Prior to recirculating the drilling fluid has to be processed and treated to regain its properties.

To restore the desired mud properties, drilled cuttings and gas have to be separated out of the drilling fluid [2, 6]. The solid control system depends on several factors such as drill fluid system (oil-based or water-based), depth of well, circulation volume, expected formation, fluids testing facilities and availability of trained personnel [8]. However, the equipment and principles used in the continuous maintenance of drilling fluids is basically the same. The equipment is arranged in manner so that larger solids are removed before smaller ones.

The first step for removing the unwanted particles out of the returning drilling fluid are the *shale shakers*. Shale shaker is a general term for vibrating devices with sized screens that filter out the unwanted particles without removing excessive amounts of drilling fluid. They are considered the most important and easiest-to-use solids removal equipment [9]. After passing through the shakers, the fluid flow into compartmentalized tanks directly beneath the shakers, known as a sand trap or namely a settling pit. The fluid is not agitated, this allows particles to settle to the bottom of the tank. The outlet is located at the top of the tank farthest away from the inlet, thus giving the particles maximal settling time. The particles that passes through the shaker screens are normally so small they will not have sufficient time in the tank to settle, so the sand pits virtually have no effect if the shakers work properly [2, 6, 9]. When drilling in gas bearing formations, gas can be entrained in the drilling fluid. This can cause problem for further removal of unwanted particles and change the density and lifting capability of the mud in the borehole. Much of the dissolved gas will be excreted when the mud pass through the shale shaker screens, provided that the viscosity of the mud is not too high. The remaining gas has to be removed by special degassing equipment before the separation of the smallest particles can take place. Hydrocyclones and centrifuges are very sensitive towards gas and they will not function optimally if the mud contains gas. Hydrocyclones is a simple mechanical device without moving parts. Its purpose is to remove the particles too fine for the shale shaker and sand pit. The separation principle is utilization of centrifugal forces, which arises when the fluid flow is forced into narrowing diameter downwards in a cone, this increases the centrifugal forces on the fluid flow and pulls the largest and heaviest particles towards the cone wall. The size of the hydrocyclon determines the diameter of the separated particles. The last option in solid removal are centrifuges, the separation principle of these are also utilization of centrifugal forces to increase the settling velocity of particles. Centrifuges are normally just used on a minor part of the total drilling fluid volume [2, 6].

It is quite simple to formulate a mud with suitable properties; the challenge is to preserve these properties while drilling. Although the drilling fluids are design to handle the physical and the chemical interaction with the formation, will it consume of the additives in the drilling fluid and influence the mud properties. Changes in mud properties can happen very swiftly, so the mud has to be closely monitored and tested several times a day during drilling operations. It is the mud engineers' responsibility to test and treat the mud and ensure that it has the desired properties [1]. During drilling mud samples are taken directly from the flow line, after the unwanted particles has been separated out, and tested immediately. The tests provide a basis for the treatment required for the reuse of the drilling fluid. The standard tests for drilling fluids will be thoroughly described in section 2.6.

2.3 Functions of Drilling Fluids

In the modern industry, drilling fluids are used for a variety of purposes. Three primary functions have previously been identified for drilling fluids; these and several other functions will be discussed briefly in the following section. How well a drilling fluid performs its function is solely determined by its inherent properties, this will be discussed in a later chapter. Below is a summarized list of essential drilling fluid functions.

- Control formation pressure
- Remove cuttings from wellbore
- Seal permeable formations – fluid loss control
- Keep cuttings and weight material suspended during circulation interruptions
- Release sand and cuttings at surface
- Cool and lubricate the bit and drill string
- Maintain wellbore stability in uncased sections
- Provide buoyancy for drill string and casings
- Control corrosion
- Ensure adequate formation evaluation data
- Transmit hydraulic energy for BHA tools

2.3.1 Control formation pressure

The most safety critical function of the drilling fluids is to prevent formation fluids entering the borehole undesired during drilling operations. The fluid column inside the borehole is the primary well barrier during drilling operations and therefore subjected to strict regulations. In Table 2.1 are the NORSOK well barrier acceptance criteria for the fluid column listed.

Table 2.1 - NORSOKs well barrier acceptance criteria fluid column [10].

15 Well barrier elements acceptance tables

15.1 Table 1 – Fluid column

Features	Acceptance criteria	See
A. Description	This is the fluid in the well bore.	NORSOK D-001
B. Function	The purpose of the fluid column as a well barrier/WBE is to exert a hydrostatic pressure in the well bore that will prevent well influx/inflow (kick) of formation fluid.	
C. Design construction selection	1. The hydrostatic pressure shall at all times be equal to the estimated or measured pore/reservoir pressure, plus a defined safety margin (e.g. riser margin, trip margin). 2. Critical fluid properties and specifications shall be described prior to any operation. 3. The density shall be stable within specified tolerances under down hole conditions for a specified period of time when no circulation is performed. 4. The hydrostatic pressure should not exceed the formation fracture pressure in the open hole including a safety margin or as defined by the kick margin. 5. Changes in well bore pressure caused by tripping (surge and swab) and circulation of fluid (ECD) should be estimated and included in the above safety margins.	ISO 10416
D. Initial test and verification	1. Stable fluid level shall be verified. 2. Critical fluid properties, including density shall be within specifications.	
E. Use	1. It shall at all times be possible to maintain the fluid level in the well through circulation or by filling. 2. It shall be possible to adjust critical fluid properties to maintain or modify specifications. 3. Acceptable static and dynamic loss rates of fluid to the formation shall be pre-defined. 4. There should be sufficient fluid materials, including contingency materials available on the location to maintain the fluid well barrier with the minimum acceptable density.	
F. Monitoring	1. Fluid level in the well and active pits shall be monitored continuously. 2. Fluid return rate from the well shall be monitored continuously. 3. Flow checks should be performed upon indications of increased return rate, increased volume in surface pits, increased gas content, flow on connections or at specified regular intervals. The flow check should last for 10 min. HTHP: All flow checks should last 30 min. 4. Measurement of fluid density (in/out) during circulation shall be performed regularly. 5. Measurement of critical fluid properties shall be performed every 12 circulating hours and compared with specified properties. 6. Parameters required for killing of the well .	ISO 10414-1 ISO 10414-2
G. Failure modes	Non-fulfillment of the above mentioned requirements (shall) and the following: 1. Flow of formation fluids.	

In order to prevent influx of formation fluids; the mud column inside the wellbore has to provide a hydrostatic pressure greater than the surrounding formation pressure acting on the wellbore. The hydrostatic pressure exerted by the drilling fluid column is proportional with its height and the density of the fluid. Accordingly, the hydrostatic pressure exerted by the fluid column at a given depth, assuming an incompressible and homogenous fluid, is given by the following equation [*2*]:

$$\mathrm{P} = \rho * g * \mathrm{h} \tag{2.1}$$

P = pressure
ρ = the fluid density
g = the gravitational constant
h = the height of the fluid column

To accurately control the bottom hole pressure while drilling, one also has to account for the frictional pressure loss in annulus and drill string during circulation. The total annular pressure in the wellbore will then consists of two components; the hydrostatic pressure exerted by the fluid and a hydrodynamic pressure loss due to fluid circulation. The combined annular pressure gradient is commonly expressed in terms of equivalent circulating density (ECD).

$$\overline{\rho_{ECD}} = \rho + \frac{\Delta P_{FA}}{g * h} \tag{2.2}$$

$\overline{\rho_{ECD}}$ = equivalent circulation density gradient
ΔP_{FA} = the frictional pressure loss in the annulus.

There are different methods for calculating this factor, with various degrees of complexity and accuracy. Since most drilling fluids are non-Newtonian they rely on certain flow models to describe their flow characteristics, elaborated in section 2.4.2. None of these models is completely accurate and involves a great number of uncertain values, when it comes to describing the drilling fluid behavior when circulated in the well. The annular width varies greatly throughout the borehole, this greatly effects the total pressure loss in the annulus. For the most accurate calculations the pressure loss various sections of the annulus should be calculated separately according to their annular width. The total pressure loss, ΔP_{FA}, is the sum of all pressure losses in the annulus [1].

One should also beware of the effect that arises when running the drill pipe into, or out of, the well. When the running the pipe into the hole, the downwards movement of the pipe acts as a piston and causes a pressure surge in addition to the hydrostatic pressure. This can cause fracturing of the formation and subsequently lost circulation. When pulling pipe out of the well the opposite effect

occurs; the effective pressure inside the borehole is reduced and cause an influx of formation fluids. All these effect must be accounted for when deciding the overall mud density [2].

The bottom hole pressure (BHP) is the sum of; the annular hydrostatic pressure, the ECD component (including the annular pressure loss), applied back pressure (used in managed pressure drilling operations) and all additional effects that affect the BHP e.g. cuttings load, swab and surge, drill string rotation, down hole temperature and pressure.

To be enable precise control of the BHP with a fitted mud weight it is essential to know the formation type it is drilling through – the depth, temperature, lithology of the rock, geology and petrophysical properties [6].

Stresses acting on the borehole wall.

Rocks are a porous material, and consist of a rock matrix and a fluid. When these rocks are subjected to a force (e.g. an overburden mass), the force is partially taken up fluids inside the pores and the rock particles. This induces a pressure inside the rock, namely *pore pressure* [11].

The pore pressure, often referred to as formation pressure, is a central term in the oil and gas industry. The pore pressure is the pressure induced on any fluid or gas within pore space of the formation by the overburden mass. The pore pressure depends on depth, density of formation fluid and the geological properties of the formation. The pore pressure can range from *normal pressure* where the formation has a self-supporting structure, and pressure inside the pores only depend on the weight of overlaying pore fluids. To *abnormal pressure formations* where pore fluids are sealed inside the rock and has to bear the weight of some or all of the overlying sediments as well as the overlying fluids, causing a overpressure inside the rock [1]. Abnormalities in pore pressure poses an increased drilling risk and can cause serious well control incidents as fluid influx, kicks and blowout if the formation pressure is not accurately predicted. Improper pore pressure predictions can lead to erroneous mud weight design, which in turn can cause wellbore instability and severe well control issues [12].

Prediction of pore pressure is mainly based on three different aspects: Pre-drill pore pressure predictions, pore pressure predictions while drilling and post-well pore pressure analysis. Pre-drill pore pressure can be predicted with the aid of seismic data collected for the planned well location, and by the use of geological, well-logging and drilling data from offset wells. Real time pore pressure data can be provided by installing Logging While Drilling (LWD) and Measurements While Drilling

(MWD) tools in the BHA near the bit, and by mud-logging data. Post-well analysis considers all available data to build a pore pressure model that can be used for pre-drilling predictions for future wells in the same basin [12].

A too high mud weight can also cause severe drilling problems. If the pressure exerted by the mud column gets higher than the rock strength, the rock will yield and the formation will start to fracture (break). The fracture pressure gradient is defined as the pressure gradient that will cause facture of the formation [13]. If fractures are induced during drilling, drilling fluid will be lost into the cracks, and the volume flow up the annulus will decrease. The consequence of this may be reduced cuttings transport, lost circulation and loss of well control [14].

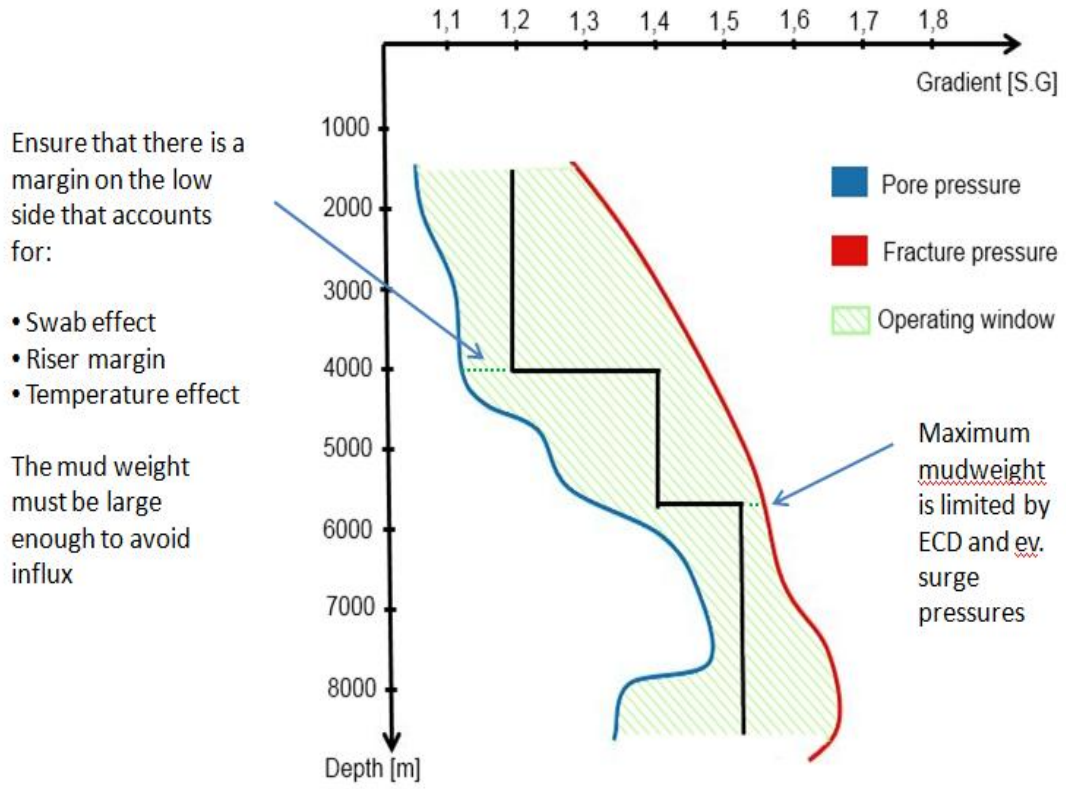

Figure 2.2 – The pore pressure gradient and fracture pressure gradient strongly influence the mud weight and casing program for the entire well.

The pore pressure and fracture pressure gradient graph are considered amongst the most important graphs in drilling. These curves strongly influence mud weight, number casing points and casing point depths for the entire well.

2.3.2 Remove cuttings from wellbore

Historically, the removal of cuttings from the borehole was the first purpose of the drilling fluids. As wellbore geometry and borehole lengths are constantly pushed towards the limits, this is more challenging and critical than ever.

An important function of drilling fluids is to remove and transport cuttings excavated by the bit from the bottom hole to the surface [2]. How efficient the circulating drilling fluid can transport cuttings depends on several factors: shape and size of the particles, wellbore size and inclination, drill fluid density and rheological properties, flow rate/annular velocity, drill pipe rotation and eccentricity [*9*, 15]. The practical use of these parameters in controlling the cuttings transport is however heavily dependent on their controllability in the field. In other words, one cannot rely on drill pipe eccentricity to control cuttings transportation. Studies done by *Rishi B. Adari et al.* indicates that drilling fluid rheology and flow rate are the two main parameters most favorable in order to control the cuttings transport [15].

For efficient removal of drilling cuttings it is essential that the drilling fluid remove the rock debris instantly after it's been excavated by the drill bit. If not instantly removed, the rock splinters will be grinded into smaller pieces that are harder to separate at the surface. The viscous properties and the density of the drilling fluid are decisive for this ability [2].

Drilled cuttings/rock particles are denser than most drilling fluids, so due to gravity, they fall through the fluid. In a static fluid column the particle will acquire a constant downwards velocity, known as *terminal settling velocity*. The settling velocity depends on density difference between particle and liquid, size and shape of particle and viscosity of the drilling fluid [1]. So in order to transport cuttings out of the wellbore the flow velocity in the annulus has to be greater than the settling velocity. The rate at which the rising fluid will carry the particles upwards is equal to the difference between the annular velocity and the slip velocity. The rheological properties strongly affect the lifting capability of the drilling fluid, and the density provides natural buoyancy to the cuttings. The buoyancy force on a particle is, in accordance with Archimedes' Principle, equal to the weight of the fluids displaced by the object. In other words, the buoyancy force on a particle is proportional to the density of the fluid in which it is submerged, hence a denser mud provides more uplift than a lighter one [2].

With increasing borehole lengths and horizontal displacements in extended reach wells, proper hole cleaning remains a major challenge. The behavior of cuttings in horizontal or highly deviated wells is

very different from that in near vertical wells, and requires a different set of methods for effective hole cleaning.

Insufficient hole cleaning can cause severe drilling problems like: stuck pipe, lost circulation, tight hole, high/fluctuating torque, excessive overpull on trips, excessive ECD, reduced ROP, and increased bit wear [1].

2.3.3 Seal permeable formations – fluid loss control

As previously mentioned the mud column inside the wellbore has to provide a hydrostatic pressure greater than the formation pressure, in order to prevent formation fluids from entering the borehole. Consequently, this overpressure inside the well will cause the drilling fluid to invade permeable formations. Suspended solids in the drilling fluid will attempts to flow into the formation with the liquid fraction, the solid particles are filtered out onto the borehole wall, thus forming a bridge that blocks the pores throats of the formation. In time, finer and finer particles fill the interstices between the larger particles, ultimately forming a filter cake. Once the filter cake is established, only liquid (filtrate) is able to penetrate it, the permeability of the filter cake now determines the flow rate into the formation. The drilling fluid should be designed to keep the cake permeability as low as possible in order to minimize the filtrate invasion to the formation and maintaining a thin filter cake. High permeability filter cakes will result in more solids flowing to and adding to the filter cake. Thick filter cakes will reduce the effective diameter of borehole and can cause various drilling problems, such as excessive torque when rotating pipe, excessive drag when pulling pipe out of well, high swab and surge pressures, and increased risk of differential sticking [1, 2, 9].

2.3.4 Keep cuttings and weight material suspended during circulation interruptions

During a drilling operation, the circulation of drilling fluids has to stop several times, for various reasons. The circulation may be interrupted for several consecutive hours. During this time it is important that the drilled cuttings and weight materials stay suspended in the drilling fluid, in order to prevent them from falling back on top of the bit and the BHA or packing off the annulus. This ability is determined by the drilling fluids thixotropic properties. This is the fluids ability form gel structure when agitations ceases. Ideally, the gel strength of the drilling fluids should be just high enough to keep cuttings and weight material suspended when circulation is stopped. Excessive gel strength is undesirable because it retards the separation of cuttings and entrained gas at the surface,

this will also increase the pressure required to restore the circulation. The gel must be revisable so that mud will return to a mobile state when the applied stress is greater than the strength of the gel structure [1, 2].

2.3.5 Release sand and cuttings at surface

In addition to properly clean the borehole and transport the cuttings to the surface, the drilling fluid must also allow efficient separation of drilled solids and entrained gas at the surface before the fluid is pumped back down hole. The drilling fluid must always have a viscosity sufficiently high to allow transportation of drilled cuttings out of the well and sufficient gel strength to keep cuttings and weight materials suspended during circulation interruptions. These requirements may complicate the separation process at the surface. For separation purposes the viscosity and gel strength should be as low as possible. In other words, a good mud is the best possible compromise of conflicting properties [1, 2].

2.3.6 Cool, clean and lubricate the bit and the drill string

When the drill bit presses and carves against the formation rock, and the drill pipe rotates against the borehole wall, as a result enormous amounts of friction and heat are generated. This can lead to overheating and failure of the drill bit, drill pipe and other equipment in the BHA. Circulation of cooler drilling fluid through the drill string and annulus removes much of the generated heat and reduces the friction between the borehole wall and drill collars/drill string. The drilling fluid absorbs much heat, this leads to a general increase in the fluid temperature, which in turn can have significant effect on the rheological properties and other drilling fluid parameters [1, 2].

2.3.7 Maintain wellbore stability in uncased sections

Maintaining a stabile borehole is one of the major challenges in drilling operations. If the wellbore cannot be kept open, a casing must be set in order to secure the hole. For the uncased sections, the drilling fluid has to preserve the wellbore stability. This can basically be divided into two main categories; one *mechanical* borehole stability primarily related to the mud density and movement of fluids, and secondly the *physicochemica*l interactions between the formation and the drilling fluid. Wellbore instability may be caused physicochemical effects alone or mechanical effects alone, or by a combination of both factors [1, 2].

2.4 Properties of Drilling Fluids

The fundamental properties of drilling fluids are; fluid density, fluid viscosity and gel strength.

The successful completion of an oil well and its cost depend, to a considerable extent, on the properties of the drilling fluid. The cost of the drilling fluid itself is relatively small, but the choice of the right drilling fluid program and maintenance of fluid properties while drilling profoundly influence the total well costs. Wrong mud design, or failure in maintaining required mud properties can lead to several costly complications and dangerous well control issues, which could put personnel and environment at risk [1].

Just as the nature of the drilling fluid properties affects the efficiency of the hole cleaning during drilling, the drilled solids also plays an integral role in the in the properties of drilling fluids, which in turn affects the performance of the solids control equipment. Figure 2.3 illustrates the intricate and very complex dynamic relationship among the drilled solids, drilling fluid and solids control equipment. Any change made to any one of these will affect the other two, and those in turn affect all three, and so on. In order to optimize the drilling operation, it is important to understand how the drilled solids will affect the bulk mud properties, in particular; rheology, hole cleaning, filtration, rate of penetration, and density [9].

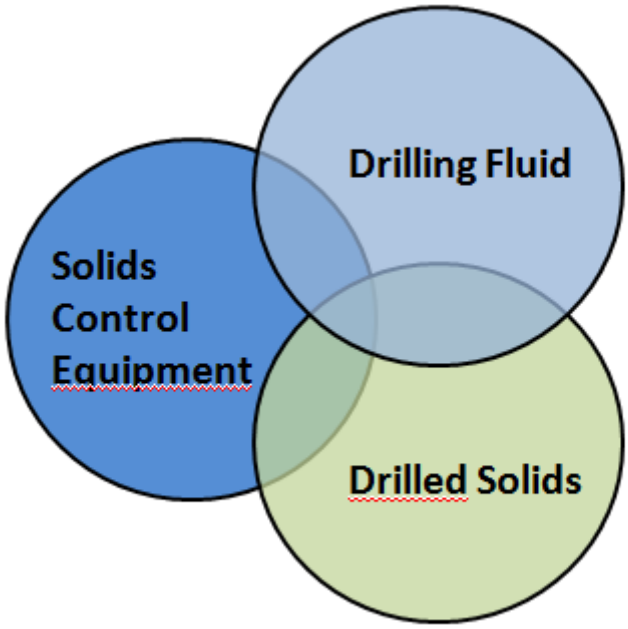

Figure 2.3 - Mud processing circle [9].

2.4.1 Fluid Density – mud weight

Density is defined as mass per volume unit. In the petroleum industry it is commonly expressed in pounds per gallon (lb/gal), pounds per cubic foot (lb/ft3), kilograms per cubic meter (kg/m3) or compared to the weight of an equal volume of water, as specific gravity (SG) [*1*]. The fundamental concepts of *equivalent static density (ESD)* and *equivalent circulation density (ECD)* will be revisited in this section.

As mentioned in section 2.3.1, the density of the drilling fluid determines the hydrostatic pressure imposed in wellbore and is the basis for controlling formation pressure during drilling operations. A too high mud weight can lead to formation fracturing and lost circulation. A too low mud weight can result in well cleaning problems, wellbore instability, and influx of formation fluids. Careful and constant monitoring of the density of the drilling fluid, both going in the hole and coming out, is therefore of the utmost importance [16]. The success or failure of the drilling operation is nearly always tied to the mud weight program [17].

Equivalent Static Density (ESD)

The equivalent static density is an expression of hydrostatic pressure exerted by the drilling fluid column, including the effect of entrained solids and fluids, which may increase or decrease the effective hydrostatic pressure in the annulus. The fluid densities are pressure and temperature dependent.

The hydrostatic pressure exerted by the fluid has previously been defined in section 2.3.1, by equation (1.1). This will give a reasonable approximation of the bottom hole drilling fluid density given that the temperature and pressure in the mud is relatively low. However, neglecting the effect of temperature and pressure on fluid density for *high pressure and high temperature* (HPHT) wells, can yield bottom hole pressures estimations that are erroneous by hundreds of psi. There have been conducted several studies to document the severity of this effect, Figure 2.4 shows the findings obtained by *W.C. McMordie et al* [18].

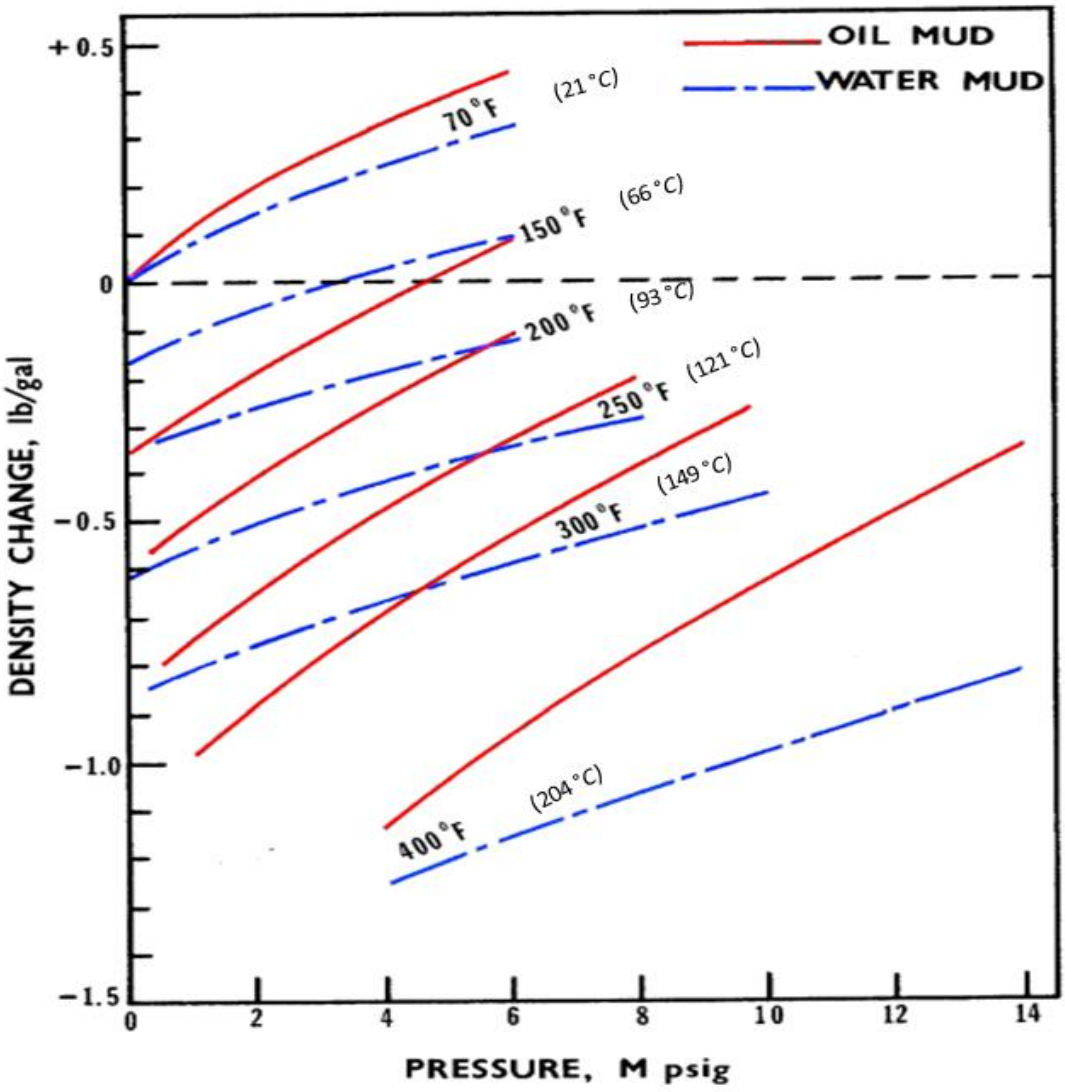

Figure 2.4 – A comparison of the effect of temperature and pressure on ESD a typical WBM and OBM [18].

When estimating the equivalent static density of drilling fluids in well, one must account for the effects of temperature and the pressure conditions present in the well. The down hole density of drilling fluids can be accurately predicted with the use of a compositional model, which takes the volumetric behavior of the liquid and solid phases in the drilling fluid [19].

Equivalent Circulating Density (ECD)

It is normal to distinguish between equivalent densities for circulating and non-circulating wells. Due to fluid circulation dynamics the bottom hole pressure will be greater, for circulation wells, than the hydrostatic pressure exerted by the mud. The major additional contribution comes from the frictional pressure loss in the annulus. The equivalent circulating density has previously been defined

by equation (1.2) in section 2.3.1. The density at the point of interest equals the total hydrostatic head and the frictional pressure loss in the annulus due to fluid flow.

Down hole temperature and pressure will affect the drilling fluid density, hence the down hole densities are often quite different from those measured at surface conditions. These effects must be accounted for when determining the mud weight program. Accurate prediction of ECD is always important in drilling operations, especially when drilling in formations where there is a narrow window between the pore pressure and the fracture pressure gradient. The generalized effect of temperature is to increase the density of drilling fluids at low temperatures and decrease the density at higher temperatures. Increased pressure on a fluid will compress the fluid and decrease the volume, therefore increase its density. The magnitude of temperature and pressure effects on drilling fluids will depend on the drilling fluid composition [19].

The drilling fluid density will also be affected by the suspended drilled cuttings, generally cuttings have a higher density than the drilling fluid itself and will therefore add to the effective fluid density and thus increase the ECD. For simple vertical wells the cuttings contribution to the fluid density could be estimated based on cutting feed rate, drilling fluid flow rate and cutting transport ratio. There is no simple method of calculating the cuttings contribution to the ECD for deviated wells [19].

2.4.2 Fluid Rheology

Rheology is the study of the deformation and flow of matter [2, 19]. The study of flow behavior of suspension in pipes and other conduits are of particular interest. This subject is of great technical importance for several industrial products, for example; paint, cosmetics, plastic, cement, the food industry and the petroleum industry. In conjunction with drilling fluids are the effect small-dispersed particles (colloidal particles) on the fluid viscosity of particularly interest [2].

Accurate prediction of down hole rheology is very important for several reasons. The rheological properties of the drilling fluid have great influence on the pressure losses in the system while circulating, and thereby have direct impact on the ECD. The fluid rheology is essential for the following determinations [19]:

- Calculation of frictional pressure losses in pipes and annuli
- Determination of ECD under down hole conditions
- Determination of prevailing flow regime in pipes and annuli
- Estimation of hole cleaning efficiency
- Estimation of swab and surge pressures
- Hydraulic optimization for improved drilling efficiency

With better prediction of down hole rheology, standard hydraulic calculations such as circulation pressure losses needed in ECD predictions, surge and swab pressure, and hole cleaning efficiencies can be determined more accurately. Obviously, more accurate predictions will lead to safer and more efficient practices, and can be of critical value for drilling operations where the margin between pore pressure and fracture pressure are narrow [19].

Influence of temperature and pressure on the rheology of drilling fluids.

As with the prediction of down hole fluid density, the effects of temperature and pressure on drilling fluid rheology must be taken into account in order to achieve maximum accuracy in the hydraulic calculations.

The rheological properties of drilling fluids under down hole conditions can be significantly different from those measured at ambient pressure and temperatures. The elevated temperatures and pressures down hole can influence the rheological properties of drilling fluids in various ways. Even quite moderate temperature changes can have significant and largely unpredictable influence on

rheological properties [1]. Consequently, hydraulic calculations made solely from surface rheology measurements, can be of limited usefulness [19].

Flow Regime

The primary interest is the relationship between flow pressure and flow rate and their effect on flow characteristics of the fluid. In single phase flow there are two fundamentally different relationships [1]:

1) The *laminar flow regime* prevails at low flow velocities. The fluid particles flow in orderly smooth lines parallel to the walls of the flow channels. The pressure-velocity relationship is a function of the inherent viscous properties of the fluid, where the pressure required to move the fluid increases with increasing flow velocity and viscosity [1, 19].

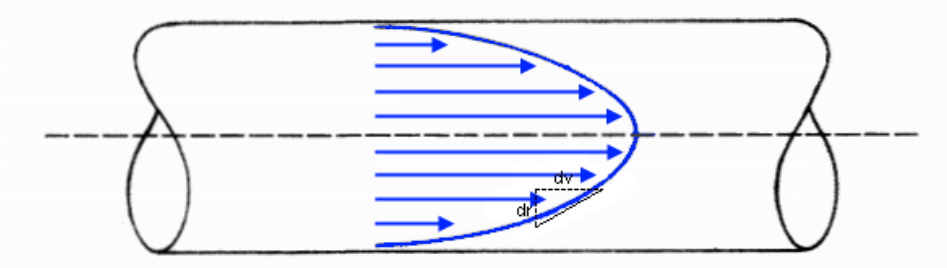

Figure 2.5 - Velocity profile for laminar flow of a Newtonian fluid in a round pipe, where the longer arrows indicate higher velocity.

2) The *turbulent flow regime* prevails at high flow velocities. The particles in the fluid moves in a chaotic manner, and the flow are primarily governed by the inertial properties of the fluid in motion. For fully developed turbulent flow, the pressure required to move the fluid, will increase linearly with density and approximately with the square of the flow velocity, hence more pump pressure is required to move the fluid in turbulent flow than in laminar flow [19].

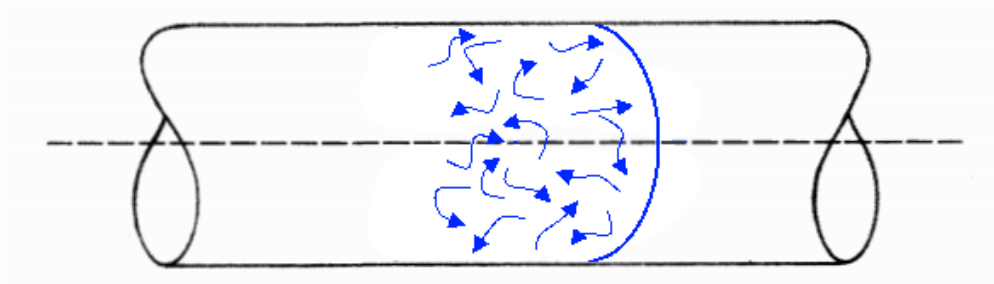

Figure 2.6 - Velocity profile for turbulent flow.

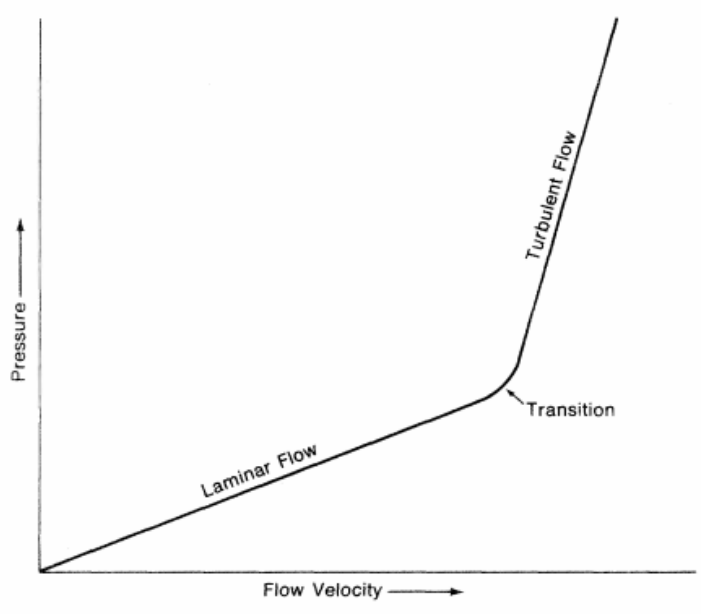

Figure 2.7 - Schematic diagram of laminar and turbulent flow regime [1].

Figure 2.7 shows how the pressure increases more rapidly when flow goes from laminar to turbulent. In the transition zone between laminar and turbulent flow the fluid movement has both laminar and turbulent characteristics.

Drilling fluid hydraulics pertains to both laminar and turbulent flow regimes, depending on fluid velocity, size and geometry of the flow channel, fluid density, and viscosity. The flow regime determines the behavior of a fluid, and thereby has a direct effect on that fluids ability to perform its basic functions. For that reason it is important to know the prevailing flow regime in order to evaluate the performance of a fluid [19].

Fluid characterization

Viscosity is a measure of the resistance for a substance to flow or deform. The conventional unit for viscosity is dyne-s/cm, which is termed Poise (P). In the oil industry, the term centiPoise (cP) is most commonly used, which is 1/100 of Poise [19].

Fluids can be classified by their rheological behavior. There are two general types; fluids whose viscosity remains constant with changing shear rate are known as *Newtonian fluids* and fluids there viscosity varies with changing shear known as *non-Newtonian fluids* [1, 19]. Fluids can exhibit different types of non-Newtonian behavior. For example:

- *Dilatant behavior*; fluids whose viscosity increases with increasing shear rate. Drilling fluids rarely exhibits in this behavior.
- *Pseudoplastic behavior;* shear thinning fluids that starts flowing as soon as any shearing force or pressure, regardless of how slight, is applied.
- *Viscoplastic behavior*; shear thinning fluids that do not start flowing until a given shear stress is applied.
- *Thixotropic behavior;* the effective viscosity of the fluid is both time and shear dependant.

For fluids that do not contain any particles larger than molecules (e.g., water, salt solutions, light oil) there is a direct proportional relationship between resistance and deforming force, in other words, these fluids have a constant viscosity and are commonly called *Newtonian fluids*. Since the viscosity of a Newtonian fluid is independent of shear rate, the viscosity determined at a single shear rate can be used for hydraulic calculations involving flow at any other share rate [1, 2].

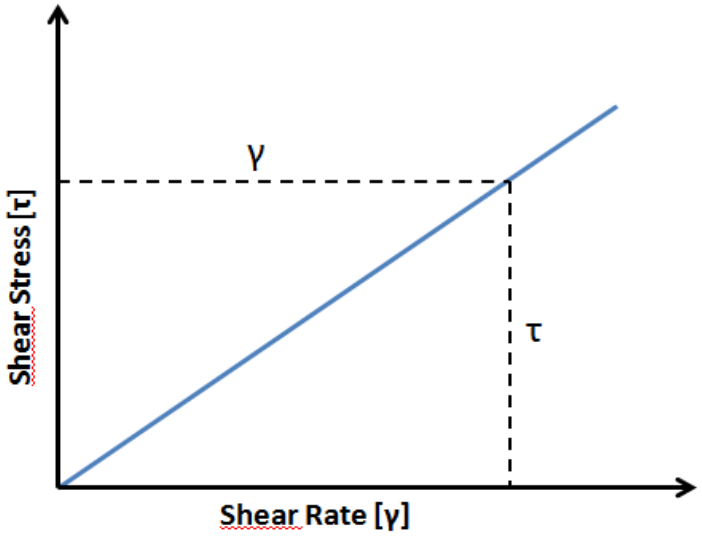

Figure 2.8 - Rheogram for a Newtonian fluid.

Viscosity for a Newtonian fluid is defined by the ratio of shear stress (τ) to shear rate (γ)[2]:

$$\mu = \tau/\gamma \qquad (2.3)$$

In short, the *shear stress* is the force per unit area required to sustain flow. *Shear rate* is, as illustrated in Figure 2.5, the rate at which the fluid velocity changes (dv) with respect to the distance (dr) from the wall.

2.5 Rheological Models

Suspensions such as drilling muds that contains particles larger than molecules (in significant quantities) do not conform to Newton's law, and are thus classified by the general title of *non-Newtonian fluids*. The *shear stress* versus *shear rate* relationship for these fluids depends on composition of the fluid. *Rheological models* are needed to describe their behavior. The most commonly used models in the petroleum industry are the *Bingham Plastic*, *Power law* and *Herschel Bulkley*. Most drilling fluids do not conform exactly to any of these models, but by using one or more of them they are sufficient accurate for practical use [*composition and properties*].

2.5.1 The Bingham Plastic Model

For a Bingham plastic fluid model, the relationship between shear rate (γ) and shear stress (τ), is defined as a function of the two parameters YP (yield point) and PV (plastic viscosity)[2]:

$$\tau = YP + PV * \gamma \tag{2.4}$$

The Bingham Plastic model is the simplest of the three rheological models discussed in this section. Drilling fluids with a high solid content behave approximately in accordance with the Bingham model for plastic flow. The fluid is characterized by two properties; a finite stress that must be applied to initiate flow, and at stresses greater than this value flow will be Newtonian. As illustrated in Figure 2.9; YP is the shear stress required to initiate flow, and PV is defined as the additional shear stress required give a shear rate increase of one unit.

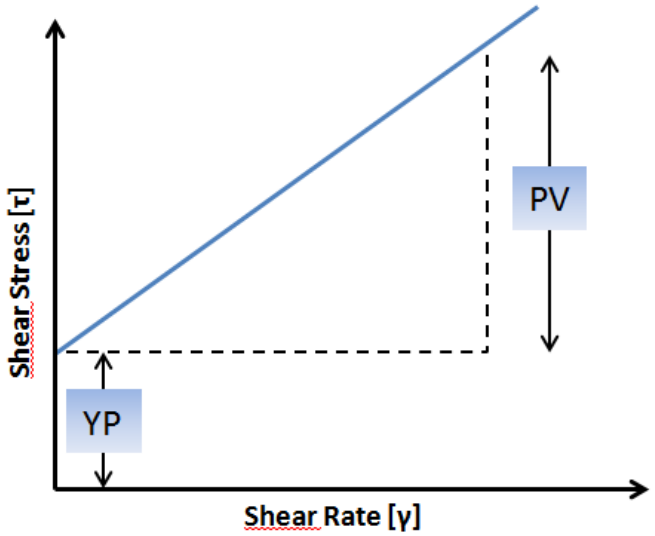

Figure 2.9 - Rheogram for a typical Bingham plastic fluid.

The total ability for a Bingham plastic fluid to resist flow could be expressed by an apparent viscosity or effective viscosity (μ_e) for a given shear stress [2].

$$\mu_e = \frac{\tau}{\gamma} = PV + \frac{YP}{\gamma} \tag{2.5}$$

Most commonly used drilling fluids are *shear thinning*, meaning their viscosity decreases with increasing shear [drilling fluid processing]. Figure 2.10 shows how the effective viscosity decreases (from $\mu_{e\,1}$ to $\mu_{e\,2}$) with increasing shear rate (from γ_1 to γ_2), and is consequently only valid for hydraulic calculations at the sear rate at which it was measured.

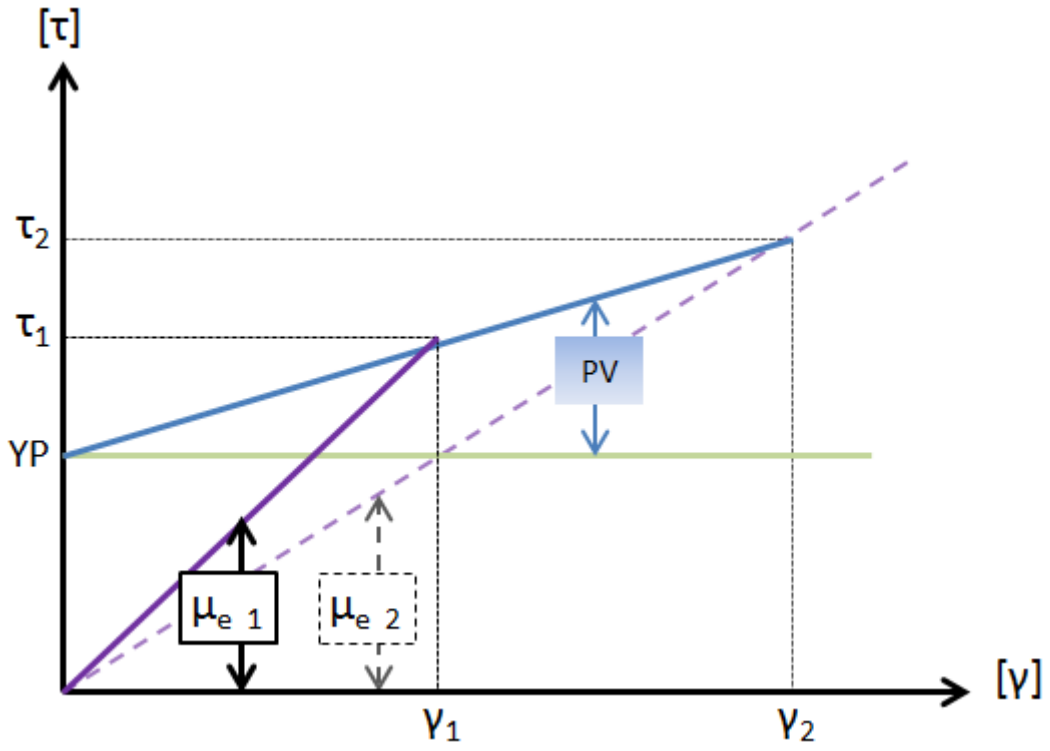

Figure 2.10 - Effective viscosity [μ_e] for a Bingham plastic fluid. The effective viscosity will decrease when shear rate increased.

Shear thinning is normally a desirable property for drilling fluids, because the viscosity will then be relatively low at high shear rates prevailing in drill pipe and thereby reduce the pump pressure, and will be relatively high at low shear rates prevailing in annulus thus increase the transporting ability of cuttings. The ratio between yield point and plastic viscosity, known as the YP/PV ratio, is a measure of shear thinning: where higher ratio equals higher shear thinning [1, 2].

The Bingham plastic model is the standard viscosity model used throughout the petroleum industry [9, 20]. The parameters YP and PV are frequently used, and are good indicators to determine the condition of the drilling fluid, especially concerning maintenance of the drilling fluid. PV gives an

indication of the concentration, shape, and size of the solids in the mud, while the YP is associated with the tendency of components to build shear resistance. The YP will also give a good indication for the cutting transporting ability in the annulus. A higher YP provides greater lifting capability in the annulus [2, 9]. Because the Bingham model only describes the flow characteristics well in a certain shear rate range, between 600 and 300 RPM (corresponding 1022 to 511 sec^{-1}), it is not suited for fluid characterization in relation to pressure loss calculations. For lower shear rates other models are needed in order to better describe drilling fluids [2].

2.5.2 The Power Law Model

The Power Law model uses a non-linear expression to describe the relationship between shear stress and shear rate, which corresponds better with the actual behavior of most drilling fluids. This gives a better and more accurate model for describing drilling fluids at low shear rates. For this model the relationship between shear rate and shear stress is defined:

$$\tau = K_p * \gamma^{n_p} \tag{2.6}$$

K_p = Power law fluid consistency index
n_p = Power law flow behavior index.

From equation (2.6) we see that K_p equals the shear stress (τ) when the shear rate (γ) is 1, for any value of n_p, and is therefore strongly related to the fluid viscosity at low shear rates and corresponds, to some extent, to the yield value. Hence, an increase in K_p will indicate an increase in the lifting capability of cuttings. The n_p parameter indicates the deviation from Newtonian behavior. In other words, it is a measure of how the viscosity changes with shear rate. A lower value of n_p implies a higher degree of shear thinning [1, 2, 9].

The Power Law model may be used to describe the behavior of three flow models by inserting the proper value of n_p:

1) Pseudo plastic fluids, $n_p < 1$, effective viscosity decreases with shear rate
2) Newtonian, $n_p = 1$, viscosity is constant for any shear rate
3) Dilatant, $n_p > 1$, effective viscosity increases with shear rate

2.5.3 Herschel-Bulkley model

The Herschel-Bulkley model, often called modified power law, alleviate the problem of underestimation of viscosity at very low share rates. It is used to describe the flow of pseudoplastic drilling fluids, which require a yield stress to initiate flow. The Herschel-Bulkley model is in many ways a hybrid between the Bingham and the Power law models, it is the Power Law model with yield stress [*9*].

The three parameters, $\tau_{0,}$ K and n, characterize this relationship:

$$\tau = \tau_0 + K * \gamma^n \qquad (2.7)$$

τ_0 = fluid yield stress,
K = consistency factor for the Herschel-Bulkley model
n = flow behavior index for the Herschel-Bulkley model

The parameter K can functionally be considered the equivalent to the plastic viscosity (PV) term in the Bingham model, but will almost always have a significantly different numerical value. The τ_0 can be considered the equivalent to the Bingham yield point (YP), but will nearly always have a lower numerical value [19].

This model is widely used because it [19]:

a) Describes the flow behavior of most drilling fluids
b) Includes a yield stress value, which is important for several hydraulic issues
c) Includes the Bingham plastic model and power law as special cases.

The API (American Petroleum Institute) recommend using the Herschel-Bulkley model, this model consistently provides good simulations of measured rheological data for both water based and non-aqueous drilling fluids. It has for this reason become the *de facto* rheological model for engineering calculations in the petroleum industry [19].

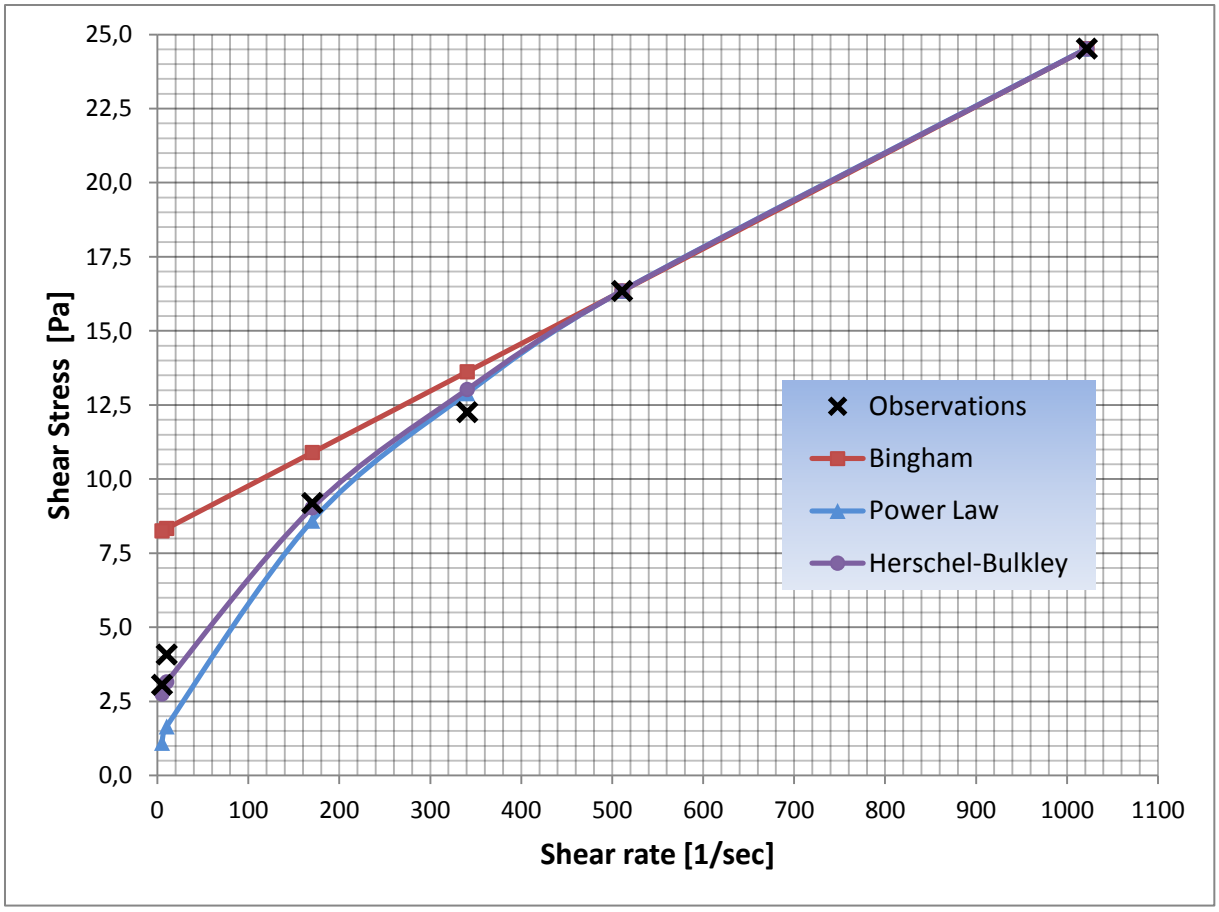

Figure 2.11 - Graphical comparison of measured rheological values compared to expected values for the Bingham, Power Law model and The Herschel-Bulkley model [Table presented in appendix E.1].

Figure 2.11 shows a graphical comparison of the three most commonly used rheological models in the industry to characterize the behavior of drilling fluids. The accuracy of the Power Law model compared to the Bingham model is illustrated in Figure 2.11, and it is clear that the Power Law provides the curve that best fit the measured values for the lower shear rates. However, the Power law model tends to underestimate the viscosity for very low shear rates. Most drilling muds exhibits a behavior intermediate between the Bingham plastic model and the Power law model, thus the Herschel-Bulkley model provides the best fit curve, as observed. The Herschel-Bulkley model is often considered the unifying model, because it fits Bingham plastic fluids, Power law fluids and everything else in between. The equations used to make this plot are presented in section 2.6.2.

A plot of shear stress versus shear rate is a great way to determine which rheological model best describes the behavior of the drilling fluid. The shape of the curve and the gel strength is used to determine the best model. Generally if the gel strength is high and near the yield point the Bingham plastic model provide the best fit, while muds without gel is better described by the other two or by the Newtonian model.

2.6 Conventional testing of drilling fluid

Due to the undisputable importance of drilling fluids during drilling operations, it is quite obvious that the drilling fluid should be closely monitored and kept within the designed parameters at all times. The drilling fluid is nearly always directly or indirectly related to most drilling problems. If the drilling fluid does not properly perform the functions listed in section 2.3 the result may be catastrophic and extremely costly for the operators.

The complexity of drilling fluid behavior has been outlined throughout this chapter. From their mixture of interacting components and continuous interaction with the formation fluids and solids, to their properties which change markedly with; pressure, temperature, time, shear rate and shear history. This makes it a virtually impossible task to devise tests that will accurately describe down hole drilling fluid behavior [1].

Maintaining the desired mud properties while drilling is the job of the *mud engineer.* There are normally two mud engineers present at the drilling rig facility at all times, working in opposite 12hr shifts. As the required maintenance depends on the mud type and the formation in which is being drilled, there are never a definitive procedure for maintaining the drilling fluids desired properties. However, the API has presented a recommended practice for drilling fluid testing, and most companies have adapted to this practice. These tests are devised to aid the mud engineer in determining whether the drilling fluid is performing its functions properly. Mud testing should be performed at regular intervals, in order to identify and correct potential drilling problems at an early stage and thereby prevent more serious situations [3, 20]. During circulation the mud density should be tested every fifteenth minute. Usually the deckhands (roughnecks) will assist the mud engineer with density measurements. The full set of API standard testes is normally conducted two times per 12 hour shift. This is the common practice of the two major drilling fluid service companies Bariod (Halliburton) and M-I SWACO (Schlumberger) [21, 22].

Another problem is that well site testing must be performed quickly and with quite simple apparatus. Consequently the standard field tests, which have been accepted by the industry, are quick and practical, yet they only approximately reflect down hole behavior of drilling fluids. It is important to be aware of the limitations these test have in terms of describing the actual fluid properties and behavior down hole. Nevertheless, by correlating test results with previous experience they suffice and give a valuable indication of fluid behavior down hole [1].

This section will present a brief description of the standard mud tests and equipment used in the routine mud check at a drilling facility and their purpose. The standard tests can basically be separated in two main groups:

1) Physical properties of the drilling fluids includes: density of drilling fluid, rheological parameters, solids content and filtration properties.
2) Chemical properties of the drilling fluid includes: Mud pH and alkalinity, Chloride and Calcium concentration, cation exchange capacity, corrosivity and electrical conductivity.

This thesis will solely focus on the physical parameters, with emphasis on evaluation of density and rheology.

2.6.1 Determination of drilling fluid density (mud weight)

Fluid density, or mud weight, is the most important parameter for the drilling fluid due to its key role in well control. Additionally the density has a direct or indirect influence on several other important functions of the drilling fluid, which has been outlined throughout section 2.3. How the drilling fluid density is affected by the bottom hole conditions is discussed in section 2.4.1.

According to API [3] any density measuring instrument having an accuracy of ± 0,01 g/cm^3, ± 10 kg/m^3, ± 0,1 lb/gal or ± 0,5 lb/ft^3 can be used.

The default apparatus for measuring drilling fluid density in the industry is the *mud balance* or the *pressurized mud balance,* shown in Figure 2.12. Their basic design is the same; a drilling fluid holding cup at one end of the beam, which is balanced by a fixed counterweight at the other end and a sliding weight rider free to move along a gradual scale. A level-bubble is mounted on the beam to allow accurate balancing. The pressurized mud balance in addition allows pressurizing the mud sample in the holding cup. By pressurizing the mud sample in the holding cup the effect of any entrained gas is minimized to a negligible volume, thus providing a more representative density [3].

The instrument should be calibrated frequently with fresh water, which should give a scale reading of 1,00 g/cm^2 or 1000 kg/m^3 at 21 °C (70 °F) [3].

The operating procedures for these mud balance scales are highly intuitive; nevertheless the API recommended procedure for operating the pressurized mud balance will be presented in *appendix A.1.*

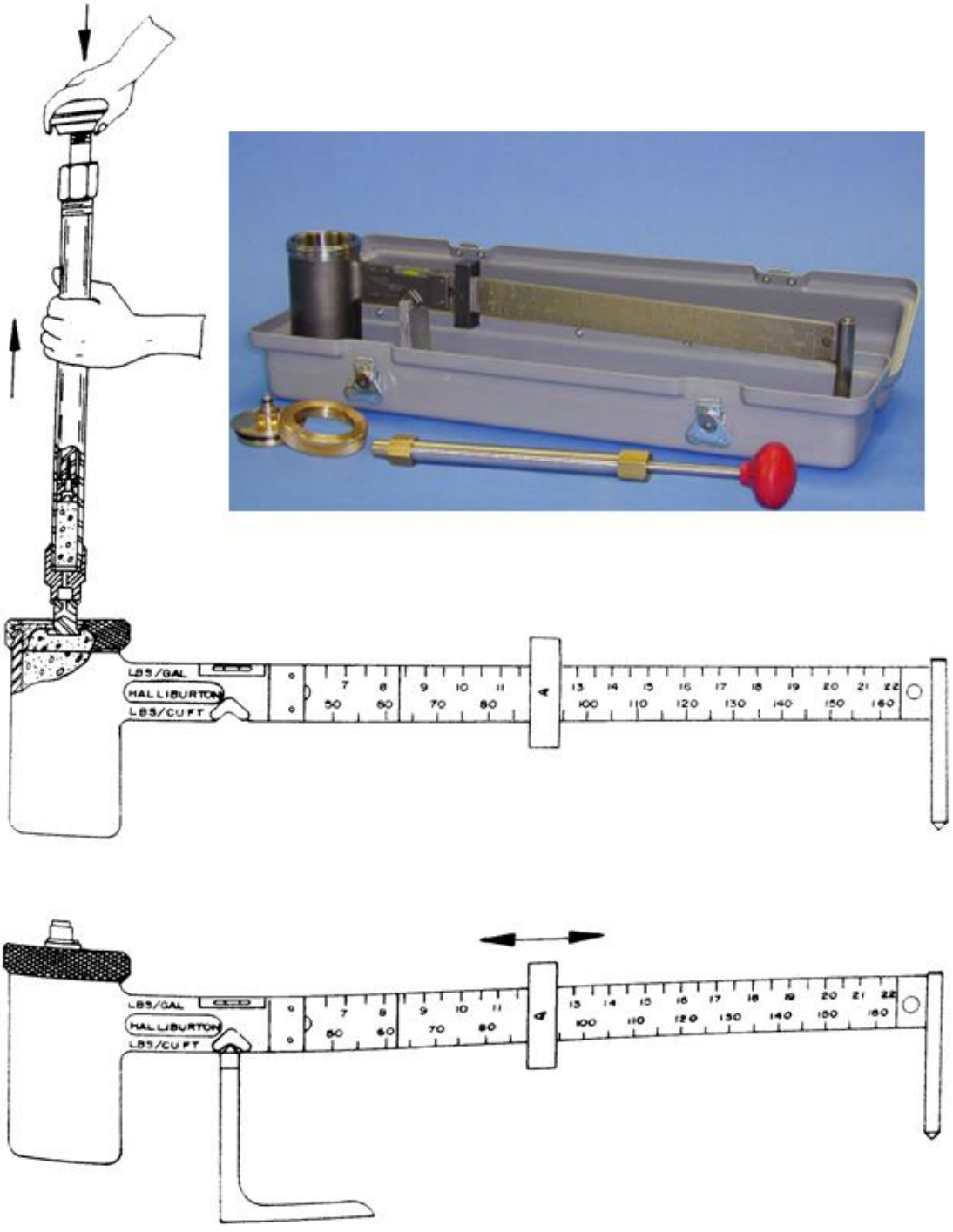

Figure 2.12 – Halliburton's pressurized mud balance.

2.6.2 Determination of viscosity and gel strength

The rheological models presented in section 2.5 provide a mathematical description of the viscous forces present in a fluid. This is required for the calculation of frictional pressure loss in a circulating well.

The Marsh funnel

The March funnel is a widely used as a field measuring instrument, mainly due to its pure simplistic concept. It consists of a conical funnel that holds 1500 cm^3 of fluid, with an orifice at the bottom of the cone. The test essentially consist of filling the funnel with a fluid sample and then measure the time it takes the fluid to fill to the 946 ml (one quart) mark of the measuring cup.

The measurement is normally referred to as the *funnel viscosity* and is usually recorded in seconds per quart (946 ml). The Marsh funnel is design so that the outflow time of 946 ml fresh water at 21°C ± 2°C is 26 s ± 0,5 s.

The Marsh funnel viscosity is a simple and rapid test that is made routinely on all liquid drilling fluid systems. Since the funnel viscosity is a one point measurement, it will not provide any information as to why the viscosity may be high or low, so test results is less meaningful for non-Newtonian fluids. It is, however, an excellent indicator of changes in mud properties and is therefore useful in regards to alert to changes in mud properties or condition. If a change in funnel viscosity is observed, the mud should be tested by a *rotational viscometer*. Detailed API operating procedure and required specifications for the Marsh funnel is included in *appendix A.2*.

The Rotational Viscometer

For routine viscosity measurements the mud engineer mostly uses a two speed concentric cylinder viscometer, such as the *Fann VG 35 viscometer* shown in Figure 2.13. This instrument enables simple calculation of the Bingham parameters (PV, YP and μ_e), the Power law parameters (n_p and K_p) and the Herschel-Bulkley parameters (τ_0, n and K). Additionally it provides a mean of measuring the gel strength of drilling fluids. The gel strength is a measurement of the required shear strength to break the internal tension of a static thixotropic fluid.

Figure 2.13 - Fann VG 35 Viscometer "Standard of the Industry".

A rotational viscometer can provide more meaningful rheological characteristics of drilling fluids than the Marsh funnel. To determine the parameters, yield point and the plastic viscosity, which describes the behavior of a non-Newtonian fluid, it is required have at least two viscosity measurements for two known shear rates. A rotational viscometer can measure the relation between shear rate and shear stress.

There are a number of different types of rotational viscometers suitable for use with drilling fluids on the marked, but in general their all built by the same principle as illustrated in Figure 2.14. The rotor sleeve and the bob are submerged in a mud sample, so the fluid fills the annular space between the rotor sleeve and the bob. Then the rotor sleeve is driven at a constant rotational velocity, there are six standard velocities; 600, 300, 200, 100, 6, 3 RPM. This way the mud is sheared at a constant rate between the bob and the rotor sleeve. The viscous drag exerted by the fluid transfers a torque onto the bob. The torsion spring restrains the movement of the bob until the force is sufficient and the bob starts rotating. A dial attached to the bob indicates the displacement of the bob in degrees. The dimensions of the bob, rotor sleeve and torsion spring are designed so that shear stress in the unit of lb/100 ft^2 is directly obtained from the dial reading [2]. The API recommended operating procedure and apparatus specifications is included in *appendix A.3*.

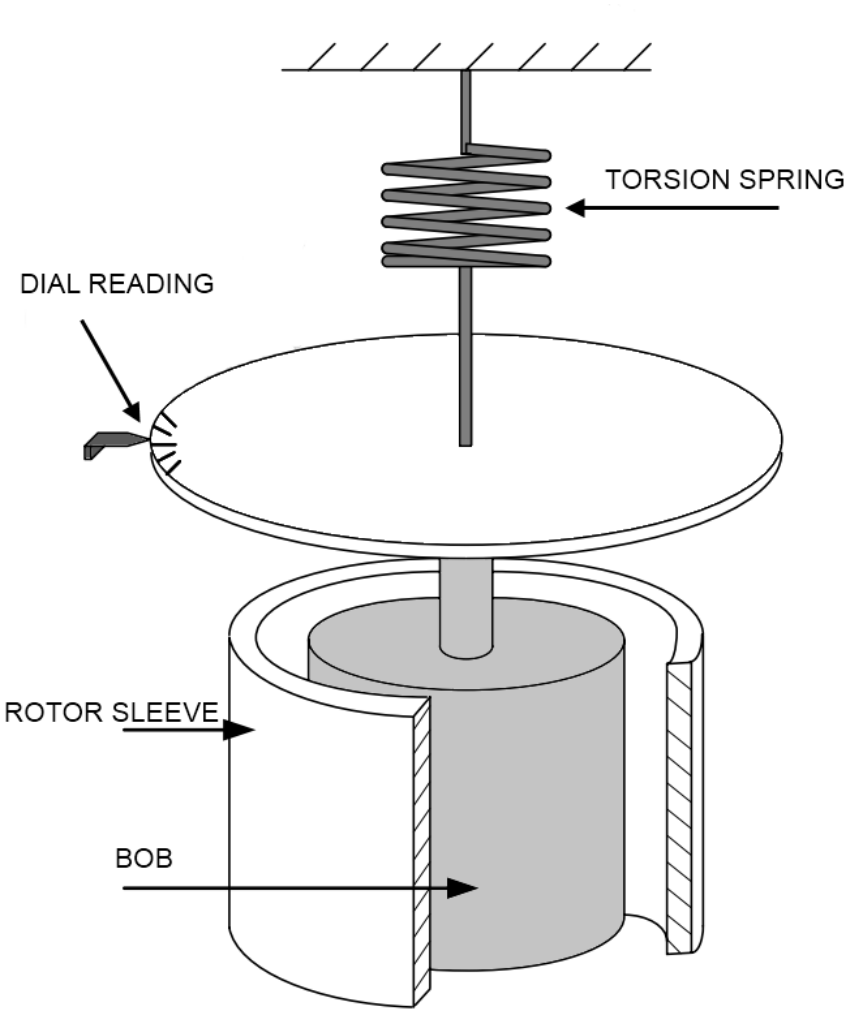

Figure 2.14 - Schematic drawing of the basic components in a concentric cylinder viscometer [19].

Equations for calculating the Bingham plastic parameters [2, 20]

The Bingham plastic model has previously been defined by *equation 2.4:*

$$\tau = YP + PV * \gamma$$

The Bingham plastic flow parameters, which are plastic viscosity (PV) and yield point (YP), can easily be calculated from the recorded shear stress values obtained with the rotating viscometer.

The plastic viscosity*, PV* (in the unit of centipoises), is normally computed by:

$$PV = \theta_{600} - \theta_{300} \tag{2.8}$$

where;

θ_{600} = Dial reading when viscometer operating at 600 RPM [$lb_f/100\ ft^2$]
θ_{300} = Dial reading when viscometer operating at 300 RPM [$lb_f/100\ ft^2$]

The yield point*, YP* (in the unit of $lb_f/100\ ft^2$), is normally computed by:

$$YP = \theta_{300} - PV \tag{2.9}$$

Equations for calculating the power law parameters [2, 20]

The power law model has previously been defined by *equation 2.6 :*

$$\tau = K_p * \gamma^{n_p}$$

The power law model uses one set of viscometer dial readings to calculate the flow parameters, which are the flow index (n_p) and the consistency index (K_p).

The flow index, n_p (dimensionless), can be calculated from:

$$n_p = \frac{\log \theta_{600} - \log \theta_{300}}{\log 1022 - \log 511} \tag{2.10}$$

where;

θ_{600} = Dial reading when viscometer operating at 600 RPM [$lb_f/100\ ft^2$]
θ_{300} = Dial reading when viscometer operating at 300 RPM [$lb_f/100\ ft^2$]

The consistency index, K_p (in the unit of $lb_f/100\ ft^2\ s$), is normally computed by:

$$K_p = \frac{\theta_{600}}{1022^{n_p}} \tag{2.11}$$

Equations for calculating the Herschel-Bulkley parameters [2, 20]

The Herschel-Bulkley model has previously been defined by *equation 2.7:*

$$\tau = \tau_0 + K * \gamma^n$$

The Herschel-Bulkley model requires two sets of viscometer readings to calculate the three parameters (τ_0, *K* and *n*).

The fluid yield stress, τ_0 (in the unit $lb_f/100\ ft^2$), commonly known as the low shear rate yield point, can be approximated by the following equation:

$$\tau_0 = 2\theta_3 - \theta_6 \tag{2.12}$$

where;

θ_6 = Dial reading when viscometer operating at 6 RPM
θ_3 = Dial reading when viscometer operating at 3 RPM

The flow index, n (dimensionless), can be calculated from:

$$n = 3.32 \log\left(\frac{\theta_{600} - \tau_0}{\theta_{300} - \tau_0}\right) \tag{2.13}$$

where;

θ_{600} = Dial reading when viscometer operating at 600 RPM
θ_{300} = Dial reading when viscometer operating at 300 RPM

The consistency index, K (in the unit of $lb_f/100\ ft^2\ s$), can be calculated from:

$$K = \frac{(\theta_{300} - \tau_0)}{511^n} \tag{2.14}$$

2.7 Frictional Pressure Loss Calculations

During circulation of drilling fluids, there is a pressure loss due to friction between the drilling fluid flow and the wall of the conducting channel (drill pipe and/or annulus). Frictional pressure loss is a function of several factors [19]:

- Flow rate
- Wellbore geometry and drill string configuration
- Fluid rheological behavior (Newtonian vs non-Newtonian)
- Flow regime (laminar, transitional or turbulent flow)
- Fluid properties (density and viscosity)

Pressures in the circulating system can be defined by fundamental relationship between initial pump pressure and the frictional pressure losses in the well. The actual pump pressure, P_P, is equal to the sum of frictional pressure losses, surface back pressure, and the difference in hydrostatic pressure between drills string and annulus [19]. The mathematical expression for this is given by the equation:

$$P_P = \Delta P_{SP} + \Delta P_{DP} + \Delta P_{DC} + \Delta P_N + \Delta P_{ADC} + \Delta P_{ADP} + \Delta P_{BP} + P_{HA} - P_{HDP} \qquad (2.15)$$

where;

P_P = Pump pressure
P_{BP} = Surface back pressure
P_{HA} = Annular hydrostatic pressure
P_{HDP} = Drill pipe hydrostatic pressure
ΔP_{SP} = Pressure loss in surface equipment (stand pipe, mud hose, swivel and kelly)
ΔP_{DP} = Pressure loss inside the drill pipe
ΔP_{DC} = Pressure loss inside the drill collars/bottom hole assembly
ΔP_N = Pressure loss across the bit nozzles
ΔP_{ADC} = Pressure loss in annulus around the drill collars/bottom hole assembly
ΔP_{ADP} = Pressure loss in annulus around the drill pipe

The bottom hole pressure (BHP) is the sum of; the annular hydrostatic mud weight, $P_{HA,}$ the ECD component (including annular pressure losses, ΔP_{FA}), and applied surface back pressure, P_{BP}. And can be expressed by the following mathematical expression:

$$BHP = \Delta P_{FA} + P_{HA} + P_{BP} \qquad (2.16)$$

Figure 2.15 shows a simple sketch of where in the circulation system the pressure losses occur, and includes example values which illustrates where in the well the pressure losses normally are most significant.

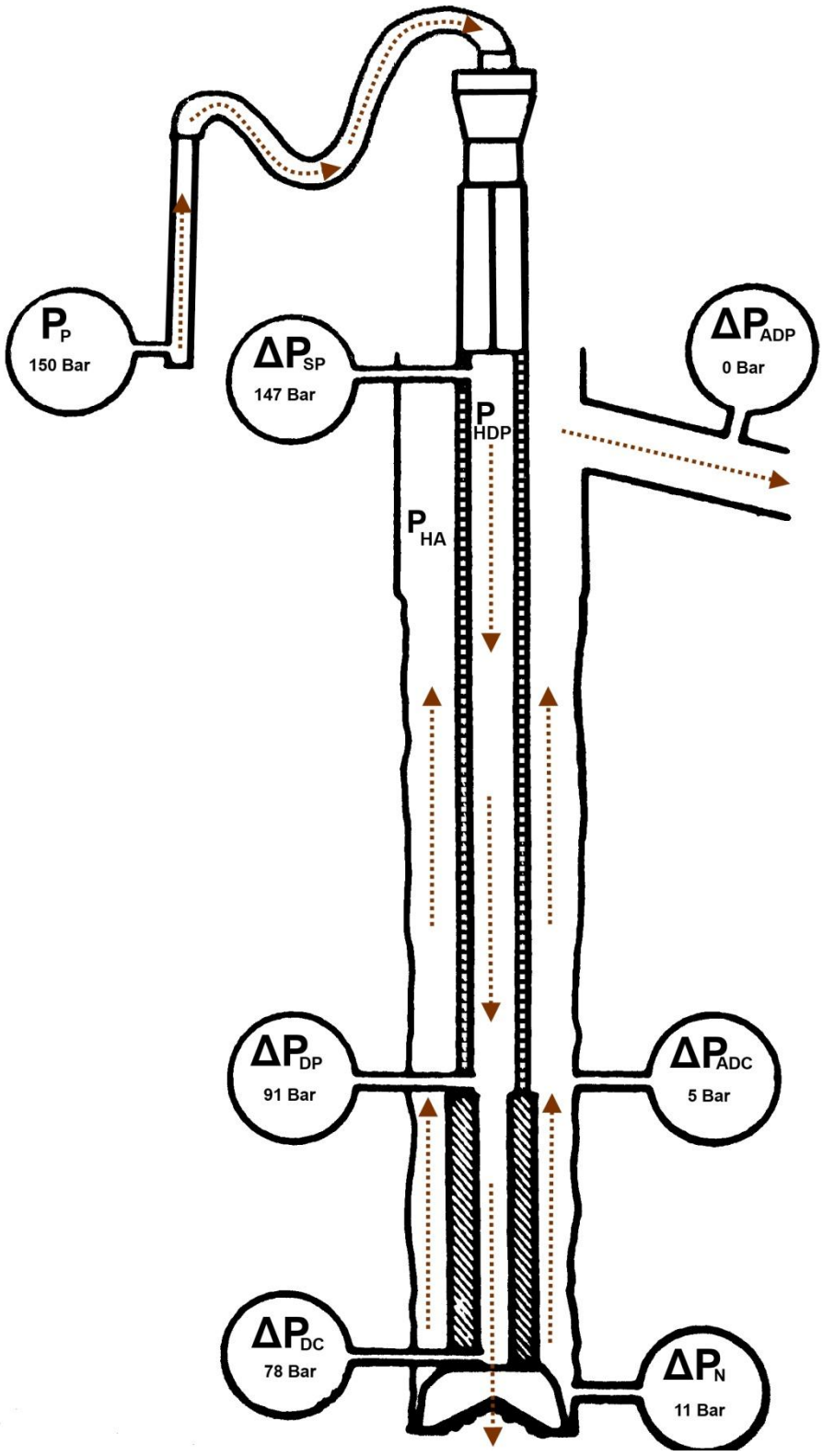

Figure 2.15 - Example of circulation pressures, for a typical well without any surface back pressure and uniform mud density throughout the well [2].

Frictional Pressure Loss

The most accurate method to calculate the ECD is to subdivide the drill string and annulus into shorter segments with respect to flow areas [2, 19]. The associated pressure loss for each segment is then directly proportional to its length, the fluid density, the fluid velocity squared and inversely proportional the conduct diameter and could be described by the mathematical expression [23]:

$$\Delta P_{FA} = \frac{2 * f_f * \rho * V^2}{D} * \Delta L \qquad (2.17a)$$

If the Darcy type friction factor is applied[23]:

$$\Delta P_{FA} = \frac{f_d * \rho * V^2}{2 * D} * \Delta L \qquad (2.17b)$$

ΔP_{FA} = Frictional pressure loss
f_f = Friction factor (Fanning type)
f_d = Friction factor (Darcy type)
ρ = Fluid density
V = Fluid velocity
D = Conduct diameter
ΔL = Conduct length

Fluid velocity

The average fluid velocity is inversely proportional to the cross sectional area of the respective fluid conduct channel.

Average fluid velocity, V_{DP}, in circular pipe flow:

$$V_{DP} = \frac{Q}{A} = \frac{4 * Q}{\pi * D^2} \qquad (2.18)$$

Average fluid velocity, V_A, in concentric annular flow:

$$V_{\mathrm{A}} = \frac{Q}{A} = \frac{4 * Q}{\pi * \left(D_2^2 - D_1^2\right)} \qquad (2.19)$$

Q = Flow rate
A = Flow area
D_1 = Inner wall of conduction channel (e.g. the OD of the drill pipe, drill collars, BHA)
D_2 = Outer wall of conduction channel (e.g. bore hole diameter or casing ID)

Flow Regime

The discrimination between laminar and turbulent flow plays a decisive role for the frictional pressure drop [23].

The Reynolds number*, Re*, which gives a measurement of the ratio of inertial forces to viscous forces. When consistent units are chosen, this ratio is dimensionless, and for pipe flow defined by [23, 24]:

$$Re = \frac{D*V*\rho}{\mu} \qquad (2.20)$$

D = Diameter of the flow channel
V = Fluid flow velocity
ρ = Fluid density
μ = Fluid Viscosity

It has been found experimentally that the change from laminar to turbulent flow always occurs at approximately the same Reynolds number. For flow of a Newtonian fluid in pipe the flow is considered laminar if the Reynolds number is less than 2000, transitional from 2000 to 3000, and turbulent for Reynolds numbers greater than 3000 [23, 24].

Fluid properties alone can cause dramatic difference in the Reynolds number and consequently the flow pattern. For fluids of variable viscosity, such as non-Newtonian fluids, and for flow in non-circular ducts, such as annular flow, special considerations must be made. This will be described later in this section.

Friction factors

Two different friction factors definitions are in common use in the literature:

- The Fanning friction factor
- The Darcy/Moody friction factor

The Darcy friction factor is 4 times the value of the fanning type, this will obviously influence the pressure loss calculations severely, and therefore one should always be specific to which factor that is employed. There is apparently no real consensus for when to use which friction factor, this varies from text to text. And they are frequently used interchangeably which may lead to very inconsistent calculations and poor comparability of results. Over the years there has been made numerous approximations of both friction factors, especially in relation to describing turbulent flow [1, 20].

The fanning friction factor for *laminar flow* is related to the Reynolds number by the following equation [20, 23]:

$$f_f = \frac{16}{Re} \quad [\mathrm{Re} < 2000] \tag{2.21}$$

f_f = friction factor (Fanning type) [dimensionless]

The roughness of pipe wall does not influence laminar flow behavior, so this relationship is the same for all grades of pipe [1].

The fanning friction factor for fully developed *turbulent flow* is described by an empirical correlation presented by Colebrook [20]:

$$\frac{1}{\sqrt{f}} = -4 * \log\left(0{,}269\frac{\epsilon}{D} + \frac{1{,}255}{Re*\sqrt{f}}\right) \quad [\mathrm{Re} > 3000] \tag{2.22a}$$

ϵ = absolute roughness in pipe
D = pipe diameter

This equation requires an iterative solution since the friction factor, f, appears both inside and outside the log term.

The friction factor is a function of the Reynolds number, Re, and a term called *relative roughness of pipe,* ϵ/D, which represents the pipe wall irregularities. Selection of an appropriate absolute roughness can in many cases be quite difficult, so a smooth pipe condition (ϵ/D = 0) is often applied for engineering calculations, and is considered sufficiently accurate since the Reynolds number seldom exceeds 100 000 for viscous drilling fluids, and the relative roughness of most well bore geometries is less than 0,0004. For smooth pipes the Colebrook equation (2.22a) is reduced to [20]:

$$\frac{1}{\sqrt{f}} = 4 * \log\left(Re * \sqrt{f}\right) - 0{,}395 \quad [\mathrm{Re} > 3000] \tag{2.22b}$$

Haaland (1983) developed a practical explicit formula (non-iterative) for the Darcy friction factor [23]:

$$\frac{1}{\sqrt{f}} \approx -1{,}8 * \log\left(\left(\frac{\varepsilon}{3{,}7D}\right)^{1{,}11} + \frac{6{,}9}{Re}\right) \quad [\mathrm{Re} > 3000] \tag{2.22c}$$

Once the friction factor has been determined the frictional pressure loss can easily calculated from equation 2.17.

Flow of non-Newtonian fluids

The fanning friction factor and the Reynolds number are used to determine the pressure losses associated with turbulent flow behavior of non-Newtonian fluids, provided that suitable flow parameters are applied. This is mainly concerned with applying the most representative viscosity for use in the calculation of the Reynolds number. As previously explained, the viscosity of non-Newtonian fluids varies with the shear rate. In section 2.4.2 the rheological properties of drilling fluids were discussed and three different rheological models were presented in section 2.5. When the best fit rheological model is decided, the flow regime can be determined by calculating the Reynolds number.

Since the experiments performed in this study, only involves Newtonian fluids, the equations required for determining pressure losses in non-Newtonian fluid are not really of any practical value. Nevertheless, I chose to present them in the form of a compact table just to illustrate how the rheological parameters obtained through conventional testing can be used to determine the pressure loss for typical non-Newtonian drilling fluids. For practical reasons the will all equations in the table will be adapted to practical field units to minimize the number of unit conversions. Note that this is only *one way* of obtaining the pressure losses for non-Newtonian drilling fluids, there are several others of varying degree of accuracy and complexity.

Table 2.2 - Nomenclature and practical input units for equations presented in Table 2.3 and Table 2.4

Symbol	Description	Input unit
D	Diameter	in
f	Friction factor	Dimensionless
He	Hedstrom number	Dimensionless
K	Consistency index	cP
n	Flow behavior index	Dimensionless
PV	Plastic viscosity	cP
Q	Flow rate	gal/min
Re	Reynolds number	Dimensionless
Re_c	Critical Reynolds number	Dimensionless
v	Average flow velocity	ft/s
YP	Yield point	$lb_f/100\ ft^2$
ΔL	Length	ft
ΔP_f	Frictional pressure loss	psi
Θ_{600}	Dial reading of rotational viscometer at 600 RPM	$lb_f/100\ ft^2$
Θ_{300}	Dial reading of rotational viscometer at 300 RPM	$lb_f/100\ ft^2$
μ_e	Apparent viscosity	cP
ρ	Fluid density	lb_m/gal

Table 2.3 - Equations for determining frictional pressure loss for non-Newtonian fluids [20]

		Bingham Plastic Model	Power-Law Model
Mean velocity	Pipe	$v = \frac{Q}{2{,}448\ D^2}$	$v = \frac{Q}{2{,}448\ D^2}$
	Annulus	$v = \frac{Q}{2{,}448(D_2{}^2 - D_1{}^2)}$	$v = \frac{Q}{2{,}448(D_2{}^2 - D_1{}^2)}$
Flow behavior Parameters		$PV = \theta_{600} - \theta_{300}$ $YP = \theta_{300} - PV$	$n = \frac{\log\theta_{600} - \log\theta_{300}}{\log 1022 - \log 511}$ $K = \frac{\theta_{600}}{1022^n}$
Apparent viscosity	Pipe	$\mu_e = PV + \frac{6{,}66\ YP * D}{v}$	$\mu_e = \frac{K * D^{(1-n)}}{96\ v^{(1-n)}} * \left(\frac{3 + \frac{1}{n}}{0{,}0416}\right)^n$
	Annulus	$\mu_e = PV + \frac{5\ YP * (D_2 - D_1)}{v}$	$\mu_e = \frac{K * (D_2 - D_1)^{(1-n)}}{144\ v^{(1-n)}} * \left(\frac{2 + \frac{1}{n}}{0{,}0208}\right)^n$
Turbulence Criteria	Pipe	$Re = \frac{928\ \rho * v * D}{\mu_e}$ *Critical Reynolds number:* $He = \frac{37100 * \rho * YP * D^2}{PV^2}$ Re_c = from Figure 2.16	$Re = \frac{89100\ \rho * v^{(2-n)}}{K} * \left(\frac{0{,}0416 * D}{3 + \frac{1}{n}}\right)^n$ *Critical Reynolds number:* Re_c = from Figure 2.17
	Annulus	$Re = \frac{757\ \rho * v * (D_2 - D_1)}{\mu_e}$ *Critical Reynolds number:* $He = \frac{24700 * \rho * YP * (D_2 - D_1)^2}{PV^2}$ Re_c = from Figure 2.16	$Re = \frac{109100\ \rho * v^{(2-n)}}{K} * \left(\frac{0{,}0208 * (D_2 - D_1)}{2 + \frac{1}{n}}\right)^n$ *Critical Reynolds number:* Re_c = from Figure 2.17
Friction factor (smooth pipe)		$\frac{1}{\sqrt{f}} = 4\ log(Re * \sqrt{f}) - 0{,}395$ Colebrook (fanning type)	$\frac{1}{\sqrt{f}} = \frac{4}{n^{0{,}75}} * \log\left(Re * f^{\left(1-\frac{n}{2}\right)}\right) - \frac{0{,}395}{n^{1{,}2}}$ Dodge-Metzner correlation (fanning type)

Table 2.4 - cont. Equations for determining frictional pressure loss for non-Newtonian fluids [20]

			Bingham Plastic Model	Power-Law Model
Frictional pressure loss	Laminar flow	Pipe	$\Delta P_f = \left(\frac{PV * v}{1500\ D^2} + \frac{YP}{225\ D}\right)\Delta L$	$\Delta P_f = \left(\frac{K * v^n * \left(\frac{3+1/n}{0{,}0416}\right)^n}{144\ 000\ {D_2}^{(1+n)}}\right)\Delta L$
		Annulus	$\Delta P_f = \left(\frac{PV * v}{1000\ (D_2 - D_1)} + \frac{YP}{200\ (D_2 - D_1)}\right)\Delta L$	$\Delta P_f = \left(\frac{K * v^n * \left(\frac{2+1/n}{0{,}0208}\right)^n}{144\ 000\ (D_2 - D_1)^{(1+n)}}\right)\Delta L$
	Turbulent flow	Pipe	$\Delta P_f = \left(\frac{f * \rho * v^2}{25{,}8\ D}\right)\Delta L$	$\Delta P_f = \left(\frac{f * \rho * v^2}{25{,}8\ (D_2 - D_1)}\right)\Delta L$
		Annulus	$\Delta P_f = \left(\frac{f * \rho * v^2}{21{,}1\ D}\right)\Delta L$	$\Delta P_f = \left(\frac{f * \rho * v^2}{21{,}1\ (D_2 - D_1)}\right)\Delta L$

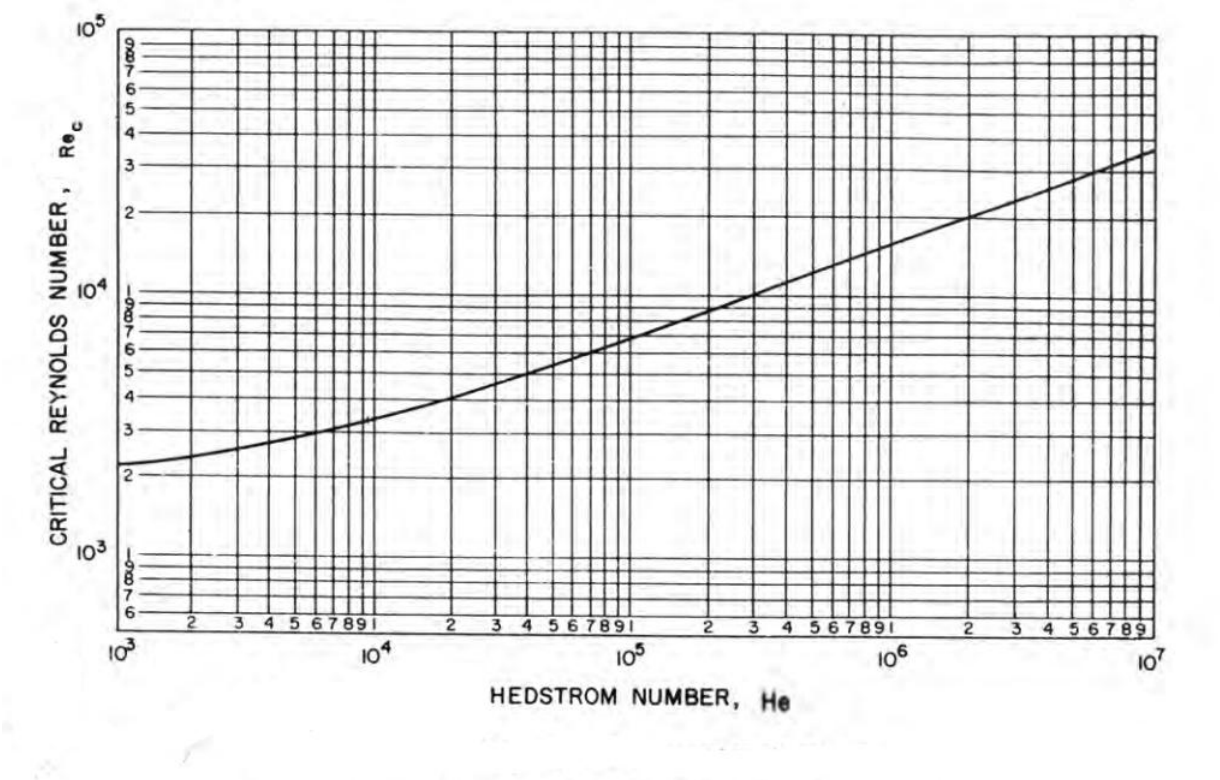

Figure 2.16 - Chart for obtaining Critical Reynolds number for Bingham plastic fluids [20]

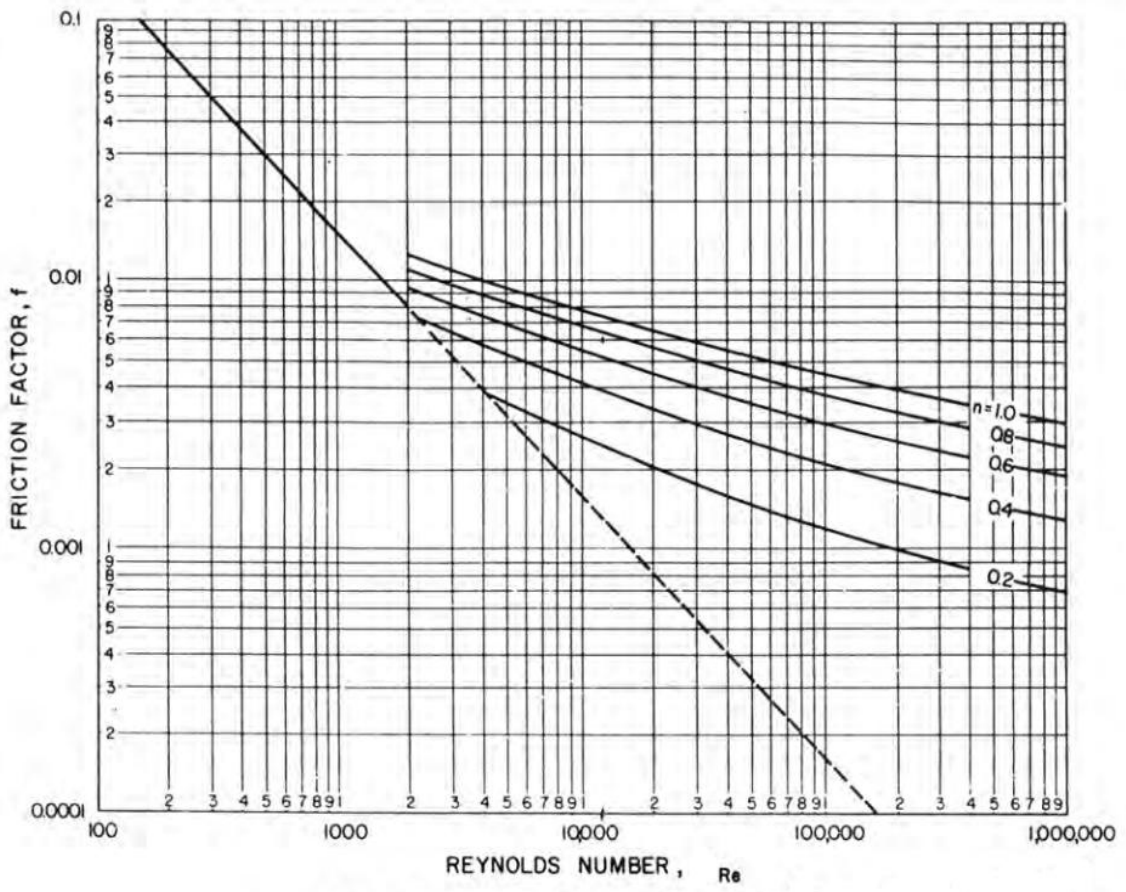

Figure 2.17 - Chart for obtaining friction factors for Power Law fluids [20]

3 AUTOMATIC EVALUATION OF DRILLING FLUID PROPERTIES

The scope of this chapter is to present a method that enables accurate, automatic and continuously monitoring of drilling fluid parameters. It contains a brief introduction of the Instrumented Standpipe concept. The main part of this chapter is concerned with the implementation of the Instrumented Standpipe concept to an existing flow loop and validation of its performance through experimental testing.

3.1 Instrumented Standpipe concept

The principle behind the Instrumented Stand pipe is to use accurate pressure sensors along the circulation path from the mud pumps to the connection to the drill string. This allows for *direct measurements* of the frictional pressure drop. Thus providing a much simpler and faster way of

performing hydraulic calculations, as opposed to the current methods, explained in chapter two, which involves manual viscometer testing and simplified rheological to estimate down hole fluid behavior.

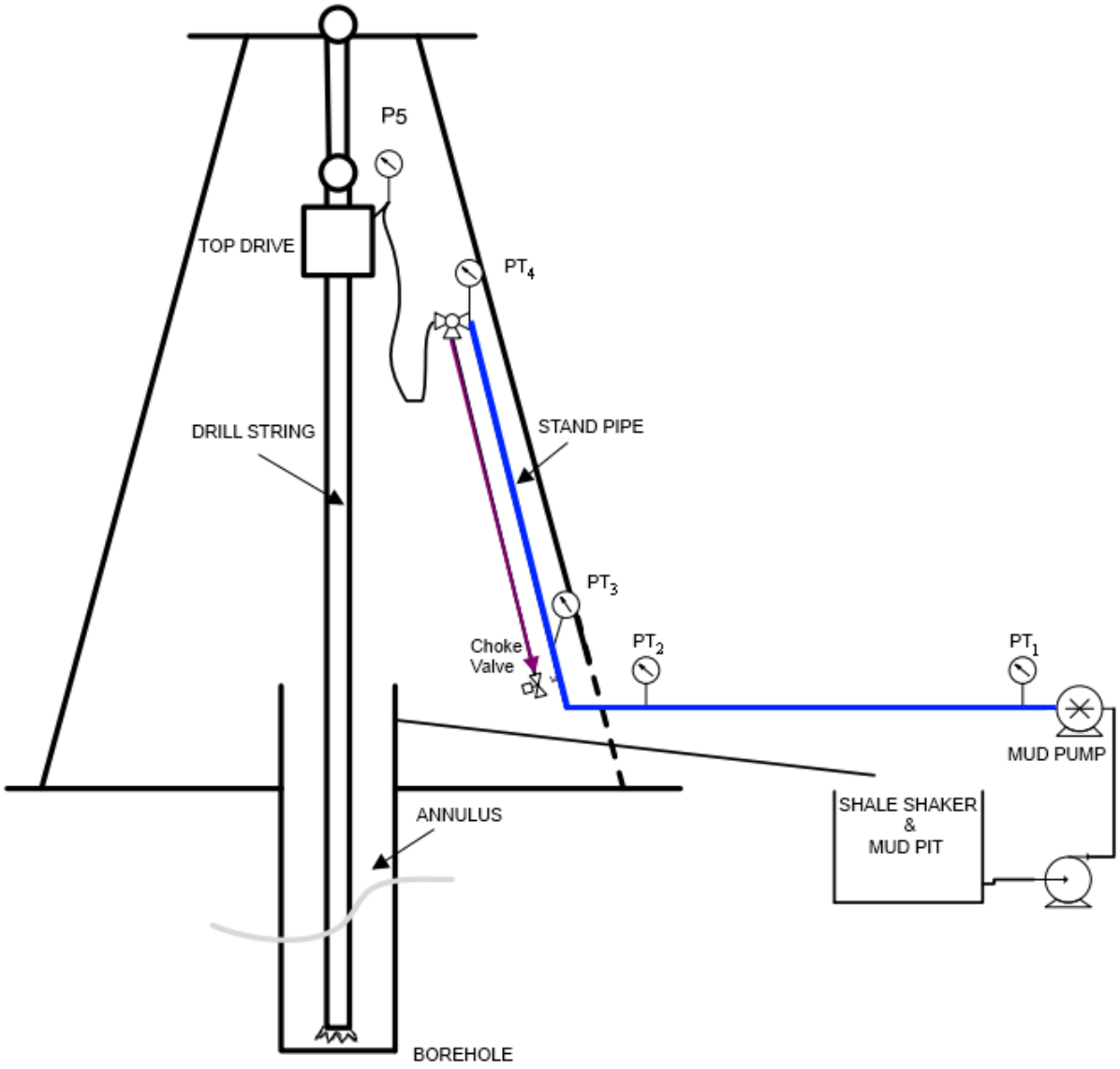

Figure 3.1 - Schematic of the Instrumented Standpipe setup. PT_1, PT_2, PT_3 and PT_4 are the pressure transmitters along the flow path [25].

Drill pipe is put together in stand of 30m, and for every 30m drilled a new pipe stand has to be connected drill sting to enable further drilling. During these periodic stops the mud pump ramps down and halts circulation drilling fluids for approximately 5 minutes [21]. The basic idea is exploit these periodic stops and measure various drilling fluid properties by diverting the mudflow from the top of the stand pipe through a return line with an adjustable choke valve as illustrated in Figure 3.1. By employing a pre-programmed sequence the mud pump and the choke valve can automatically

adjust the flow rate and back pressure in this inner loop, so that the frictional pressure losses and densities at different pressures can be calculated from the pressure measurements in the flow path.

The frictional pressure drop across the horizontal section (between PT_1 and PT_2) is equal to the differential pressure between PT_1 and PT_2 :

$$\Delta P_{Hor} = PT_1 - PT_2 \tag{3.1}$$

The pressure loss in a circular pipe has previously been defined by *equation (2.17) in section 2.7*. By rearranging this equation respect to the *f*, a friction factor coefficient for the horizontal section can be found from following equations:

$$f_f = \frac{\Delta P_{HOR} * D}{2 * \rho * v^2 * \Delta L} \qquad \text{(Fanning type)} \tag{3.2a}$$

$$f_d = \frac{2 * \Delta P_{HOR} * D}{\rho * v^2 * \Delta L} \qquad \text{(Darcy type)} \tag{3.2b}$$

ΔL = distance between pressure measurement
D = pipe inner diameter
ρ = fluid density
v = fluid velocity

The fluid density can be estimated, at various pressures, from vertical section between PT_3 and PT_4 and ΔP_{Hor}. As opposed to the conventional testing method, this method also account for the pressure effect (compressibility) on fluid density, as discussed in section 2.4.1. The fluid density is estimated with following mathematical expression:

$$\rho = \frac{\Delta P_{Ver} - \Delta P_{Hor}}{g * h} \tag{3.3}$$

where;

ΔP_{Ver} = $PT_3 - PT_4$

g = gravitational constant
h = vertical height between PT_3 and PT_4

For laminar flow can fluid viscosity and shear stresses be estimated by combining following equations; 2.3, 2.20, 2.21, and 3.2a. But since it is impossible to achieve steady laminar flow from the current flow loop set up is this not included in this thesis.

Differential pressure measurements can also be used in calculation of flow rates, but this will not be further elaborated in this thesis. There are several existing methods for accurate measuring of flow rates.

3.2 Flow loop description

In order to evaluate the potential of the Instrumented Standpipe concept several practical experiments have been performed in a small scale flow loop located in the two-phase flow lab, on the first floor in the west-section of Kjølv Egeland building, at the University of Stavanger.

The flow loop was originally built by *Magnus Tveit Torsvik* as part of his Master thesis in the spring of 2011 and was further developed by *Alexander Wang* during the autumn 2011 [26, 27]. This section will provide a very brief and general description of the flow loop and some its existing components, followed by a detailed description of the equipment I installed on the rig to enable the execution of my planned experiments.

A picture of the flow loop is shown in Figure 3.2 and the corresponding process flow diagram (PFD) is shown in Figure 3.3.

A 300 liter tank supplies the flow loop with fluid. The fluid is pumped, by a screw pump, through the approximately 65m of PVC pipes (with inner diameter of 3,33cm), before terminating back into the tank at atmospheric pressure. Figure 3.2 also illustrates how the rig model is built to emulate the circulation system used in real drilling operations. For a more detailed description of the flow loop instrumentation and rig construction I refer to *Magnus T. Torsviks thesis* [26].

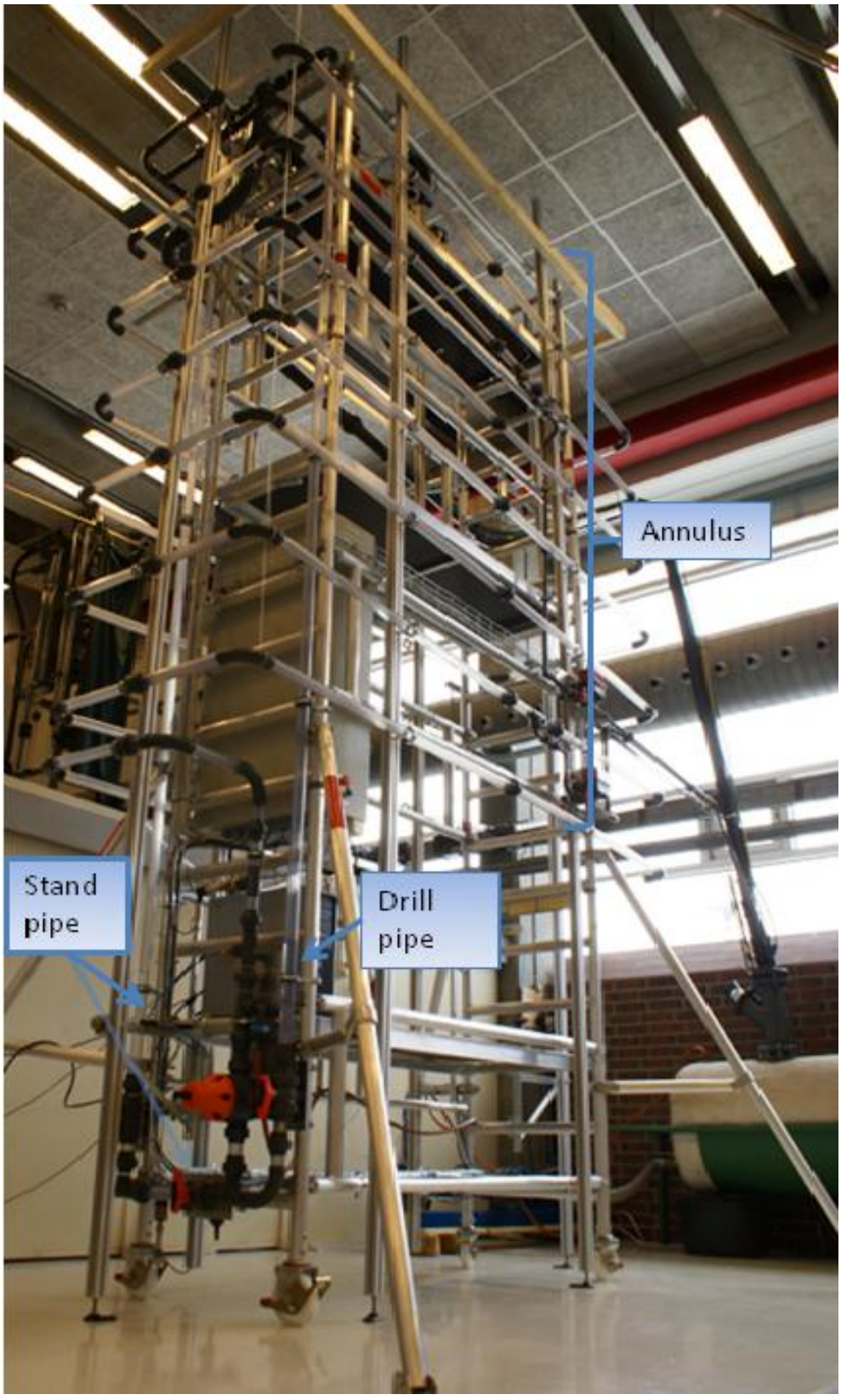

Figure 3.2 – Picture of the flow loop

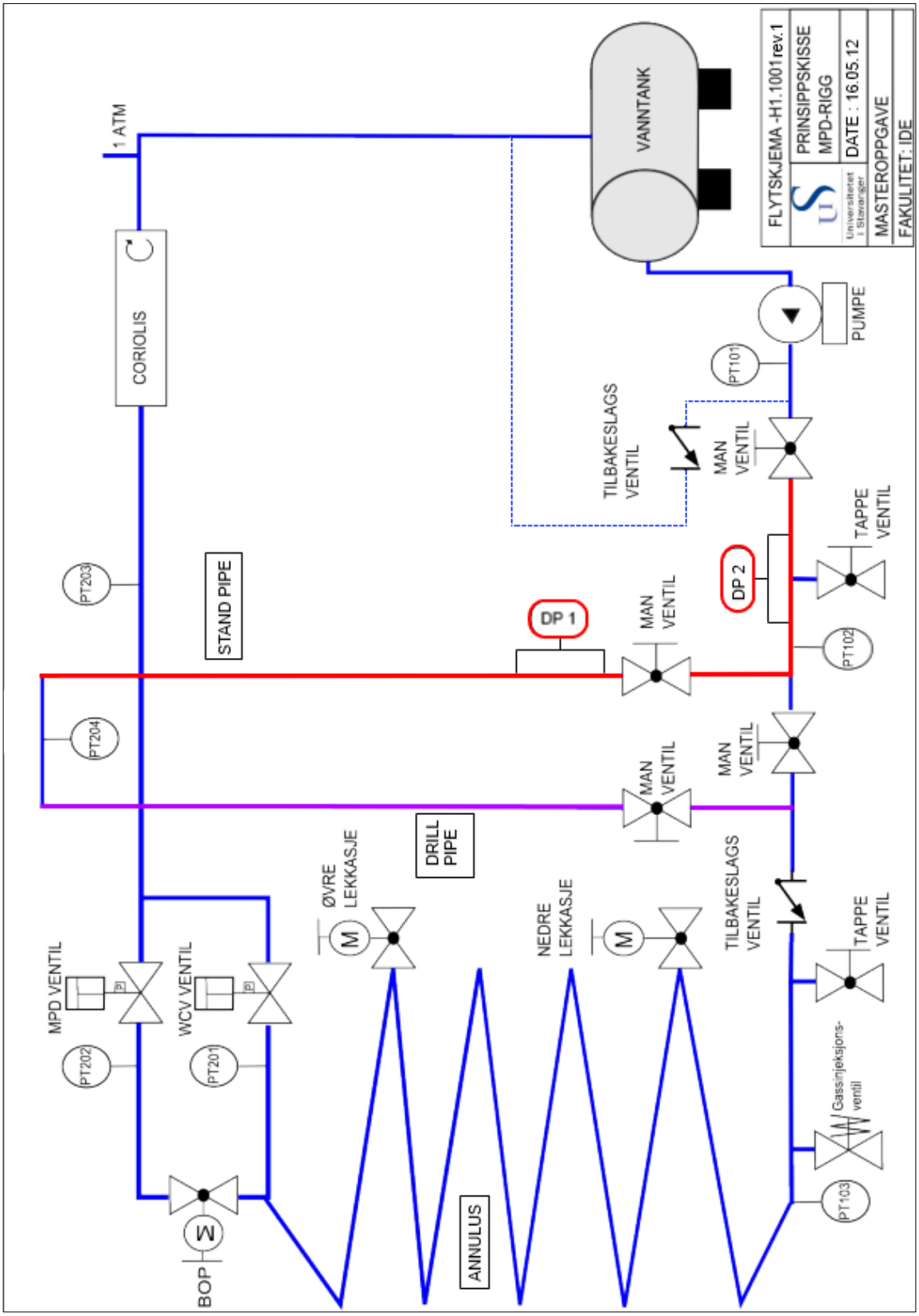

Figure 3.3 - Process flow diagram (PFD) for the flow loop

3.3 Implementation of differential pressure transmitters on flow loop

The first part of my experiments was to install two differential pressure (DP) transmitters onto the flow loop and implement them into the existing control systems. Both DP transmitters are of the type Rosemount 3051S Series Pressure Transmitter with HART® Protocol. All technical documentation related to these differential pressure transmitters can be found at the vendor webpage [28].

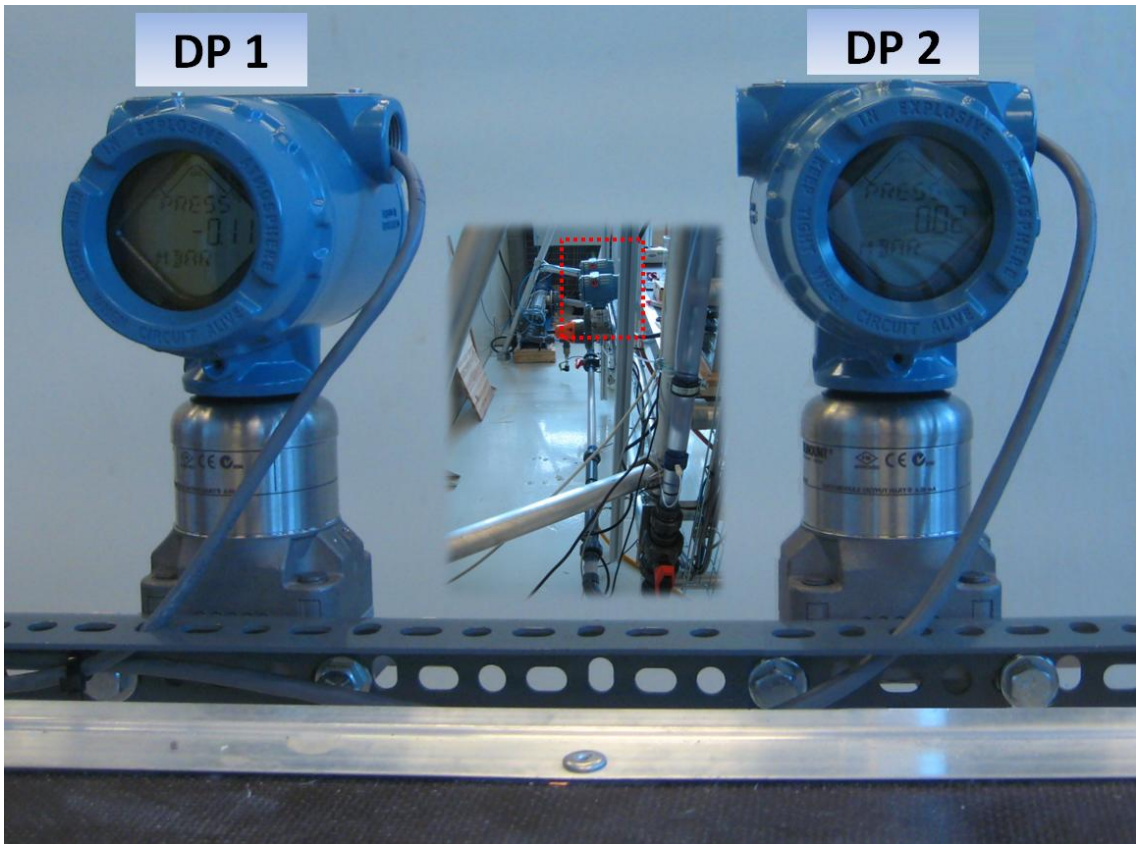

Figure 3.4 - Picture of DP transmitters and their placement on the flow loop

The Instrumented Stand pipe set up, illustrated in Figure 3.1, use four pressure transmitters to obtain pressure measurements at given points in the flow path, and the differential pressure between two sensors is obtained by subtraction. The differential pressure transmitters used in this case measures the differential pressure between two points directly, but the basic principle is exactly the same.

The PFD in Figure 3.3 also illustrate the position of the differential pressure transmitter and, one DP transmitter was connected to the vertical “stand pipe section” of the flow loop and the other DP transmitter was connected to the horizontal section, respectively DP 1 and DP 2. The impulse lines from each DP transmitter were taped into the flow loop pipe with the identical spacing of 0,855m.

A control card from National Instruments combined with Matlab (Simulink), enables communication between the instruments and processes in the flow loop and a Computer, as illustrated in Figure 3.5.

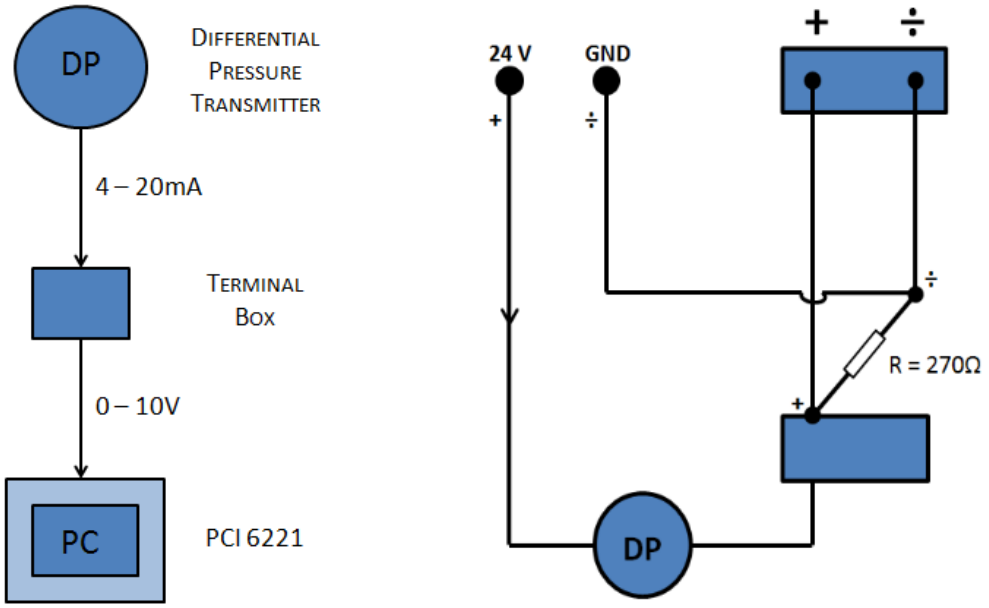

Figure 3.5 - Levels included in the link between the DP transmitters and the PC input card.

A 24 VDC current is supplied to the DP transmitters, and a 4 – 20 mA return goes through a 270 ohms resistance. This converts the current into a 0 – 10 voltage signal, in accordance with Ohms Law, which is directly transmitted into the analog input ports of the control card (PCI 6221). Relevant technical documentation concerning the connection is included in *appendix B - Technical documentation related to the installation DP transmitters on the flow loop.*

There are actually two control cards connected to the computer; one *input card (PCI 6221)* which receive and logs measurements from the different instruments on the flow loop, such as the one illustrated in Figure 3.5 And one *output card (PCI 6703)* which delivers control signals to the process i.e. adjusting the pump rate. Both control cards, power supply and other electrical components for the flow loop instrumentation is placed within a cabinet which keeps the wiring neat and tidy and provide shielding against electromagnetic interference (EMI) and fluid spillage. For further reading regarding the cabinet set up and EMI and Electromagnetic compatibility (EMC) issues at the flow loop site, I refer to *Magnus T. Torsvik* and *Alexander Wang's* master thesis[26, 27].

3.3.1 Matlab scaling factor

Since the information from the DP transmitter is received as a voltage on the computer, a scaling factor is needed to convert this information into mBar in Matlab. A *Rosemount HART 375 Field Communicator* was used to measure the true relationship between voltage and mBar on the DP transmitters in order to ensure maximum accuracy. The following relation was obtained by the Field Communicator:

Table 3.1 - Relationship between voltage signal and mBar obtained with the Rosemount HART 375 Field Communicator.

DP1 (vertical section)		DP2 (horizontal section)	
1,080 Volt	0 mBar	1,083 Volt	0 mBar
5,400 Volt	62 mBar	5,410 Volt	62 mBar

A linear equation (y = ax + b) gives the argument for the scaling factor, graphically presented in Figure 3.6.

The differential pressure transmitter operates with a scale from approximately *1.08 – 5.4 volt*, which corresponds to the minimum- and the maximum reading, respectively 0 mBar and 62 mBar. Minor differences in the 270 ohms resistors may be the cause of the slight difference between the two relationships.

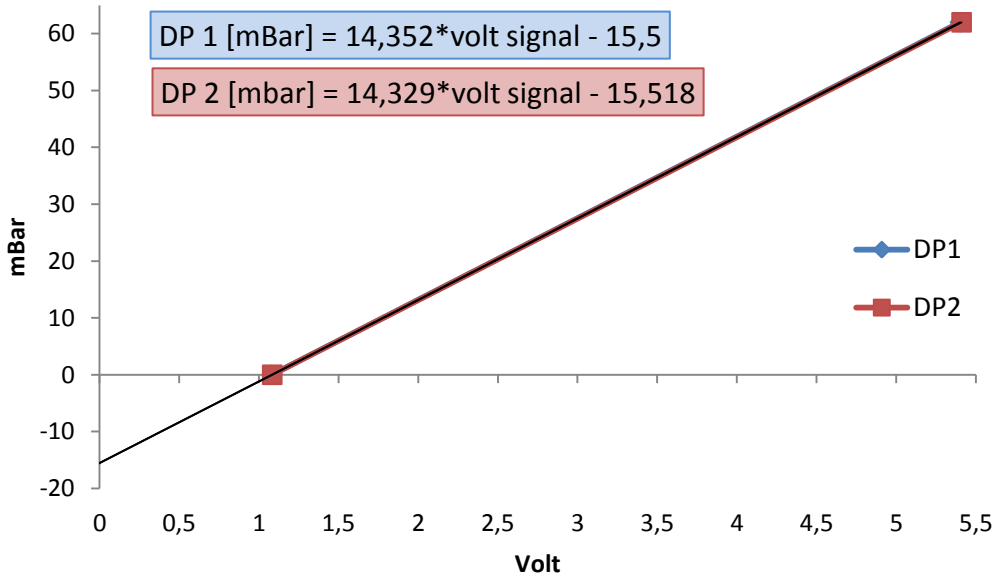

Figure 3.6 – Graphical presentation of scaling factor argument

3.3.2 Verification of scaling factor

The scaling factor was verified by comparing the actual readings from the DP transmitters and the scaled values in Matlab. The Rosemount DP transmitters are delivered pre-calibrated from the vendor, and can therefore with a great deal of certainty be regarded as very accurate.

The update frequency on the DP transmitters display however, is quite low (about every third second) and only displays the moment value. Unfortunately the displayed values proved to fluctuate quite a lot, possibly due to pulses from the screw pump.

Matlab samples at much higher frequency, approximately 70 samples per sec, additionally the raw signal from the DP transmitters goes through a *Low-Pass filter*, which basically reduces the amplitude of signals with frequencies higher than a cutoff frequency. In other words, a low pass filter provides a smoother form of signal, by removing the short term fluctuations and leaving the longer term trend [29]. I decided to correlate the display values with the filtered values rather than the raw signal because all further testing will be based on the filtered signal.

I therefore devised a method for correlating the displayed readings with the filtered and scaled Matlab values, which resulted in following procedure:

- Set the pump to a constant rate, start the circulation, and wait 20 seconds to ensure stable flow conditions.
- Monitor the displayed readings for both DP transmitters, for example with a video camera, over a 70 second time interval (unfortunately the current settings in Matlab only allows for logging data over a approximately 70 seconds interval before the memory is full and it starts overwriting data)
- Stop the circulation and the video recording. Review the “scope” plot in Matlab and ensure that logged differential pressures are reasonably constant/stable.
- Play off the video recording and log the displayed readings in a spread sheet. Find the corresponding datasets in Matlab and import it into the same spread sheet. There might be some disturbances in the flow when the pump shuts down, so I discarded the last 10 seconds data from all datasets.
- Finally, calculate the average values from both datasets.

By repeating this procedure in series for different pump rates, the following correlations between displayed reading and Matlab data logger values was obtained:

Differential pressure transmitter 1 (DP 1)

Table 3.2 - Correlation between display reading and Matlab data logger for DP 1 @ 30% of maximum pump rate.

Series:	2	3	4	5	SUM
DP1 display average:	5,28	5,03	5,60	5,64	5,39
DP1 matlab average:	4,93	4,89	5,71	5,52	5,26
Difference:	0,34	0,14	-0,10	0,12	0,13
Correlation between series =					0,924

Table 3.3 - Correlation between display reading and Matlab data logger for DP 1 @ 40% of maximum pump rate.

Series:	1	2	3	SUM
DP1 display average:	8,89	8,67	8,53	8,70
DP1 matlab average:	8,96	8,69	8,47	8,71
Difference:	-0,07	-0,02	0,06	-0,01
Correlation between series =				0,998

Differential pressures transmitter 2 (DP 2)

Table 3.4 - Correlation between display reading and Matlab data logger for DP 2 @ 30% of maximum pump rate.

Series:	2	3	4	5	SUM
DP2 display average:	4,52	4,86	4,46	4,12	4,49
DP2 matlab average:	4,23	4,17	4,76	4,63	4,45
Difference	0,29	0,69	-0,30	-0,51	0,04
Correlation between series =					-0,70

Table 3.5 - Correlation between display reading and Matlab data logger for DP 2 @ 40% of maximum pump rate.

Series:	1	2	3	SUM
DP2 display average:	7,81	7,61	7,65	7,69
DP2 matlab average:	7,82	7,51	7,63	7,65
Difference:	-0,01	0,10	0,02	0,04
Correlation between series =				0,98

The test indicates a very strong correlation between the displayed reading of both pressure transmitters and the data logger in Matlab. There is also a very small difference in the summed total for the corresponding display and Matlab series. This evidence supports that the scaling factor provides a credible scaling.

It is however, important to beware the great differences in sample populations for the compared datasets series. The Matlab average is based on approximately 4700 values while the display average is based on 24 values; in other words, there are almost 200 Matlab values for every display reading. The "random" nature of the display readings adds some uncertainty, and might not always give a representative impression of the true differential pressure in the pipe section. This may very well be the cause of the altering positive and negative difference between the series, and the negative correlation factor in Table 3.4. Ideally one should do several more series to obtain an even stronger relationship argument and minimize uncertainties; yet I find the presented verification sufficiently compelling to proceed with the experiment.

Negative initial values in Matlab data logger

Additionally there is a minor unresolved issue with the signal from the DP transmitters when the rig does not run. Negative pressure values are logged in the Matlab for both DP transmitters, the initial value is equal to the respective interception point with the y-axis in Figure 3.6. This probably means that no signal is send form the transmitters when the loop is not operated, when there should have been a 1,08 V signal from DP1 and 1,083 V from DP 2 which would have given a initial reading of 0 mBar in Matlab data logger.

There were also some initial negative values in Coriolis measurements; these had to be filtered out in the Matlab code to permit later calculation of theoretical friction factor and theoretical pressure loss. The Matlab code is included in *Appendix C – Matlab script for measured data and plots.*

3.4 Pre-testing of small scale Instrumented Standpipe set up on flow loop

In this section a pre-test phase will be conducted in order to ensure that the flow loop and all relevant instrumentation works according and produces reliable data.

3.4.1 Pump characteristics

How the pump delivers the feed is very decisive for experiments performed in this paper. For this reason is it briefly described in this section. The pump can be regulated from Matlab Simulink via the output control card that sends a direct analog 0 – 10 volt signal to the *frequency converter* that regulates the pump rate. The screw pump is manufactured by PCM and has a maximum output capacity of 14 m^3/hr. This will however induce a higher pressure in the flow loop piping than what it is designed for, so the upper working area of the pump is for operational safety reasons therefore limited to 45% of maximum. Additionally is the lower limit set to 20% of maximum, due to overheating and subsequent release of the *pump motor thermal protector* when the pump is operated at lower rates. So the pump working range is therefore in the interval between 20% – 45% of maximum capacity.

Alexander Wang investigated the relationship between pump rate [0 – 1] and mass rate [kg/hr], and found the following linear relationship when the MPD valve is fully open:

$$\gamma = 1{,}4495 * 10^4 x - 0{,}0012 \tag{3.4}$$

This relationship has been used in all calculations depending on pump rate and fluid flow in the flow loop system. This relationship has not been rechecked in this thesis [27].

3.4.2 Inconsistent measurements for DP transmitters

During the testing phase an odd inconsistency in the DP measurements was discovered, the obtained results were significantly different depending on the time of day they were made. To clarify; measurements made during working hours is consistent with other measurements done in the same period of time other days, however, measurements made at night after normal working hours has a significantly different trend from those made during the day. In the Matlab plots depicted in Figure 3.7 to Figure 3.10 this difference can be observed for two different pump rates; respectively 30% and 40% of maximum pump rate. All other conditions are the same for these series. It is show that DPhor (DP2) switches from high side to the lower side of DPver (DP1) and the measured values are

higher for both DP transmitters when testing is performed after normal working hours. This change is observed for other pump rates as well.

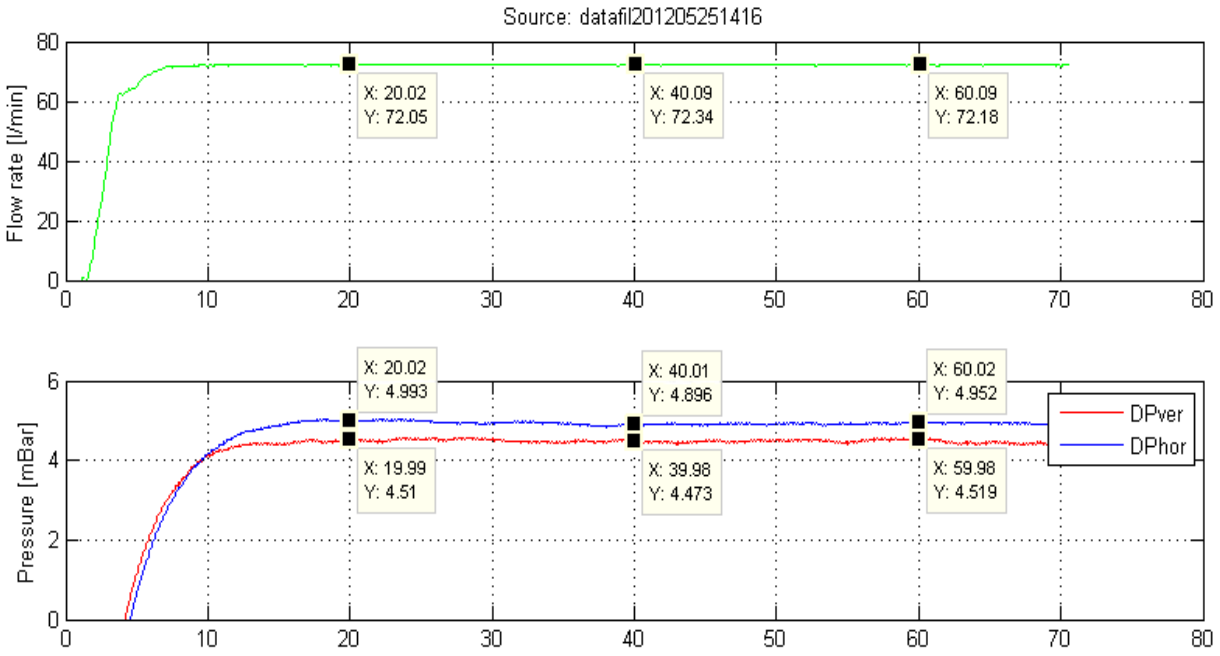

Figure 3.7 - Differential pressures at 30% of maximum pump rate measured during working hours.

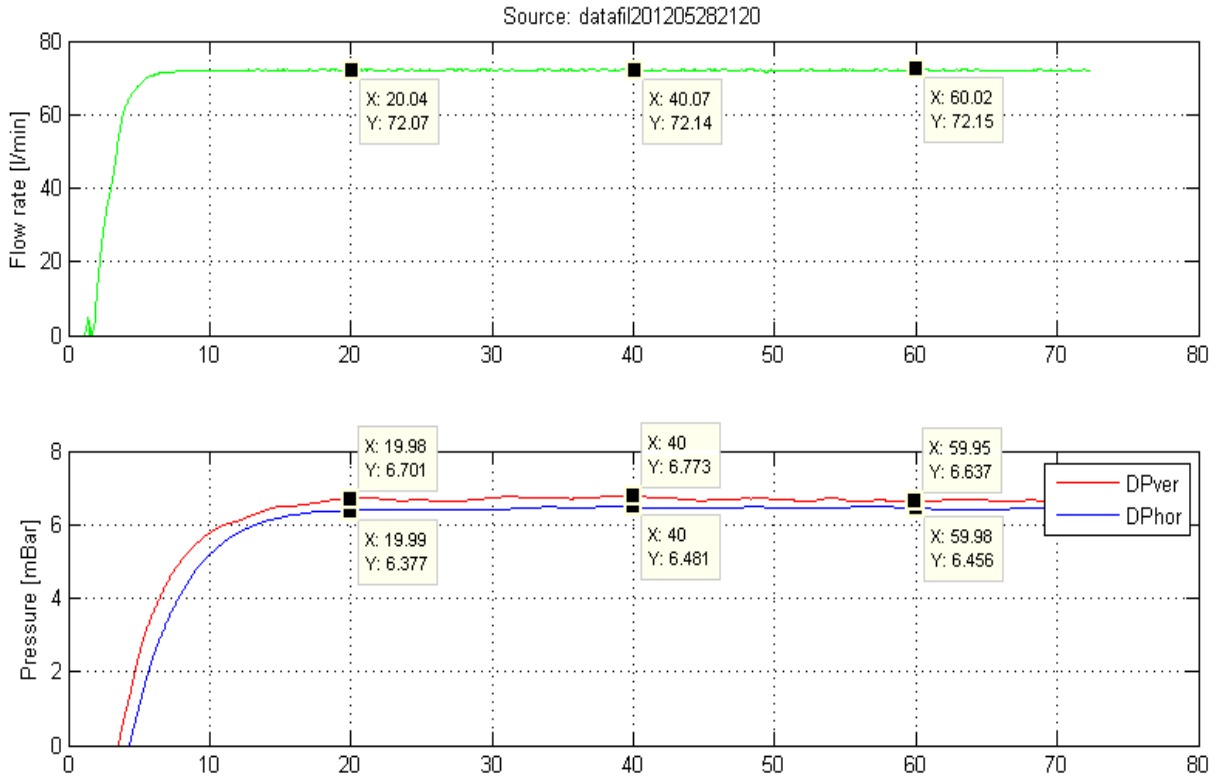

Figure 3.8 - Differential pressures at 30% of maximum pump rate measured after working hours.

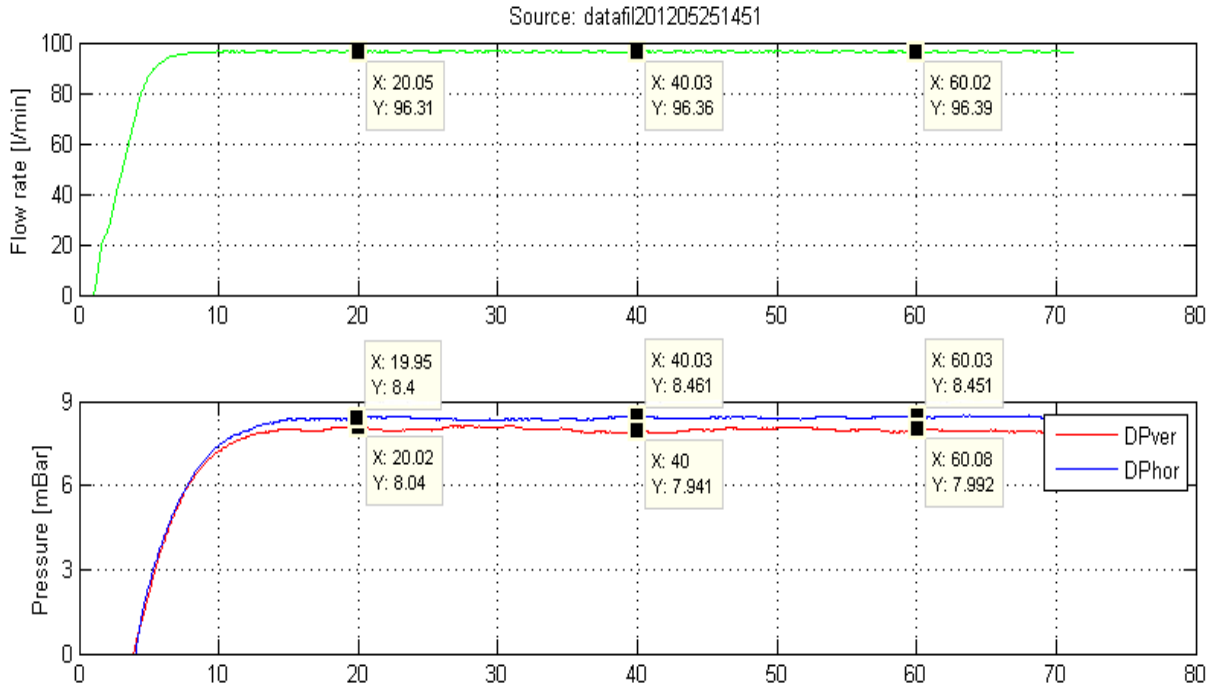

Figure 3.9 - Differential pressures at 40% of maximum pump rate measured during working hours.

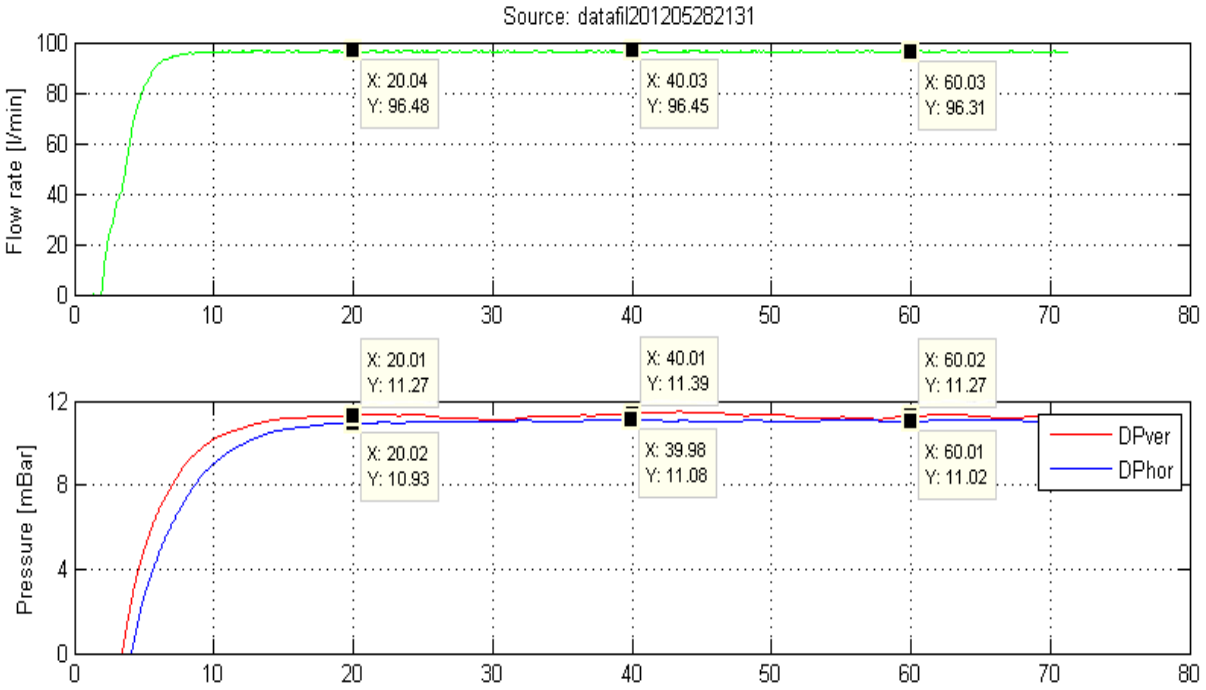

Figure 3.10 - Differential pressures at 40% of maximum pump rate measured after working hours.

The most immediate explanation for this is electromagnetic interference (EMI) from other electrical equipment used in the hall during work hours. This has previously been highlighted as a problem in the current flow loop location and some measures has already been taken [26, 27].

A comparison of Matlab data series obtained after working hours and during working hours shows that the after working hours data provides a smoother curve and a seemingly less disturbed signal than the ones obtained during work hours, as seen in Figure 3.11. Also, the data series obtained after working hours also displays an almost identical trend to the theoretical pressure loss values, especially if a more conservative roughness factor (ε) for the PVC pipes is applied. The absolute roughness factor for the PVC pipes is not know, but will great certainty lay somewhere between the smooth pipe (ε/D = 0) and the more conservative ε/D = 0,0015 [24]. The theoretical pressure loss is calculated from the equations presented in section 2.7. Each data point in the plot represents an average value for over 6000 measurements. Flow loop hard data given in Table 3.6.

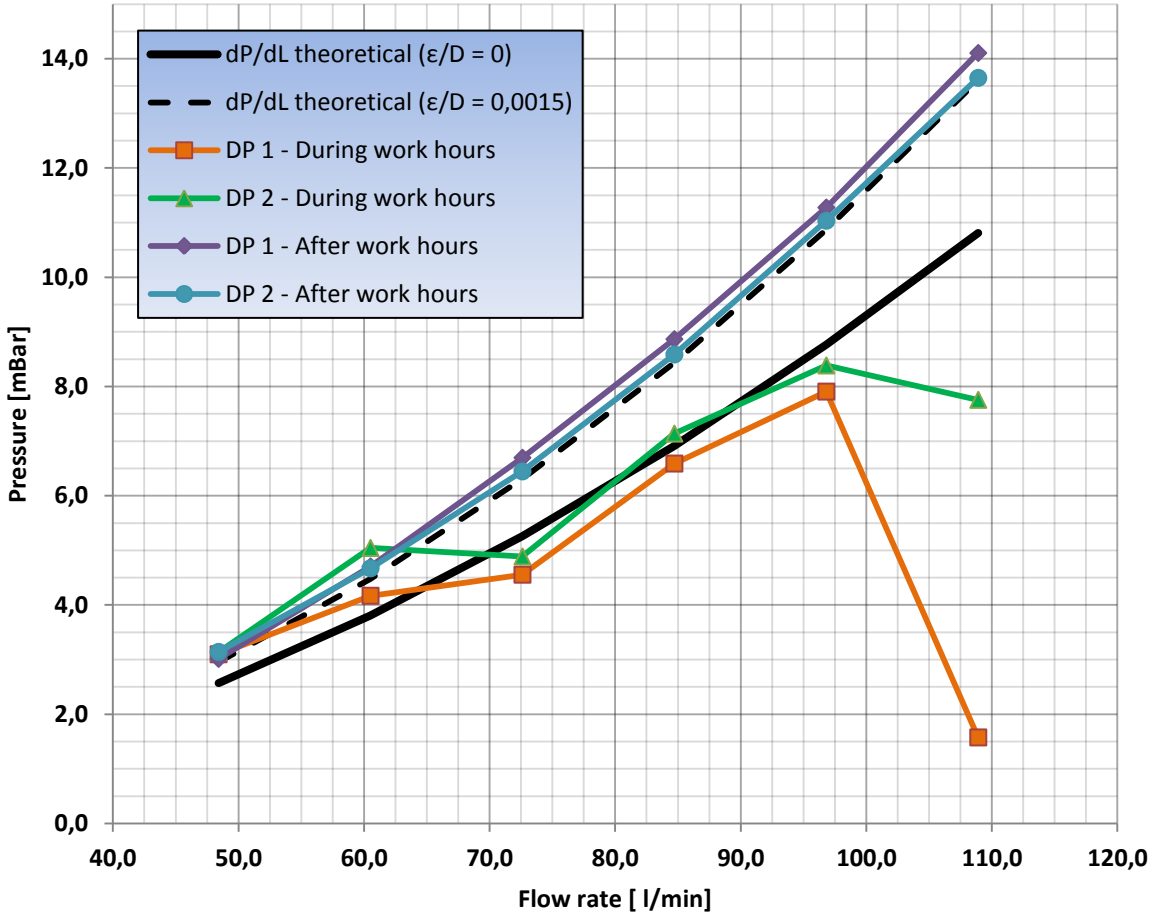

Figure 3.11 - Comparison of Matlab data obtained during and after normal working hours.

Comparison of DP transmitter display readings:

Furthermore is the problem with fluctuating readings in the DP transmitter display, discussed in section 3.3.2, more or less gone. A comparison of the display readings obtained after working hours and during working hours also supports the notion of a less disturbed signal and thus a higher quality of the data obtained after normal working hours.

The box plots in Figure 3.12 and Figure 3.13 provides a visual summary of the display reading data sample statistics. From these plots it can be observed that the range (max – min) of the data series made after working hours is significantly less than for the daytime series. And the inter quartile range, Q75 – Q25, which contains 50% of the data, is for the after working hour data very narrow compared to the daytime data thus indicating a much smaller spread in data. The medians position inside the boxes indicates the skeweness in the distributions; in other words, whether there are more values towards the upper or the lower quartiles, respectively Q75 and Q25. The box plots generally indicate little skeweness in the display readings data, with the exception of the DP 1 display readings at 30% of maximum pump rate during day time. The same trends can be seen for both pump rates. A brief summary of error analysis is given in *appendix D – Error analysis.*

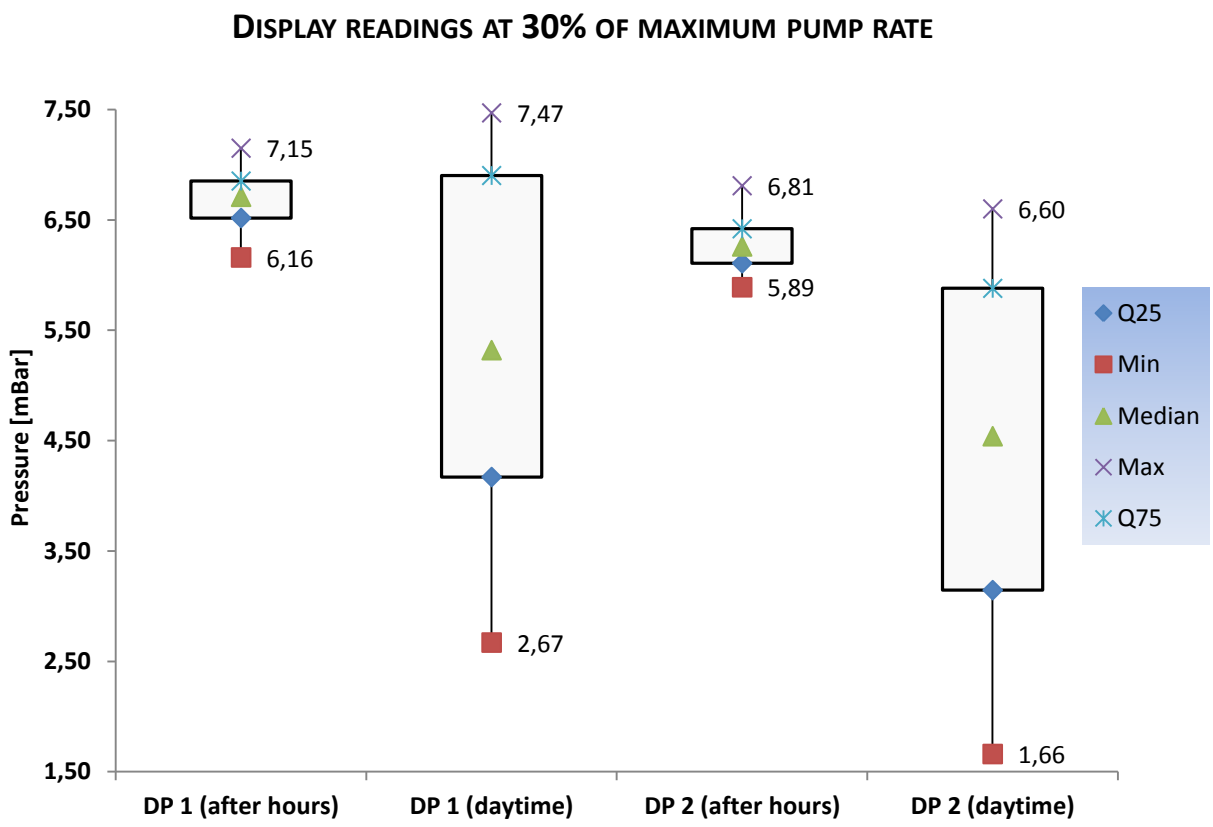

Figure 3.12 - Box plot comparison of data quality for DP display readings obtained after work hours and during work hours, at 30% of maximum pump rate.

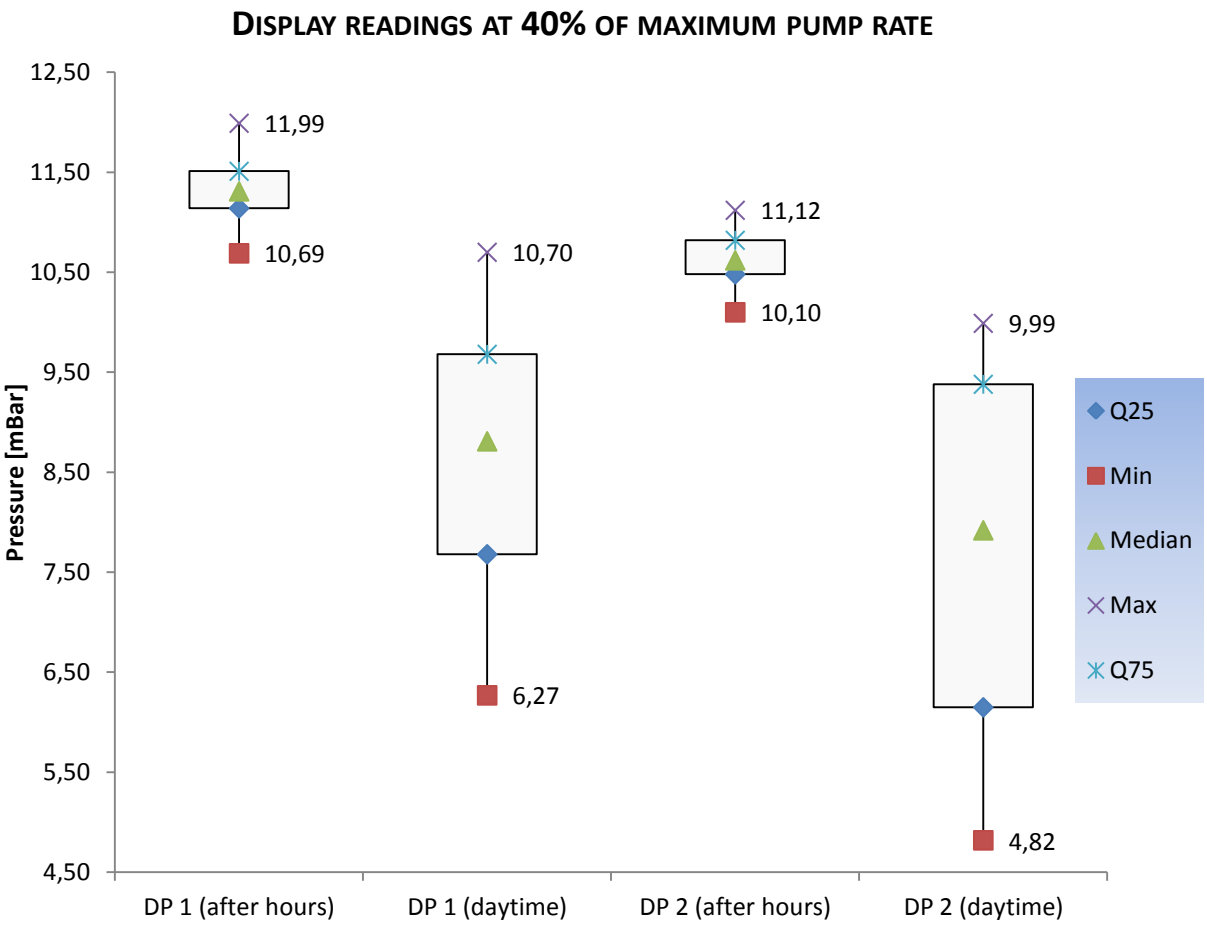

Figure 3.13 - Box plot comparison of data quality for DP display readings obtained after work hours and during work hours, at 40% of maximum pump rate.

An even more detailed table concerning the data quality and error analysis calculations is presented in *appendix E.2*

These findings are, in my opinion, a very strong indication of an electromagnetic compatibility (EMC) problem, rather than the disturbances caused by pulses from the pump, as previously claimed in this thesis. Also the results strongly implies that the source of this disturbances is external, in other words coming from some of the other equipment used in the e-hall during working hours.

Due to limited time and an imminent deadline, is no further effort put into resolving this problem. However, I will urge other students to investigate this problem further if future experiments are to be conducted.

3.5 Results of small scale testing with Instrumented Standpipe set up on flow loop

Since the pre-test phase proved quite poor testing conditions during normal work hours, is the results in presented in this section solely based on data obtained after normal work hours. The main objective in this section is to evaluate how well the Instrumented Standpipe setup performs on a small scale flow loop.

Table 3.6 - Flow loop hard data and fluid properties used in all subsequent calculations.

Symbol	Description	Numerical Value	Unit
ΔL	Length of horizontal section, associated with DP 2	0,855	m
Δh	Height of vertical section, associated with DP 1	0,855	m
ID	Inner diameter of flow loop piping	0,03325	m
ε/ID	Relative roughness of pipe	0	
g	Gravitational constant	9,81	m/s^2
ρ	Water density at 20c°	998,2	Kg/m^3
μ	Water viscosity at 20c°	0,001002	Pa*s

The relative roughness factor is set to 0 (smooth pipe assumption) for all following calculations, unless otherwise is specified, even though the plot depicted in Figure 3.11 shows a more congruent relationship between the theoretical frictional pressure loss and the measured pressure losses when a more conservative relative roughness factor is applied. The non-zero roughness factor used in Figure 3.11 is highly speculative and cannot be used in calculations without further evidence, while the smooth pipe is a very common assumption in pressure loss calculations and will therefore be applied here.

As previously mentioned, the current settings in Matlab only allows for logging data over an approximately 70 seconds time interval before the memory fills up and starts to overwrite data. This is highly inconvenient and makes it practically impossible to display the measured data for different pump rates in the same Matlab plot in a sensible way. So instead the measurements for different pump rates are presented in individual plots, with a brief description. Lastly a comparison of averaged pressure measurements values obtained at different flow rates will be presented with a more detailed description.

3.5.1 Formulas used in the Matlab plots

Flow rate

$$Q\ [l/min] = \frac{1000 * Coriolis\ [kg/hr]}{60 * \rho\ [kg/m^3]} \tag{3.5}$$

The friction factor coefficient

The friction factor in the Matlab plots is calculated from equation 3.2b, which has been modified to fit the Matlab input data units:

$$Darcy\ friction\ factor = \frac{162\ 000\ 000 * DP2\ [mBar] * \rho[kg/m^3] * ID^5[m] * \pi^2}{Coriolis^2\ [kg/hr] * \Delta L\ [m]} \tag{3.6}$$

The theoretical friction factor coefficient

The theoretical friction factor coefficient is calculated from the Haaland correlation presented in equation 2.22c;

$$Darcy\ friction\ factor_{teo} = \left(\frac{1}{-1{,}8 \log\left(\left(\frac{\varepsilon/ID}{3{,}7} \right)^{1{,}11} + \frac{6{,}9}{Re} \right)} \right)^2 \qquad [\mathrm{Re} > 3000] \tag{3.7}$$

where ;

$$Re = \frac{\rho[kg/m^3] * v[m/s] * ID[m]}{\mu[Pa*s]} \quad \text{and} \quad v\ [m/s] = \frac{4 * Coriols\ [kg/hr]}{3600 * \pi * ID^2 * \rho[kg/m^3]}$$

The theoretical frictional pressure loss

$$(dP/dL)_{teo}[mBar] = \frac{Darcy\ friction\ factor_{teo} * \rho[kg/m^3] * v^2[m/s] * \Delta L[m]}{200 * ID[m]} \tag{3.8}$$

Matlab coding is included in *appendix C – Matlab script for measured data and plots.*

3.5.2 Measurements at 20% of maximum pump rate

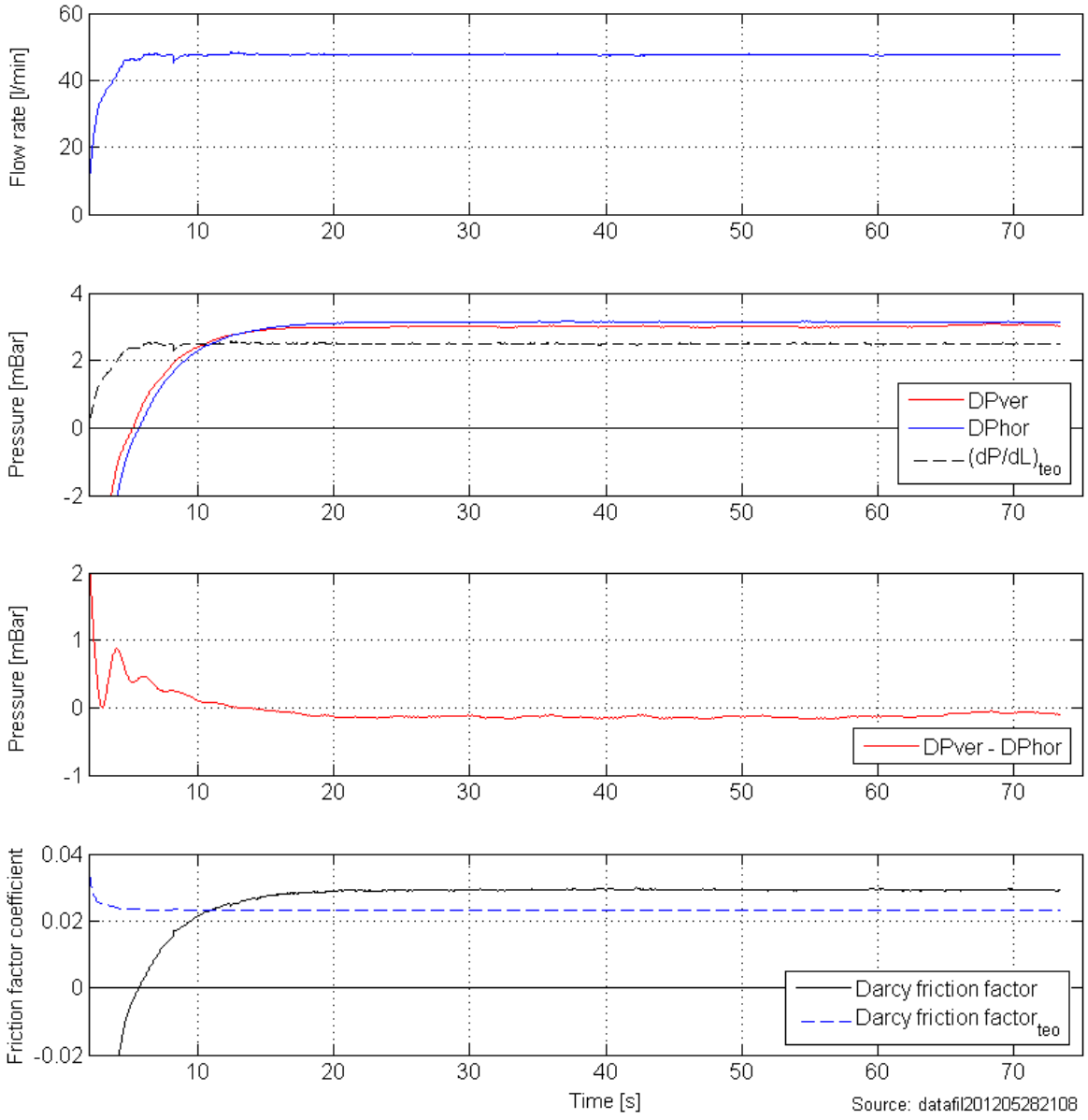

Figure 3.14 - Measurements at 20% of maximum pump rate

The measurement obtained at 20% of maximum pump rate shows a slight negative difference between the vertical and the horizontal frictional pressure loss. There is also a minor difference between measured pressure loss and the theoretical pressure loss, consequently also a small difference between the measured friction factor (which depends on DPhor), and the theoretical friction factor. The theoretical pressure loss ramps up to the plateau level a couple seconds before the plateau level is reached for the measured values, because it is based on the flow rate obtained from the Coriolis meter displayed in the uppermost subplot.

3.5.3 Measurements at 25% of maximum pump rate

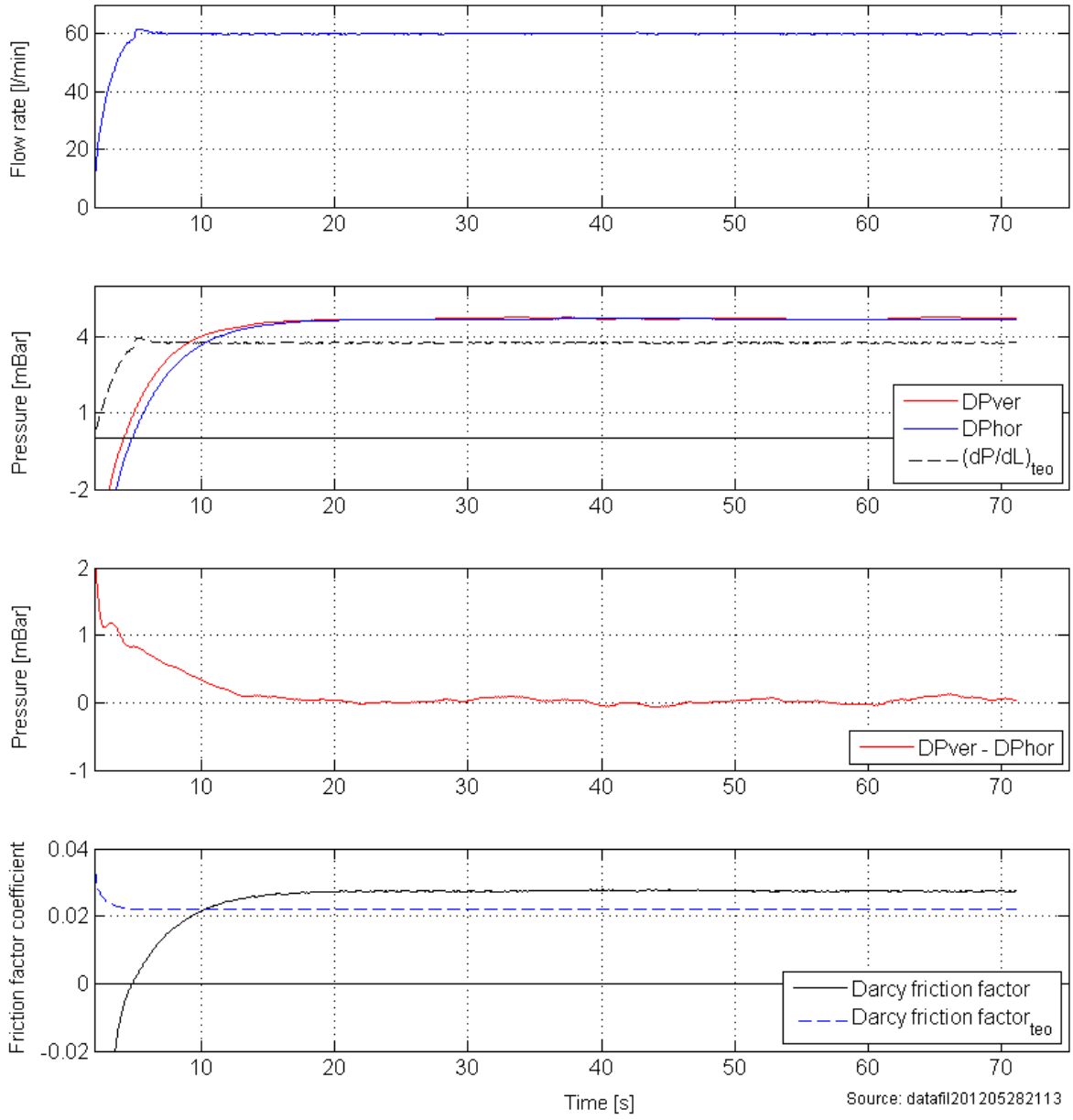

Figure 3.15 - Measurements at 25% of maximum pump rate

Figure 3.15 shows that the pressure loss for DPver (DP1) and DPhor (DP2) coincides for the measurement obtained at 25% of maximum pump rate, the difference between them is shown in third lowest plot. It is observed that the frictional pressure loss increases with the increased flow rate, while the friction factor coefficients decreases.

3.5.4 Measurements at 30% of maximum pump rate

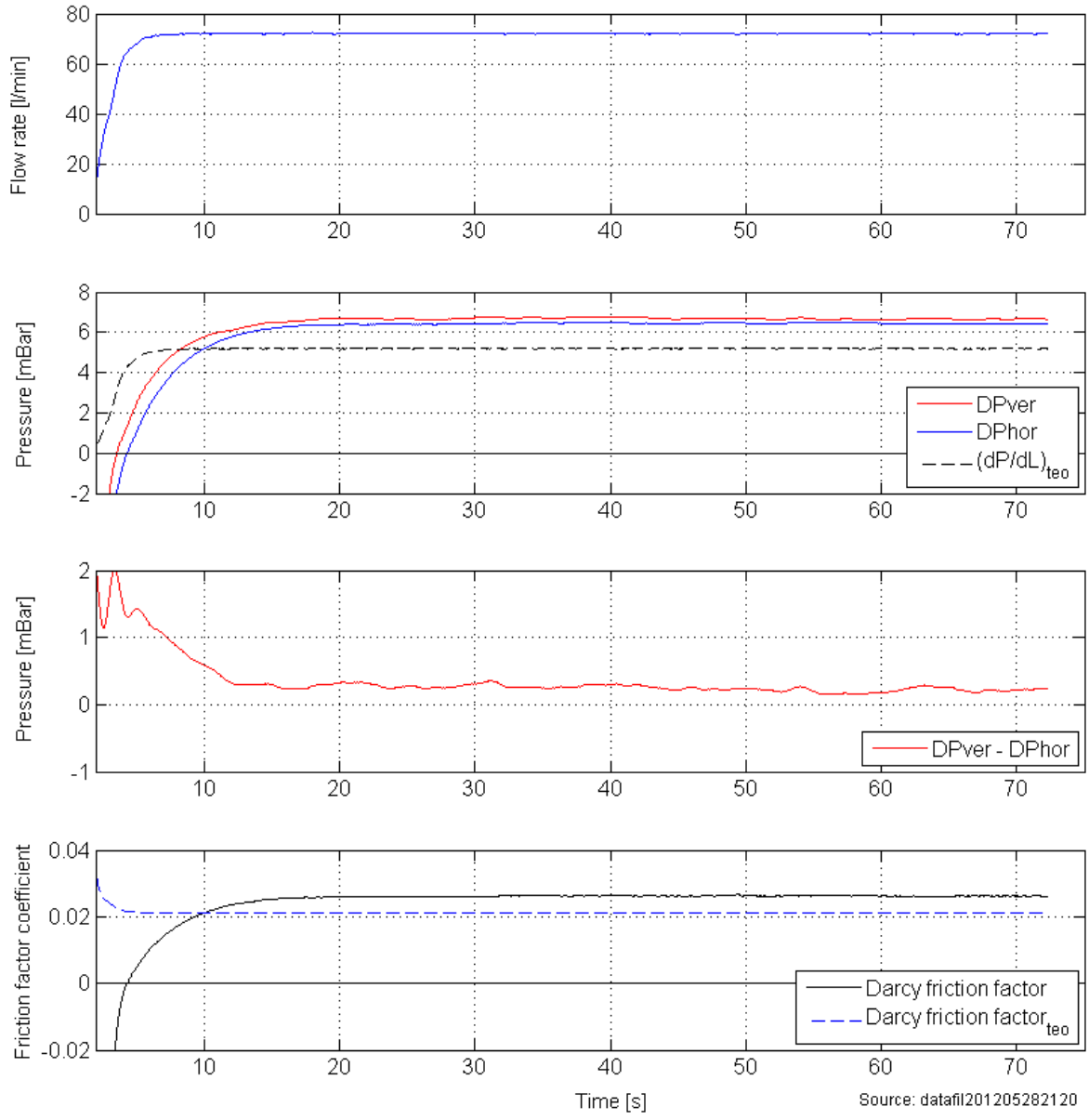

Figure 3.16 - Measurements at 30% of maximum pump rate

At this flow rate, 30% of maximum, the frictional pressure loss in the vertical section is now greater than the one in the horizontal section, and there is consequently a positive difference between DPver and DPhor. The cause of this shift is not known.

3.5.5 Measurements at 35% of maximum pump rate

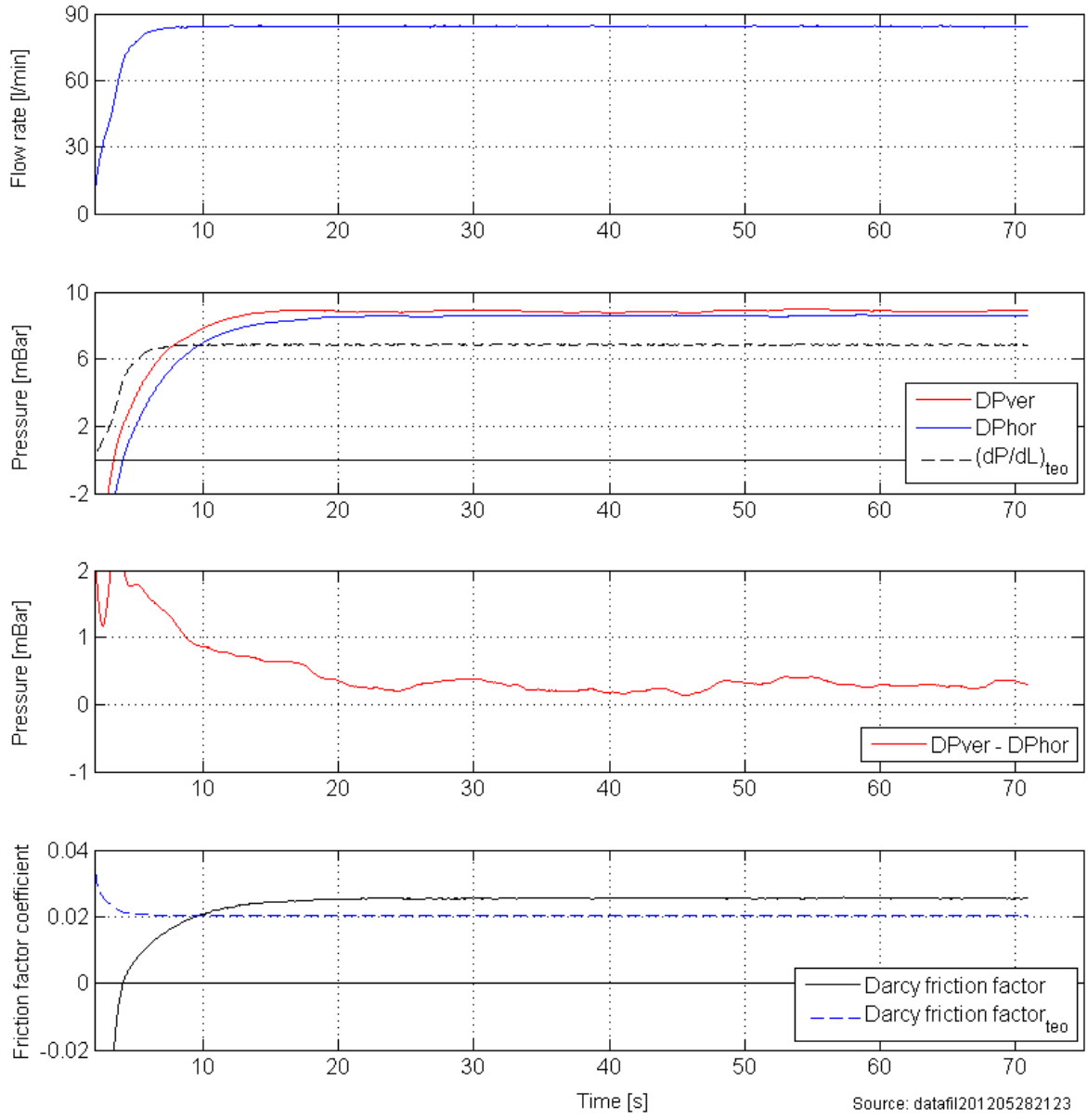

Figure 3.17 - Measurements at 35% of maximum pump rate

The trend from the previous pump rate continues. It is observed an increasing difference between the theoretical and measured frictional pressure losses compared to the lower pump rates.

3.5.6 Measurements at 40% of maximum pump rate

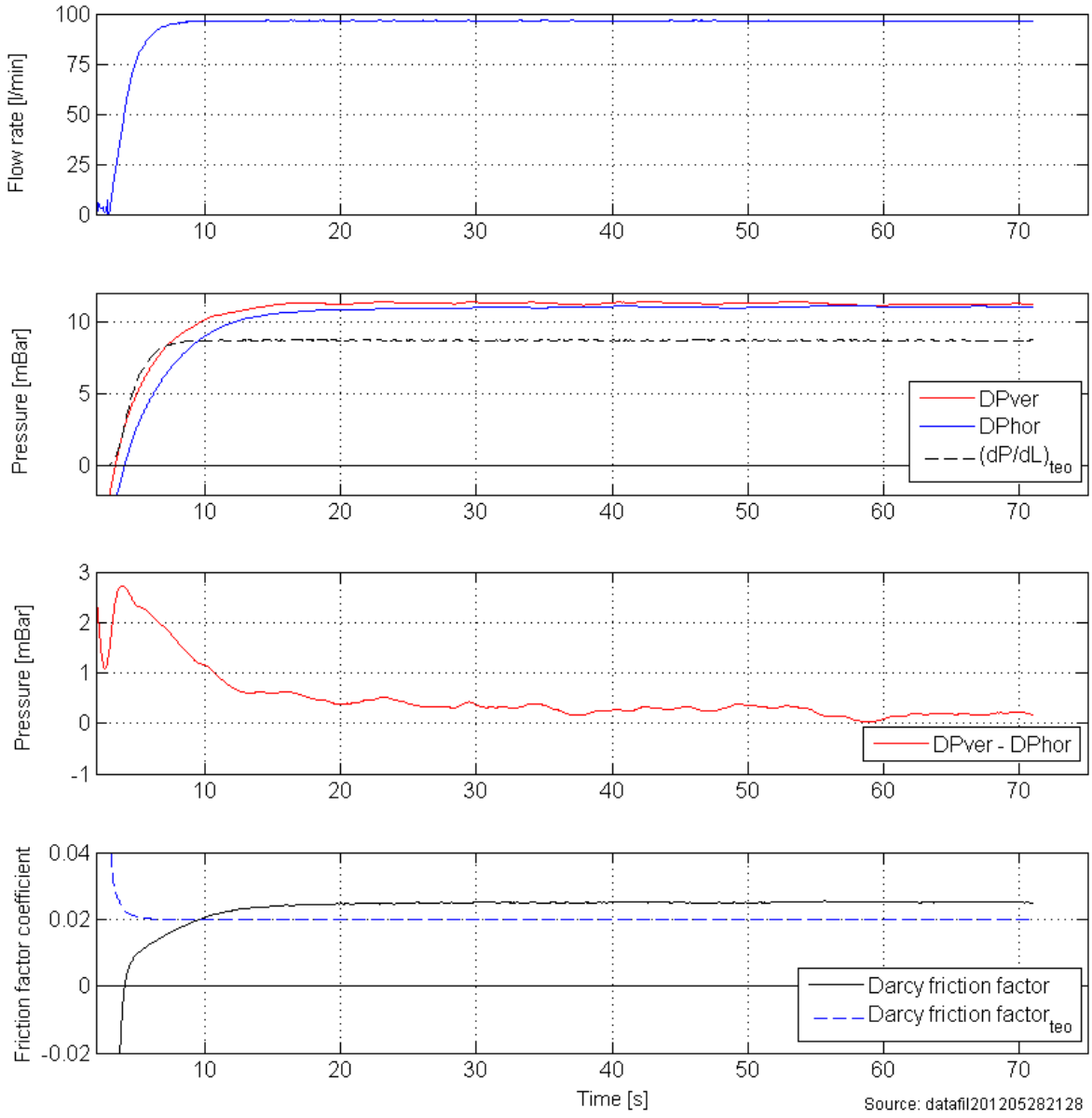

Figure 3.18 -Measurements at 40% of maximum pump rate

The difference between theoretical pressure loss and measured is consistently increasing, this trend is better displayed in section 3.5.8. The mirrored symmetry between the theoretical friction and the measured friction factor, displayed in Figure 3.14 – Figure 3.19, is caused by the difference in their respective mathematical expressions.

3.5.7 Measurements at 45% of maximum pump rate

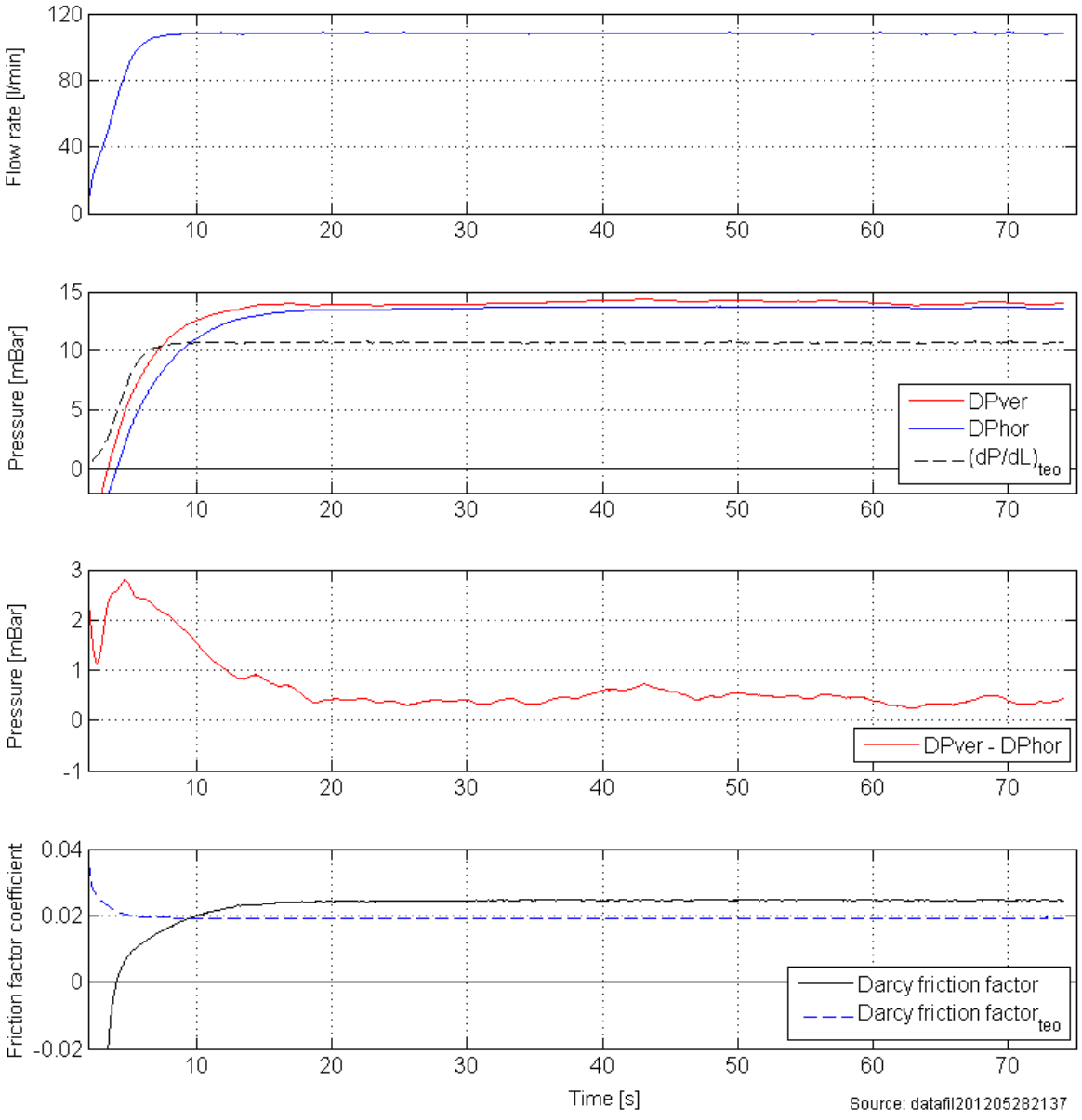

Figure 3.19 - Measurements at 45% of maximum pump rate

The general trends from previous flow rates continue.

3.5.8 Measured pressure losses compared to theoretical at different flow rates

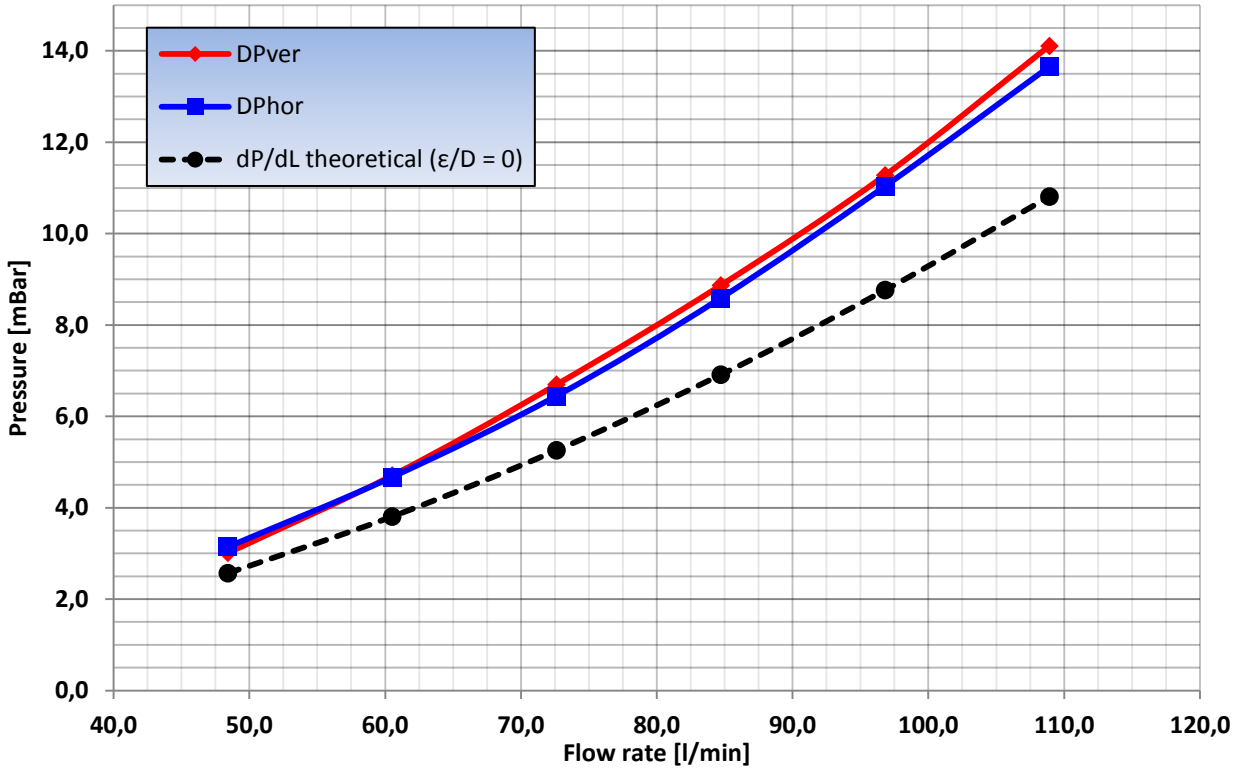

Figure 3.20 - Measured pressure losses compared with the theoretical pressure loss for different flow rates.

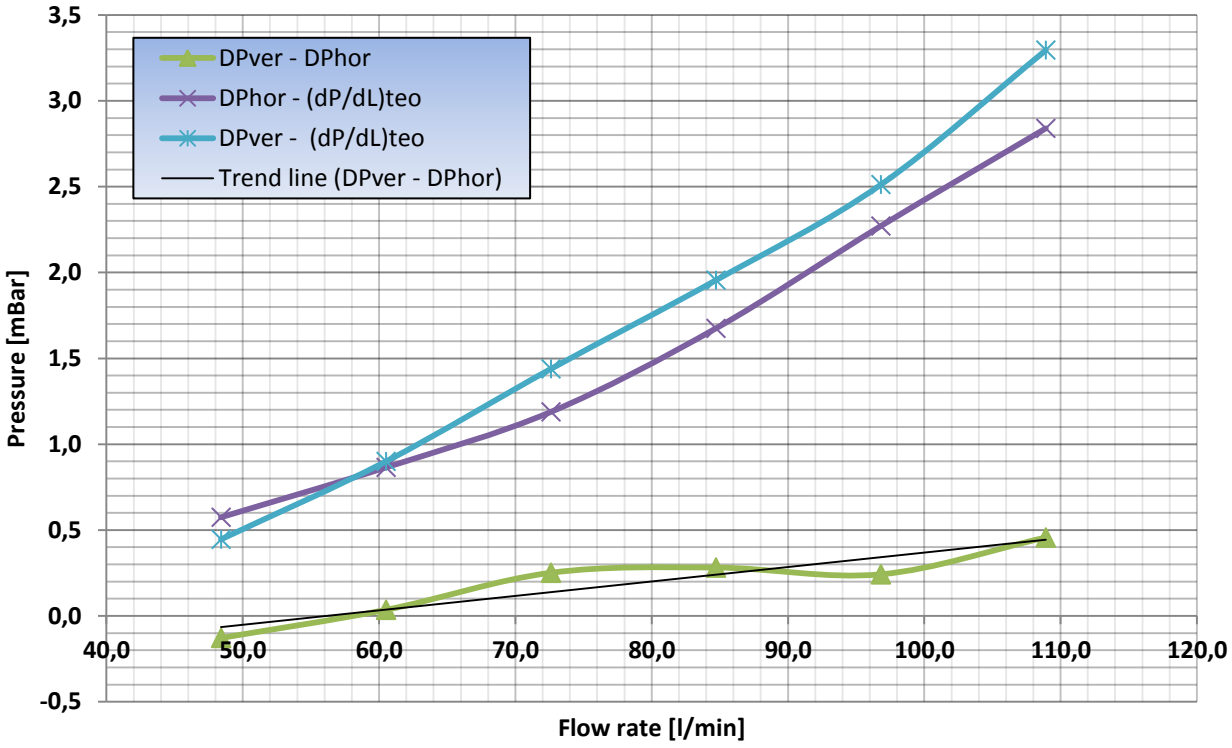

Figure 3.21 - Pressure difference between: DPver and DPhor, DPver and $(dP/dL)_{teo}$, and DPhor and $(dP/dL)_{teo}$

Figure 3.20 and Figure 3.21 show the relationship between frictional pressure loss and flow rate for both the measured and the theoretical values, and is basically a visual summary of the three upper subplots in each Matlab plot presented in Figure 3.14 - Figure 3.19. As before; each point on the graphs in Figure 3.20 and Figure 3.21 represents an averaged value of over 6000 Matlab measurements at a given flow rate. The first 20 seconds of every data set is neglected to ensure a representative average value based on stable flow conditions.

In Figure 3.20 and Figure 3.21 the previously mentioned, continuously increasing difference between measured and theoretical pressure loss is seen more clearly. This trend is shown for both the DP transmitters. The theoretical pressure loss in this case is based on friction factor which involves a smooth pipe assumption. This development can be explained by the smooth pipe assumption and is in accordance with theory (section 2.7) which states that the effect of the pipe wall irregularities increases with increasing Reynolds numbers. It can also be seen from equation 3.7, that the term containing the relative roughness factor (ε/D) will be increasingly more dominant for higher Reynolds numbers. The ε/D term is a constant value for any Reynolds number, so the friction factor coefficient will converge towards a value determined by this term when Reynolds numbers goes towards infinity. However if the ε/D term is set to zero, like here, the friction factor coefficient will converge towards zero as the Reynolds number goes towards infinity.

Figure 3.21 also shows the pressure difference between the measurements made at the vertical pipe section and horizontal pipe section, namely DPver (DP1) and DPhor (DP2). Even though the plotted line is quite erratic, a generally increasing trend is indicated for the available flow rates, illustrated by the trend line. The reason for this increasing trend is not known. The varying difference between the DPver and DPhor and hence the erratic shape of the line, could very well be due to uncertainties related to the measurements. Although the standard deviance in the measurements these plots are based on is very small (at most 0,01 mBar). Is for instance the standard deviance in the display readings discussed in section 3.4.2 closer to 0,2 mBar. There is in both cases too little data to determine the standard deviance conclusively; the point is that there are a lot of uncertain aspects related to measurements at this stage.

3.5.9 Fluid density estimation for different pump pressures

The hydrostatic pressure contribution from the fluid column in the vertical section is not measured by the DP transmitter. The hydrostatic pressure in the vertical section is necessary for the estimation of the fluid density from equation 3.3. The contribution from the water column in the vertical section is constant for any flow rate, and is calculated from equation 2.1 and data from table 3.6. This yields a constant pressure difference between the top and bottom connection point for DPver equal to 83,72 mBar. Figure 3.22 shows the estimated fluid density at different pump pressures when the hydrostatic pressure is added to the measured differential pressure for the vertical section. The pump pressures are measured with a preexisting pressure transmitter mounted near the pumps outlet, shown as PT101 in the PFD Figure 3.3. The pump pressure measurements are averaged in the same way as before and obtained from the corresponding Matlab data logs.

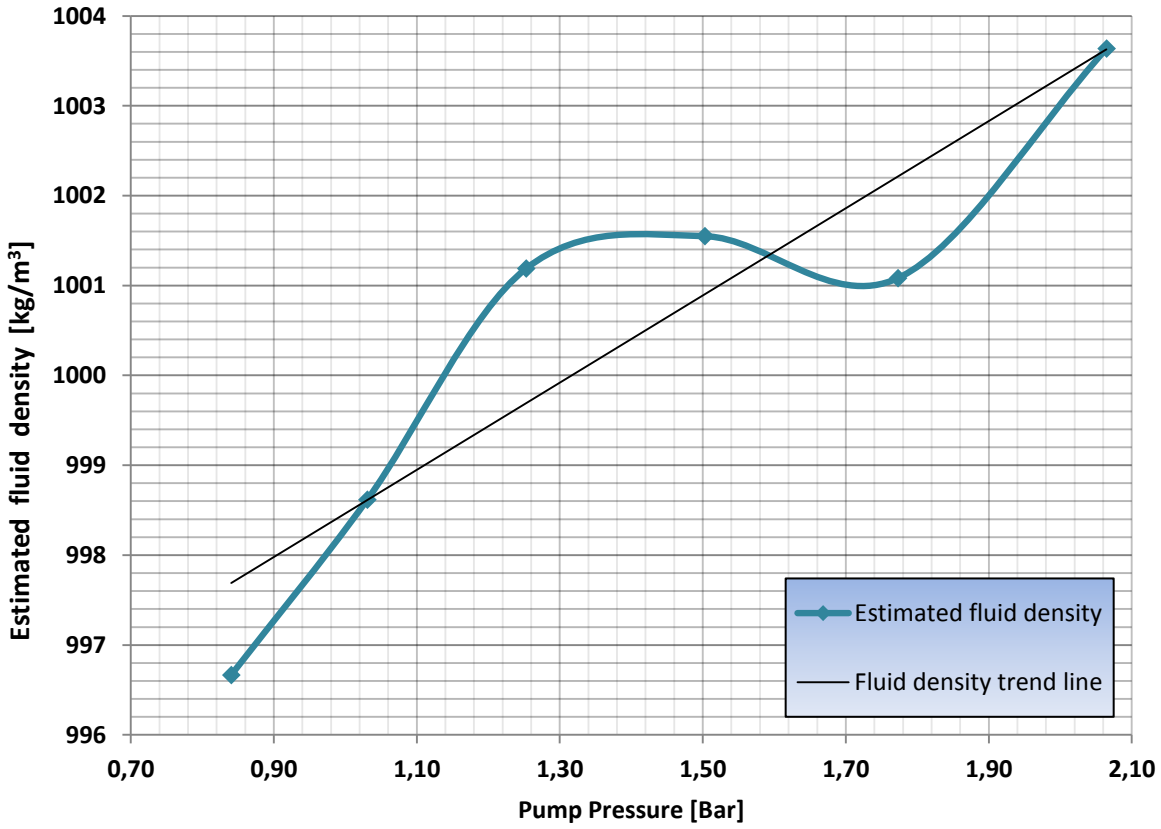

Figure 3.22 - Graphical presentation of estimated fluid densities at corresponding pump pressures

The varying difference between DPver and DPhor, discussed in previous section, causes the erratic shape of the line as that density estimate is based on the difference between them. From Figure 3.22 it is also shown that the increasing pressure difference between DPver and DPhor causes the estimated fluid density to increase. Since the current test fluid is fresh water, with a density of

998,2kg/m3, this increase in density is quite unlikely due to the low compressibility of water coupled with relatively low pressures.

3.5.10 Measured friction factor vs. theoretical friction factor at different flow rates

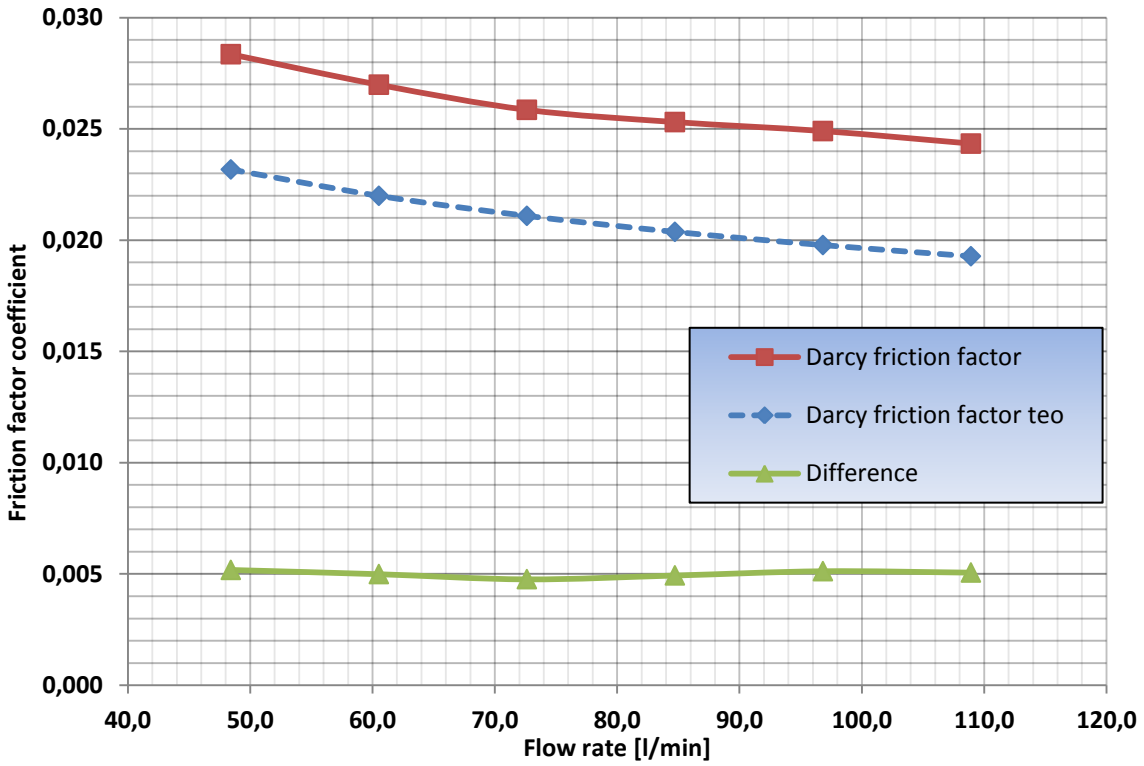

Figure 3.23 - Graphical comparison of the measured friction factor coefficient and theoretical friction factor coefficient at different flow rates.

Figure 3.23 displays a more or less constant difference of 0,005 between the measured friction factor coefficient and the theoretical friction factor coefficient. This indicates a very strong correlation (0,995) between the two. The reason for this difference is not fully understood, but the smooth pipe assumption could be one contributing factor and of course the uncertainties that is inherent in the measurements.

CONCLUSION & LESSONS LEARNED

Although a lot of effort was put into assuring the highest possible quality of data, there is still a great deal of uncertainties related to the data. The pressure losses obtained from the installed DP transmitters generally yields a higher pressure loss than theory suggests. Although this might partially be due to the smooth pipe assumption, it is hard to ignore that this could be caused by disturbances in the signal.

There are some obvious weaknesses with the current flow loop configuration. The restricted pump rates constitute a major limitation as it restrains the possibility of laminar flow with water as flow medium. Additionally there is an unresolved issue with the data logger in Matlab, which only allows logging over a 70 seconds interval before the memory fills up and data is overwritten. This is impractical because one often wants the possibility of running longer series of measurements.

Since all the experiments in this thesis have been performed with water as test medium, and the properties of water is well-established, it is practically meaningless to conduct the conventional standard tests for comparison. Most drilling fluids do not conform to the Newtonian behavior as water do. So in order to validate the Instrumented Standpipe concept against the existing standard tests, one should perform experiments on fluids with different fluid characteristics and more relevant properties.

In conclusion: The flow loop in its current condition and the experiment performed in this thesis is not sufficient to validate the Instrumented Standpipe concept.

FURTHER WORK

EMC issues

From the conclusion of this thesis it emerges that the current flow loop configuration must be rectified before the flow loop can be a useful tool in validation of the Instrumented Standpipe concept. The most critical issue is the inconsistency between measurements obtained during normal work hours and those obtained after normal work hours. This problem should be resolved before any further testing is conducted. A suggestion that might resolve or improve the situation:

- Install additional *isolating amplifiers* in the control cabinet and connect the DP Transmitters through these. The preexisting PTs are set up in this way [26]. Isolating amplifiers provide electrical safety barrier and protect data acquisition components from common mode voltages, which are the potential difference between instrument ground and signal ground. This is a potential source of signal disturbances [26, 30].

Restricted pump rates and Matlab data logger limitation.

The current pump is oversized for its purpose and can only be operated within a limited range of pump rates. Although pump pulses have not been proven to be a problem, it could also be appropriate to modify the flow loop with an additional looped pipe extension after the pump outlet to ensure stable flow conditions for the measurements made in the horizontal and vertical "standpipe" section.

- Replace the current pump with a pump better suited for its purpose, preferably as pulse-free as possible.
- Upgrade Control Computers physical memory or rewrite Matlab code to enable longer measurement series.

Perform experiments with different fluids

- Perform experiments with weighted brine.
- Perform experiments with a viscosified fluid.
- Perform experiments with a weighted & viscosified fluid.

ABBREVIATIONS

WBM	Water-based mud
OBM	Oil-based mud
ROP	Rate of penetration
BHA	Bottom hole assembly
ECD	Equivalent circulation density
BHP	Bottom hole pressure
LWD	Logging while drilling
MWD	Measurements while drilling
SG	Specific gravity
ESD	Equivalent static density
HPHT	High pressure and high temperature
YP	Yield point
PV	Plastic viscosity
RPM	Rotations per minute
API	American Petroleum Institute
PT	Pressure transmitter
PFD	Process flow diagram
DP	Differential pressure
EMI	Electromagnetic interference
EMC	Electromagnetic compatibility

NOMENCLATURE

Symbol	Description	Practical unit
A	Flow area	m^2
BHP	Bottom hole pressure	Bar
D	Diameter	m
f	Friction factor	dimensionless
f_f	Friction factor (Fanning type)	dimensionless
f_d	Friction factor (Darcy type)	dimensionless
g	Gravitational constant	m/s^2
h	Height of the fluid column	m
K	Fluid consistency factor for the Herschel-Bulkley model	$lb_f/100\ ft^2 * s$
K_p	Power law fluid consistency index	$lb_f/100\ ft^2 * s$
L	Length	m
n	Flow behavior index for the Herschel-Bulkley model	dimensionless
n_p	Power law flow behavior index	dimensionless
P	Pressure	Bar
P_{BP}	Surface back pressure	Bar
P_{HA}	Annular hydrostatic pressure	Bar
P_{HDP}	Drill pipe hydrostatic pressure	Bar
P_P	Pump pressure	Bar
PV	Plastic viscosity	cP
Q	Flow rate	m^3/s
Re	Reynolds number	dimensionless
V	Fluid velocity	m/s
V_A	Average fluid velocity in Annulus	m/s
V_{DP}	Average fluid velocity in pipe	m/s

YP	Yield point	$lb_f/100\ ft^2$
ε	Absolute roughness in pipe	m
γ	Shear rate	RPM
ΔP_{ADC}	Pressure loss in annulus around drill collars	Bar
ΔP_{ADP}	Pressure loss in annulus around drill pipe	Bar
ΔP_{DC}	Pressure loss inside the drill collars	Bar
ΔP_{DP}	Pressure loss inside the drill pipe	Bar
ΔP_{FA}	Frictional pressure loss in the annulus	Bar
ΔP_N	Pressure loss across the bit nozzles	Bar
ΔP_{SP}	Pressure loss in surface equipment	Bar
θ_3	Dial reading when viscometer operating at 3 RPM	$lb_f/100\ ft^2$
θ_{300}	Dial reading when viscometer operating at 300 RPM	$lb_f/100\ ft^2$
θ_6	Dial reading when viscometer operating at 6 RPM	$lb_f/100\ ft^2$
θ_{600}	Dial reading when viscometer operating at 600 RPM	$lb_f/100\ ft^2$
μ	Viscosity	cP
μ_e	Apparent/effective viscosity	cP
ρ	The fluid density	kg/m^3
ρ_{ECD}	Equivalent circulation density gradient	SG
τ	shear stress	$lb_f/100\ ft^2$
τ_0	The fluid yield stress	$lb_f/100\ ft^2$

BIBLIOGRAPHY

[1] Ryen Caenn, H.C.H. Darley, George R. Gray (2011) *Composition and properties of drilling and completion fluids 6th Ed*, ISBN: 9780123838599

[2] Olaf Skjeggestad (1989) *Boreslamteknologi : teori og praksis*, ISBN: 82-419-0010-4

[3] American Petroleum Institute (March, 2005) *Recommended practice 13 B-2: For field testing oil-based drilling fluids, 4th edition*

[4] Halliburton's Internet homepage (May, 2012) *Automated mud monitoring equipment*, http://www.halliburton.com/public/bar/contents/Data_Sheets/web/Sales_Data_Sheets/H08287-A4.pdf

[5] Egil Ronaes, Truls Fossdal, and Tore Stock, M-I SWACO (2012) *Real-Time Drilling Fluid Monitoring and Analysis - Adding to Integrated Drilling Operations,* Society of Petroleum Engineers, Document ID: 151459-MS

[6] Kjell Thorbjørnsen (2009) *Brønnvæsketeknologi,* ISBN: 978-82-315-0014-8

[7] Erik Skaugen, University of Stavanger (2000) *Drilling – Introduction,* Compendium in BIP180 – Boring

[8] V. J. Pandey, S. O. Osisanya (September, 2001) *Development of an Expert System for Solids Control in Drilling Fluids,* Journal of Canadian Petroleum Technology Volume 40, Number 9, Society of Petroleum Engineers, Document ID: 01-09-05

[9] ASME: Shale Shaker Committee (2005) *Drilling fluids processing handbook*, ISBN: 0-7506-7775-9

[10] NORSOK STANDARD D-010, Rev. 3 (August, 2004) *Well integrity in drilling and well operations, http://www.standard.no/*

[11] Bernt S. Aadnøy, University of Stavanger (2009) *An introduction to Petroleum Rock Mechanics*

[12] Shuling Li, Jeff George, and Cary Purdy, SPE, Landmark Halliburton (February, 2012) *Pore-Pressure and Wellbore-Stability Prediction To Increase Drilling Efficienc,* Journal of Petroleum Technology Volume 64, Number 2, Society of Petroleum Engineers, Document ID: 144717-MS

[13] Luiz A.S. Rocha, Jose L. Falcão, C.J.C. Gonçalves, Petrobras; Cecilia Toledo, Karen Lobato, Silvia Leal, Helena Lobato, PUC-RJ (2004) *Fracture Pressure Gradient in Deepwater,* Society of Petroleum Engineers, Document ID: 88011-MS

[14] Schlumberger's Oilfield Glossary (February, 2012) *Lost circulation*, http://www.glossary.oilfield.slb.com/Display.cfm?Term=lost%20circulation

[15] Rishi B. Adari, Stefan Miska, Ergun Kuru, University of Tulsa; Peter Bern, BP-Amoco; Arild Saasen, Statoil (2000) *Selecting Drilling Fluid Properties and Flow Rates For Effective Hole Cleaning in High-Angle and Horizontal Wells,* Society of Petroleum Engineers, Document ID: 63050-MS

[16] Jerome J. Schubert , PE (December, 1995) *Well Control Procedures for the Identification and Handling of Kicks for the Prevention of Blowouts*,Texas A&M University

[17] Bernt S. Aadnøy (2010) *Modern Well Design 2nd edition*, ISBN: 978-0-415-88467-9

[18] McMordie Jr., W.C., Bland, R.G., Hauser, J.M., Hughes Drilling Fluids (1982) *Effect of Temperature and Pressure on the Density of Drilling Fluids*, Society of Petroleum Engineers, Document ID: 11114-MS

[19] American Petroleum Institute (May, 2010) *Recommended Practice 13 D: Rheology and Hydraulics of Oil-well Drilling Fluids, 6th Edition*

[20] A.T. Bourgoyne Jr, K.K. Millheim, M.E. Chenevert , F.S. Young Jr. (1986) *Applied drilling engineering vol. 2***,** Society of Petroleum Engineers, ISBN: 1-55563-001-4

[21] Correspondence with Patrik Haak, Drilling fluids engineer, Halliburton

[22] Correspondence with Emil Frestad, Drilling fluids engineer, M-I SWACO

[23] Rune W. Time, University of Stavanger (January, 2009) *Two-Phase Flow in Pipelines course compendium*

[24] Frank M. White, University of Rhode Island (2006) *Viscous fluid flow 3rd edition*, ISBN:007-124493-x

[25] Liv A.Carlsen, IRIS, Gerhard Nygaard, IRIS, Rune W. Time (December, 2011) *Utilizing Instrumented Stand Pipe for Monitoring Drilling Fluid Dynamics for Improving Automated Drilling Operations*

[26] Magnus T. Torsvik, University of Stavanger (June, 2011) *Laboratory model of well drilling oricess. Construction, instrumentation, startup and regulation*, Master thesis, UiS, Faculty of science and technology, Cybernetics

[27] Alexander Wang, University of Stavanger (January, 2012) *MPD og automatisk brønnsparkhåndtering anvendt på boreriggmodell*, Master thesis, UiS, Faculty of science and technology

[28] Emerson Process Management, Datasheet and technical documentation *Rosemount 3051S Series Pressure Transmitter with HART® Protocol,* 5th of May- 2012 from: http://www2.emersonprocess.com/en-US/brands/rosemount/Pressure/Pressure-Transmitters/3051S-Series-of-Instrumentation/Pages/index.aspx

[29] Wikipedia (15.May, 2012), *Low Pass filter,* http://en.wikipedia.org/wiki/Low-pass_filter

[30] Wikipedia (11.June, 2012), *Isolation amplifier*, http://en.wikipedia.org/wiki/Isolation_amplifier

[31] Wikipedia (02.June, 2012), Systematic error, http://en.wikipedia.org/wiki/Systematic_error

[32] Wikipedia (02.June, 2012), *Random error*, http://en.wikipedia.org/wiki/Random_error

APPENDICES

A – Operating procedures

A.1 API Recommended practice for determination of mud density using the Pressurized Mud Balance [3]

1. Place the instrument base on a flat, level surface.
2. Measure and record the temperature of the fluid to be measured.
3. Fill the holding cup to a level approximately 6 mm below the upper edge.
4. Ensure that the check valve in the lid is in the open position. Place the lid on top of the holding cup and press it downward until it lands on the outer skirt of the lid. Any excess mud will be expelled through the check valve. Rinse off the cup and threads and screw the threaded cap onto the cup.
5. Fill the plunger with the mud sample. To ensure that the plunger volume is not diluted with liquid remains from previous tests or clean up, the volume should be expelled and refilled a couple of times.
6. Push the nose of the plunger onto the mating nipple on the cap. Pressurize the holding cup by maintain a downward force on the cylinder housing in order to keep the check valve open, at the same time push the piston rod downwards and force the mud into the cup.
7. The check valve in the lid is pressure actuated, so when the holding cup is pressurized the check valve is pushed upwards into the closed position. The best way to close the valve and maintain pressure inside the cup is to maintain a pressure on the rod, while lurking the housing gradually upwards. When the check valve closes (in top position) relax the pressure in the rod prior to disconnecting.
8. Clean the exterior of the cup. Place the instrument on the base knife edge and move the sliding weight until the beam is balanced. Read the drilling fluid density at the edge of the arrow side (towards the holding cup) of the sliding weights.
9. Release the pressure inside the cup, by reconnection the empty plunger and push the check valve down.
10. Empty the holding cup and clean up the used equipment.

A.2 API Recommended procedure for determination of viscosity using the Marsh Funnel (scanned from [3])

For conversions, use the formulas given in 4.4.2.

6 Viscosity and gel strength

6.1 Principle

Viscosity and gel strength are measurements that relate to the flow properties (rheology) of drilling fluids. The following instruments are used to measure viscosity and/or gel strength of drilling fluids:

a) Marsh funnel — a simple device for indicating viscosity on a routine basis;

b) direct-indicating viscometer — a mechanical device for measurement of viscosity at varying shear rates.

NOTE Information on the rheology of drilling fluids can be found in API RP 13D.

6.2 Determination of viscosity using the Marsh funnel

6.2.1 Apparatus

a) **Marsh funnel**, calibrated to deliver 946 cm^3 (1 quart) of fresh water at a temperature of 21 ± 3 °C (70 ± 5 °F) in 26 ± 0,5 s, with a graduated cup as a receiver.

The Marsh funnel shall have the following characteristics:

1) **funnel cone**, length 305 mm (12,0 in), diameter 152 mm (6,0 in) and a capacity to bottom of screen of 1 500 cm^3 (1,6 quarts);

2) **orifice**, length 50,8 mm (2,0 in) and inside diameter 4,7 mm (0,185 in);

3) **screen**, with 1,6 mm (0,063 in) openings (12 mesh); fixed at 19,0 mm (0,748 in) below top of funnel.

b) **Graduated cup,** with capacity at least 946 cm^3 (1 quart).

c) **Stopwatch**.

d) **Thermometer**, with a range of 0 °C to 105 °C (32 °F to 220 °F).

6.2.2 Procedure

6.2.2.1 Cover the funnel orifice with a finger and pour freshly sampled drilling fluid through the screen into the clean, upright funnel. Fill until fluid reaches the bottom of the screen.

6.2.2.2 Remove finger and start the stopwatch. Measure the time for drilling fluid to fill to the 946 cm^3 (1 quart) mark of the cup.

6.2.2.3 Measure the temperature of the fluid, in degrees Celsius (degrees Fahrenheit).

6.2.2.4 Report the time (6.2.2.2), to the nearest second, with the volume, as the Marsh funnel viscosity. Report the temperature (6.2.2.3) of the fluid to the nearest degree Celsius (degree Fahrenheit).

A.3 API Recommended procedure for determination of viscosity and/or gel strength using a direct-indication viscometer (scanned from [3])

6.3 Determination of viscosity and/or gel strength using a direct-indicating viscometer

6.3.1 Apparatus

a) **Direct-indicating viscometer,** powered by an electric motor or a hand crank.

Drilling fluid is placed in the annular space between two concentric cylinders. The outer cylinder or rotor sleeve is driven at a constant rotational velocity. The rotation of the rotor sleeve in the fluid produces a torque on the inner cylinder or bob. A torsion spring restrains the movement of the bob, and a dial attached to the bob indicates displacement of the bob. Instrument constants should be adjusted so that plastic viscosity and yield point are obtained by using readings from rotor sleeve speeds of 300 r/min and 600 r/min.

The components shall meet the following specifications.

1) **Rotor sleeve**

Inside diameter	36,83 mm (1,450 in)
Total length:	87,0 mm (3,425 in)
Scribed line:	58,4 mm (2,30 in) above the bottom of sleeve, with two rows of 3,18 mm (0,125 in) holes spaced 120° (2,09 rad) apart, around rotor sleeve just below scribed line.

2) **Bob**, closed, with flat base and tapered top

Diameter:	34,49 mm (1,358 in)
Cylinder length:	38,0 mm (1,496 in)

3) **Torsion spring constant:**

386 dyne-cm/degree deflection

4) **Rotor sleeve speeds**

High speed:	600 r/min
Low speed:	300 r/min

NOTE Other rotor speeds are available in viscometers from various manufacturers.

b) **Stopwatch.**

c) **Thermostatically controlled viscometer cup.**

d) **Thermometer**, with a range of 0 °C to 105 °C (32 °F to 220 °F).

6.3.2 Procedure

6.3.2.1 Place a sample of the drilling fluid in a thermostatically controlled viscometer cup. Leave enough empty volume (approximately 100 cm^3) in the cup for displacement of fluid due to the viscometer bob and sleeve. Immerse the rotor sleeve exactly to the scribed line. Measurements in the field should be made with minimum delay from the time of drilling fluid sampling. Testing should be carried out at either (50 ± 1) °C [(120 ± 2) °F] or (65 ± 1) °C [(150 ± 2) °F]. The place of sampling should be stated on the report.

The maximum recommended operating temperature is 90 °C (200 °F). If fluids have to be tested above this temperature, either a solid metal bob, or a hollow metal bob with a completely dry interior should be used.

CAUTION Liquid trapped inside a hollow bob may vaporize when immersed in high-temperature fluid and cause the bob to explode.

6.3.2.2 Heat (or cool) the sample to the selected temperature. Use intermittent or constant shear at 600 r/min to stir the sample while heating (or cooling) to obtain a uniform sample temperature. After the cup temperature reaches the selected temperature, immerse the thermometer into the sample and continue stirring until the sample reaches the selected temperature. Record the temperature of the sample.

6.3.2.3 With the sleeve rotating at 600 r/min, wait for the viscometer dial reading to reach a steady value (the time required is dependent on the drilling fluid characteristics). Record the dial reading R_{600} in pascals for 600 r/min.

6.3.2.4 Reduce the rotor speed to 300 r/min and wait for the dial reading to reach steady value. Record the dial reading R_{300} in pascals for 300 r/min.

6.3.2.5 Stir the drilling fluid sample for 10 s at 600 r/min.

6.3.2.6 Allow drilling fluid sample to stand undisturbed for 10 s. Slowly and steadily turn the hand-wheel in the appropriate direction to produce a positive dial reading. Record the maximum reading as the initial gel strength. For instruments having a 3 r/min speed, the maximum reading attained after starting rotation at 3 r/min is the initial gel strength. Record the initial gel strength (10-second gel) in pounds per 100 square feet.

NOTE To convert the dial reading to pounds per 100 square feet: 1 Pa = 0,48 lb/100 ft^2.

6.3.2.7 Restir the drilling fluid sample at 600 r/min for 10 s and then allow the drilling fluid to stand undisturbed for 10 min. Repeat the measurements as in 6.3.2.6 and report the maximum reading as the 10-minute gel in pascals (pounds per 100 square feet).

NOTE To convert the dial reading to pounds per 100 square feet: 1 Pa = 0,48 lb/100 ft^2.

6.3.3 Calculation

$$\eta_P = R_{600} - R_{300} \quad (6)$$

$$\eta_Y = 0{,}48 \times (R_{300} - \eta_P) \quad (7)$$

$$\eta_A = R_{600}/2 \quad (8)$$

where

η_P is the plastic viscosity, in millipascal seconds;

NOTE Plastic viscosity is commonly known in the industry by the abbreviation PV.

η_Y is the yield point, in pascals;

η_A is the apparent viscosity, in millipascal seconds;

R_{600} is the dial reading at 600 r/min, in pascals (pounds per 100 square feet);

R_{300} is the dial reading at 300 r/min, in pascals (pounds per 100 square feet).

NOTE 1 To convert to CGS units of centipoise, 1 mPa·s = 1 cP.

A.4 Procedure for startup and shutdown of flow loop [26]

STARTUP

1. Make sure all extension cords are connected.
2. Manually activate the fuses in the control cabinet and the pump cabinet.
3. Manually open the vent valve for the “rørbuesløfe” (hose located at flow loop’s outlet to tank).
4. Turn on the contactor, green indication light is shown
5. Ensure that all the red manual valves in flow direction are in open position. And that blue drain valves are in closed position.
6. Compile and connect to the system in the Matlab (Simulink)
7. Start the process, with preferred settings.
8. Run for a while, when water starts returning to the tank close the vent valve on the “rørbuesløfe”.

SHUTDOWN

1. Stop the system in Matlab (Simulink)
2. Drain water from flow loop to tank, with blue drain valves
3. Turn off the contactor, green indication light goes dark
4. Turn off the computer
5. Clean up your mess

B - Technical documentation related to the installation DP transmitters on the flow loop

B.1 Table of analog input ports on control card (PCI 6221)

Innskjema for PCI 6221				
Innganger	**Kanalnr**	**Skilleforsterkerkort**	**Tilkobling**	**Signaltype**
PT101	0	G1	68, 67	Analog
PT102	8	G2	34, 67	Analog
PT103	1	G3	33, 32	Analog
PT201	9	G4	66, 32	Analog
PT202	2	G5	65, 64	Analog
PT203	10	G6	31, 64	Analog
PT204	3	G7	30, 29	Analog
Tilbakemeld MPD-ventil	4	G8	28, 27	Analog
Tilbakemeld WCV-ventil	12	G9	61, 27	Analog
Motor monitorering	5		60, 59	Analog
DP1	6		25, 24	Analog
DP2	14		58, 24	Analog

SCB-68 Quick Reference Label

M SERIES DEVICES

NATIONAL INSTRUMENTS

CONNECTOR 0

(AI 0-15)

P/N 192187A-01

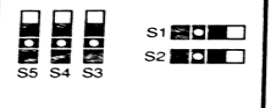

Temperature Sensor Disabled
(Factory Default Setting)

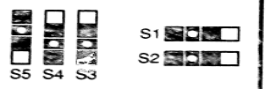

Temperature Sensor Enabled
(Single-ended)

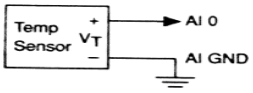

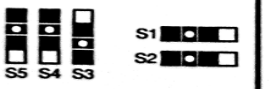

Temperature Sensor Enabled
(Differential)

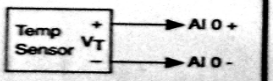

PIN #	SIGNAL
68	AI 0
34	AI 8
67	**AI GND**
33	AI 1
66	AI 9
32	**AI GND**
65	AI 2
31	AI 10
64	**AI GND**
30	AI 3
63	AI 11
29	**AI GND**
62	**AI SENSE**
28	AI 4
61	AI 12
27	**AI GND**
60	AI 5
26	AI 13
59	**AI GND**
25	AI 6
58	AI 14
24	**AI GND**
57	AI 7
23	AI 15

PIN #	SIGNAL
12	**D GND**
46	PFI 11/P2.3
13	**D GND**
47	P0.3
14	**+5 V**
48	P0.7
15	**D GND**
49	P0.2
16	P0.6
50	**D GND**
17	P0.1
51	P0.5
18	**D GND**
52	P0.0
19	P0.4
53	**D GND**
20	APFI 0
54	**AO GND**
21	AO 1
55	**AO GND**
22	AO 0
56	**AI GND**

PIN #	SIGNAL
1	PFI 14/P2.6
35	**D GND**
2	PFI 12/P2.4
36	**D GND**
3	PFI 9/P2.1
37	PFI 8/P2.0
4	**D GND**
38	PFI 7/P1.7
5	PFI 6/P1.6
39	PFI 15/P2.7
6	PFI 5/P1.5
40	PFI 13/P2.5
7	**D GND**
41	PFI 4/P1.4
8	**+5 V**
42	PFI 3/P1.3
9	**D GND**
43	PFI 2/P1.2
10	PFI 1/P1.1
44	**D GND**
11	PFI 0/P1.0
45	PFI 10/P2.2

B.2 Circuit diagram for Differential Pressure transmitters

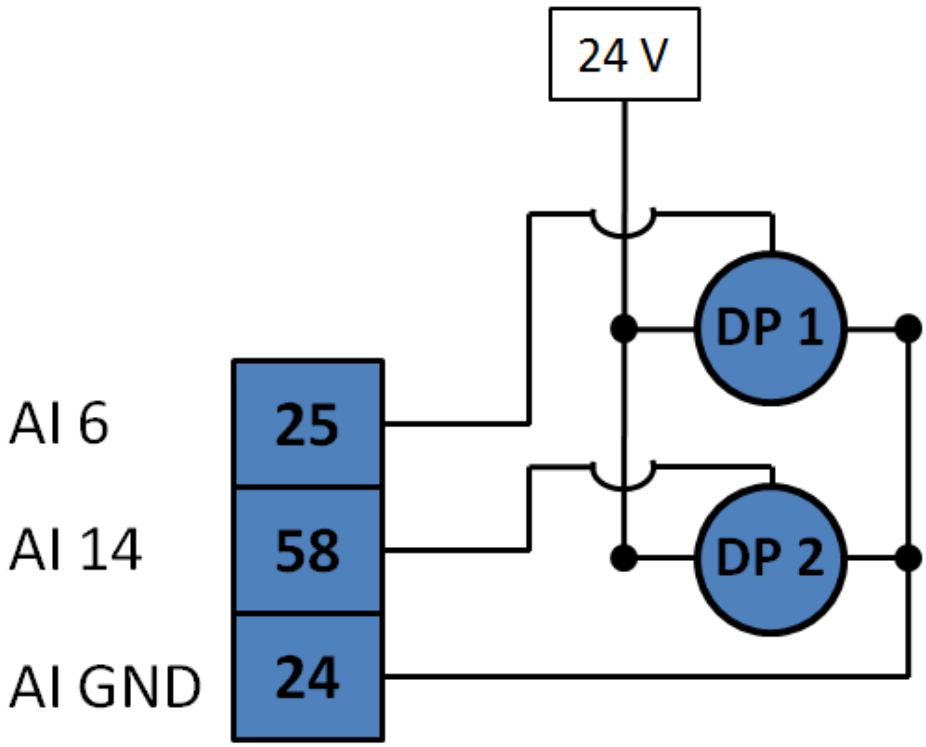

B.3 Terminal blocks (rekkeklemmer) in the control cabinet

Rekkeklemmeliste								
Rad	Nr	Tilkobl.	Led. Farg	Spenning	Sig.type	Type utstyr	Kabelnr	G.kabelnr
X1	1	L	Brun	230VAC		Stikkontakt	MPD-Stikk230V	17
	2	N	Blå	230VAC		Stikkontakt		
	3		Rød	24V		Trykkluft	MPD-AIR100-80	15
	4		Sort	Gnd		Trykkluft		
	5					SPARE		
	6		Sort			Nivåbryter i tank	MPD-LS100-10	16
	7		Hvit			Nivåbryter i tank		
	8		Rød	24VDC		Trykk transmitter 1	MPD-PT100-20	12
	9		Sort	Gnd		Trykk transmitter 1		
	10		Rød	24VDC		Trykk transmitter 2	MPD-PT100-30	13
	11		Sort	Gnd		Trykk transmitter 2		
	12		Rød	24VDC		Trykk transmitter 3	MPD-PT100-40	14
	13		Sort	Gnd		Trykk transmitter 3		
	14		Rød	24VDC		Trykk transmitter 4	MPD-PT200-10	3
	15		Sort	Gnd		Trykk transmitter 4		
	16		Rød	24VDC		Trykk transmitter 5	MPD-PT200-20	1
	17		Sort	Gnd		Trykk transmitter 5		
	18		Rød	24VDC		Trykk transmitter 6	MPD-PT200-30	4
	19		Sort	Gnd		Trykk transmitter 6		
	20		Rød	24VDC		Trykk transmitter 7	MPD-PT200-40	8
	21		Sort	Gnd		Trykk transmitter 7		
	22	N	Sort	230VAC		BOP	MPD-BOP200-80	9
	23	L1	Brun	230VAC		BOP		
	24		Hvit	230VAC		BOP		
	25	N	Sort	230VAC		Lekkasje øvre	MPD-LV100-60	2
	26	L1	Brun	230VAC		Lekkasje øvre		
	27		Hvit	230VAC		Lekkasje øvre		
	28	N	Sort	230VAC		Lekkasje nedre	MPD-LV100-50	5
	29	L1	Brun	230VAC		Lekkasje nedre		
	30		Hvit	230VAC		Lekkasje nedre		
	31		Rød	24VDC		Coriolis	MPD-CI200-70	11
	32		Blå	Gnd		Coriolis		
	33		Rød	+	Status inn	Coriolis	MPD-CI200-71	6
	34		Blå	-		Coriolis		
	35		Sort	+	Status ut	Coriolis		
	36		Brun	-		Coriolis		
	37		Gul	+	Freq ut	Coriolis		
	38		Grønn	-		Coriolis		
	39		Lilla	+	HART	Coriolis		
	40		Hvit	-		Coriolis		
	41		Rød	+		Diff.Trykk transmitter 2		
	42		Sort	-		Diff.Trykk transmitter 2		
	43		Lilla	+	Settpkt	Reg. Ventil Høyre	MPD-RV200-50	10
	44		Hvit	-		Reg. Ventil Høyre		

	45		Sort	+	Tilb.mld	Reg. Ventil Høyre		
	46		Brun	-		Reg. Ventil Høyre		
	47		Rød	24VDC	Driftsp.	Reg. Ventil Høyre		
	48		Blå	Gnd		Reg. Ventil Høyre		
	49		Lilla	+	Settpkt	Reg. Ventil Venstre	MPD-RV200-60	7
	50		Hvit	-		Reg. Ventil Venstre		
	51		Sort	+	Tilb.mld	Reg. Ventil Venstre		
	52		Brun	-		Reg. Ventil Venstre		
	53		Rød	24VDC	Driftsp.	Reg. Ventil Venstre		
	54		Blå	Gnd		Reg. Ventil Venstre		
X2	1	L1	Sort	230VAC		Tilførsel		
	2	N	Blå	230VAC		Tilførsel		
	3	L1	Sort	230VAC		Ut fra -F4		
	4	N	Blå	230VAC		Ut fra -F4		
	5	FC	4			Frekvensomformer ØLFLEX		
	6	L1	Sort	230VAC		Ut fra start/stopp br		
	7	AM	5			Frekvensomformer ØLFLEX		
	8	AC	6			Frekvensomformer ØLFLEX		
	9		Rød	+		Diff.trykk transmitter 1		
	10		Sort	-		Diff.trykk transmitter 1		

C – Matlab script for measured data and plots

```
close all;
clear all;
clc;
load 'datafil201205282105'

% figure;
% plot(inngang.time,inngang.signals(1).values);
% print motor;
% figure;
% plot(inngang.time,inngang.signals(2).values);
% print PT101;
% figure;
% plot(inngang.time,inngang.signals(11).values);
% print Coriolis;
```

```
%% Input data
rho = 998.2;
mu = 0.001002;
DL = 0.855;
Di = 0.03325;
pi = 3.14;
ks = 0.000; % smooth pipe roughness factor
cor = inngang.signals(11).values;
```

```
%% Flow rate
Q = inngang.signals(11).values.*(1000/(60*rho));
% figure;
% plot(inngang.time,Q);
% legend('Flow rate')
```

```
%% Darcy friction factor
f3 = (162000000*inngang.signals(13).values.*rho*Di^5*pi^2);
f4 = (inngang.signals(11).values.^2*DL);
% f=f3/f4;
% fd=diag(f)
```

```
%% Sorting zeros from the V vector
% The V vector contains a lot of values which are below zero, and these
values
% disturbs the plot, therefore V, t, f3, f4 and fte have to be rearranged
so these
% values are dismissed.

V = (4.*inngang.signals(11).values)/(3600*pi*Di^2*rho);
Re = (rho*V*Di)/mu;
ut = log10((ks/3.7)^(1.11)+(6.9./Re));
fte = (1./(-1.8*(ut))).^2;
DPte = (rho*fte*(V'.^2)*DL)./(2*Di*100);
DPT = diag(DPte);

[V ind1] = sort(V(:));% Making V a sorted vector with min values first
t = inngang.time(:);  % Rearranging t to vector
t = t(ind1);          % Rearranging t so the values correspond to the right
                      % velocity values.
f3 = f3(:);     f4 = f4(:);      fte = fte(:);
f3 = f3(ind1); f4 = f4(ind1);  fte = fte(ind1);
```

```
for i = 1:length(V)    % counting to the indices number where V is not
    if V(i) <= 0       % equal to zero.

    else
        break
    end
end

V = V(i:end);          % Clearing the zero values from the vector
f3 = f3(i:end); f4 = f4(i:end); fte = fte(i:end);
t = t(i:end);          % Clearing the corresponding values from t vector
[t ind2] = sort(t);    % Sorting the t vector so it is ascending
V  =  V(ind2);         % Rearranging so the right values correspond
f3 = f3(ind2); f4 = f4(ind2); fte = fte(ind2);

t2 = inngang.time;
x  = 0*t2;
xt = 0*t;
```

```
%% Plot
fd=f3./f4;
figure
subplot(4,1,1)
plot(inngang.time,Q,'b');
title ('Source: datafil201205282137');
ylabel('Flow rate [l/min]');
grid on;
ylim([0 120]);
xlim ([2 75]);

subplot(4,1,2)
plot(t2,inngang.signals(12).values,'r',t2,inngang.signals(13).values,'b',...
    'linewidth',1);
hold on;
plot( t2, DPT,'k--',t2,x,'k');
hold off;
legend('DPver','DPhor','(dP/dL)_{teo}');
ylabel('Pressure [mBar]');
grid on;
xlim ([2 75]);
ylim([-2 15]);

subplot(4,1,3)
plot(t2,inngang.signals(12).values-inngang.signals(13).values,'r');
legend('DPver - DPhor');
ylabel('Pressure [mBar]');
grid on;
xlim ([2 75]);
ylim ([-1 3]);

subplot(4,1,4)
plot(t,fd,'k');
hold on;
plot(t,fte,'b--',t,xt,'k');
legend('Darcy friction factor','Darcy friction factor_{teo}');
xlabel('Time [s]');ylabel('Friction factor coefficient');
grid on;
axis([2 75 -0.02 0.040]);
```

D – Error analysis

All measured data used in calculations contributes with their inherent measurements errors and uncertainties to the uncertainties in the calculated value. How this affects the results is commonly called error analysis. There are two main types of errors associated with measured data:

Systematic errors [31]

Systematic errors are biases in measurements, which causes measured values to be systematically too large or too small. They may be caused by:

1) Measuring instrument. For example imperfect calibration.
2) Environmental. For example electromagnetic interference with measurement process
3) Observational. For example an Offset scale
4) Theoretical. Simplified models or assumptions in the equations that describes it, will cause a systematical deviation between the measured and the theoretical values.

Random error [32]

All measurements are prone to random errors. Random errors lead to measured values being inconsistent when measurements of a constant attribute or quantity are taken. They may be caused by:

1) The experimenter's interpretation of the instrumental reading.
2) Unpredictable fluctuations in the readings of a measuring instrument. For example due to environmental disturbances as; vibrations, electromagnetic interference, voltage fluctuations

The concept of random error is closely related to the concept of accuracy and precision. If the variance (standard deviance) in the measurements is small, is also the spread in the measurements small, ergo the precision in the measurements is high.

E – Excel calculations

E.1 Comparison of rheological models

The rheometer measurements are obtained from [2 (page 40 table 5,1)].

Rheometer Measurements		Measurments in Equvialent SI-units		Estimated shear stress [Pa]		
RPM	**Dial Reading [lb/100 ft^2]**	**Shear Rate [1/s]**	**Shear Stress [Pa]**	**Bingham**	**Power Law**	**Herschel-Bulkley**
600	48	1022	24,53	24,52	24,53	24,52
300	32	511	16,35	16,35	16,35	16,35
200	24	341	12,26	13,63	12,90	13,03
100	18	170	9,20	10,90	8,60	9,04
6	8	10	4,09	8,34	1,66	3,16
3	6	5	3,07	8,26	1,11	2,76

Bingham Parameters		
PV	0,016	[Pa*s]
YP	8,176	[Pa]
Power Law Parameters		
n	0,58	[dimentionless]
K	0,43	[Pa*s]
Herschel-Bulkley Models		
ty	2,044	[Pa]
n	0,652	[dimentionless]
K	0,246	[Pa*s]

E.2 Statistical analysis of measured data quality

This table is just a summary of the recorded data. The actual recorded data sets are too big to be presented in an orderly manner.

	After normal working hours				During normal working hours			
	0,30 pump rate		0,40 pump rate		0,30 pump rate		0,40 pump rate	
	DP 1	**DP 2**	**DP 1**	**DP 2**	**DP 1**	**DP 2**	**DP 1**	**DP 2**
Nr. obs	72	72	69	69	96	96	69	69
Mean	6,69	6,27	11,34	10,65	5,39	4,49	8,69	7,73
Std.dev	0,22	0,19	0,28	0,23	1,43	1,44	1,18	1,64
Variance	0,05	0,04	0,08	0,05	2,03	2,08	1,38	2,68
Q25	6,52	6,11	11,14	10,48	4,17	3,15	7,68	6,15
Min	6,16	5,89	10,69	10,10	2,67	1,66	6,27	4,82
Median	6,71	6,26	11,31	10,62	5,32	4,54	8,81	7,92
Max	7,15	6,81	11,99	11,12	7,47	6,60	10,70	9,99
Q75	6,85	6,42	11,51	10,82	6,90	5,88	9,68	9,38